EFFECT OF END ANCHORAGE ON CFRP STRENGTHENED CONCRETE BEAMS

Dewage Manasi Narmada Wijerathna

14 8024 D

Degree of Masters of Science

Department of Civil Engineering

University of Moratuwa
Sri Lanka

March 2015

EFFECT OF END ANCHORAGE ON CFRP STRENGTHENED CONCRETE BEAMS

Dewage Manasi Narmada Wijerathna

148024 D

Dissertation submitted in partial fulfilment of the requirements for the degree Master of Science

Department of Civil Engineering

University of Moratuwa

Sri Lanka

March 2015

DECLARATION

"I declare that this is my own work and this thesis does not incorporate without acknowledgement any material previously submitted for a Degree or Diploma in any other University or institute of higher learning and to the best of my knowledge and belief it does not contain any material previously published or written by another person except where the acknowledgement is made in the text.

Also, I hereby grant to University of Moratuwa the non-exclusive right to reproduce and distribute my thesis, in whole or in part print, electronic or other medium. I retain the right to use this content in whole or part in future works (such as articles or books).

Signature: Date:

The above candidate has carried out research for the Masters dissertation under my supervision.

Signature of the supervisor: Date:

ABSTRACT

Reinforced concrete structures are often being subjected to modifications and improvements during their service life. The main causes for improvements are design errors, changes in use, degradation due to corrosion of reinforcing steel, damage due to seismic loads, vehicular impact and excessive wear and excessive loading. Precautions for these issues are mainly in two types; repair and strengthening. Restoring the structures which became structural malfunction is known as repair. Improvements done in structures in order to achieve higher service loads or longer service lives are known as strengthening. As far as strengthening techniques are concerned, concrete jacketing, steel jacketing, precast concrete jacketing, prestressed concrete jacketing and external application of Fibre reinforced polymer (FRP) composite materials are the available upgrading methods.

Structural strengthening with fibre reinforced polymers is a popular strengthening technique worldwide, due to its extensive advantages. The important properties of FRP's are high strength, light weight, good rigidity, corrosion resistance, high elastic modulus etc. FRP's are used to improve structures by means of increasing flexural capacity, enhancing shear capacity and confining concrete columns to improve axial compression load carrying capacity. When flexural strengthening with FRP is concerned, research studies show that a significant strength increment can be achieved with use of CFRP sheets as an external reinforcement. It also improves serviceability of structures.

Failure of a CFRP strengthened beam for flexure can be due to flexure, shear, concrete crushing or debonding. The failure modes can be categorized in to two main types; classical failure and premature failure. Failure of an element due to yielding of steel bars, tensile failure of FRP sheets and crushing of concrete in compression zone are known as classical failure. Failure of element in any other method such as debonding of FRP, peeling off of FRP and concrete cover separation are premature failure modes.

End debonding is the most common failure mode which has been experienced in practice. This mode of failure, limits the capacity by 60% to 80% of ultimate capacity (Mostofinejad 2014, Xiong 2007) of the system and induce sudden failure without prior warning. Different methods have been proposed in literature to delay end debonding. They are Mechanical fasteners, FRP pin and pan shape anchors, Near Surface Mount reinforcement, End wraps and use of wire mesh–epoxy composite. Among these techniques, end wraps are more beneficial since it contribute to shear capacity of the beam and help to improve ductility apart from preventing debonding failure. Although these techniques are advantages, they are not popular in the industry due to lack of technical data to quantify the effects.

Previous research studies emphasise the need of proper design method to predict the strength enhancement gained due to end wraps. There are few studies (Sawada et al,2003 Hawileh et al. 2013) carried out to investigate the interaction between resistance to debonding and the strength gain. Moreover, studies conducted in tropical countries are even less. This has lead to less confidence of using this technique by practicing engineers. Although there are several design guides available on design of externally bonded FRP systems, none of these guides address the effect of end anchorage on flexural strength gain. This study investigates the effect of end anchors on enhancing flexural capacity of reinforced concrete members, flexural strengthened with CFRP sheets.

An extensive experimental program was carried out using reinforced concrete beams to understand the failure behaviour, stress distribution, deflection behaviour and flexural strength enhancement. It was observed that 98.53% strength increment could achieved by the

specimens flexural strengthened with CFRP external reinforcement over control specimens. When the flexural strengthened beams were anchored at the ends, the strength enhancement was 145% compared with that of unstrengthened beams. It was also observed that strain levels at the ends of longitudinal CFRP strips reduces significantly, when end wrap anchorage is provided. End debonding can be fully prevented by providing sufficient amount of end anchorage. The failure mode of beams changed from cover debonding to CFRP rupture, in existence of end wraps.

A new theoretical model was developed based on experimental observations, design guidelines and data collected literature. It is capable of predicting both failure load and failure mode of flexural strengthened and end anchored beams. The model was compatible with experimental results of current study as well as experimental results collected from literature.

Two papers were published from the work of this study and are attached in appendix E.

Keywords: *CFRP/concrete, flexural performance, de-bonding failure, end anchorage*

ACKNOWLEDGEMENT

TABLE OF CONTENT

LIST OF FIGURES

LIST OF TABLES

LIST OF ABBREVIATIONS

Abbreviation   Description

ACI	American Concrete Institute
AFRP	Aramid Fibre Reinforced Polymer
BRE	Building Research Establishment
CEB	Comité euro-international du béton
CFRP	Carbon Fibre Reinforced Polymer
EBR	Externally Bonded Reinforcement
EMI	Electromagnetic Interference
FIB	Fédération internationale du béton
FIP	Fédération internationale de la précontrainte
FRP	Fiber Reinforced Polymer
GFRP	Glass Fiber Reinforced Polymer
GI	Galvanized Iron
HIT	High Heat Treatment
HM	High Modulus
HT	High Tensile
IHT	Intermediate Heat Treatment
IM	Intermediate Modulus
JCI	Japanese concrete institute
LHT	Low Heat Treatment
NSMR	Near Surface Mount Reinforcement
RC	Reinforced concrete
SHT	Super Heat Tensile
UHM	Ultra High Modulus

LIST OF SYMBOLS

Symbol	Description	Units
A_f	$nt_f w_f$, area of FRP external reinforcement	[mm^2]
A_{fv}	area of FRP shear reinforcement	[mm^2]
A_s	area of non pre-stressed steel reinforcement	[mm^2]
a_s	cover to steel tension reinforcement	
a_u	effective bond length	
A_{sv}	provided area of shear reinforcement	[mm^2]
A_{s1}	area of tensile steel reinforcement	[mm^2]
A_{s2}	area of compressive steel reinforcement	[mm^2]
b	width of beam	[mm]
b_f	width of the FRP strip	[mm]
b_w	minimum width of cross section over the effective depth	[mm]
c	distance from extreme compression fiber to the neutral axis	[mm]
C_1	Factors obtained through calibration of test results (for CFRP strips, the value is 0.64)	
C_2	Factors obtained through calibration of test results (for CFRP strips, the value is 2)	
d	effective depth of the member	[mm]
d_f	depth of FRP shear reinforcement	[mm]
d_2	distance from centroid of compressive steel to extreme compressive fibre	[mm]
E_f	modulus of elasticity of FRP	[N/mm^2]
E_{fu}	elastic modulus of FRP in the principal fibre orientation	[N/mm^2]
E_{s2}	modulus of elasticity of steel	[N/mm^2]
f_c	prism compressive strength of concrete	[N/mm^2]
f_{ctm}	mean value of the concrete tensile strength	[N/mm^2]
f_{cu}	characteristic strength of concrete	[N/mm^2]

F_d	tensile force before the debonding of CFRP sheets	
f_f	stress level in the FRP reinforcement	[N/mm^2]
f_{fe}	effective stress in the FRP	[N/mm^2]
f_s	stress in non pre-stressed steel reinforcement	[N/mm^2]
F_t	force in main tension reinforcement	[N]
F_u	effective shear force	[N]
f_y	characteristic strength of main reinforcement	[N/mm^2]
f_{yd}	design value of the steel yield strength	[N/mm^2]
f_{yv}	characteristic strength of shear reinforcement	[N/mm^2]
G_f	interfacial fracture energy	[Nmm]
h	overall thickness of a member	[mm]
k_b	geometry factor	
k_c	factor accounting for the state of compaction of concrete	
l	length of specimen	[mm]
$l_{b,max}$	maximum anchorable length	[mm]
L_e	active bond length of FRP laminate	[mm]
L_{ue}	effective bond length of FRP shear wraps	[mm]
M	expected maximum moment	[N mm]
M_n	nominal moment strength	[N mm]
M_{Rd}	resisting design moment	
$N_{fa,max}$	maximum anchorable FRP force in tensile steel reinforcement	
P	externally applied force	[N]
s_f	spacing FRP shear reinforcing	
t_f	thickness of FRP	
V_f	nominal shear strength provided by FRP stirrups	
W	applied external point load	[N]
w	uniformly distributed self-weight of concrete element	[N/mm]
x	depth of the compression zone	
α	reduction factor, (approximately equal to 0.9)	

α	angle between principal fibre orientation and longitudinal axis of member
β_1	ratio of the depth of the equivalent rectangular stress block to the depth of the neutral axis
δ_f	interfacial slip
δ_G	stress block centroid coefficient
ε_f	FRP strain
$\varepsilon_{fd,e}$	design value of effective FRP strain
ε_{s2}	compressive steel strain
θ	angle of diagonal crack with respect to the member axis
τ_f	interfacial shear stress at failure
τ_{max}	maximum interfacial shear stress
φ_f	additional FRP strength-reduction factor
λ	a factor depends on δ_f, τ_f, elastic modulus of FRP and thickness of FRP

CHAPTER 1

1 Introduction

1.1 Background

Reinforced concrete structures often require some improvements in them during their service lives. Increasing their load carrying capacity, recovering structural damages and extending their service lives are the intentions for structural repair. The improvement done in reinforced concrete structures are categorized into two main types namely repair (retrofit) and strengthening (upgrading). Measures taken to recover the structural damages and restore the functionality are known as repair. Strengthening or upgrading means the improvements done in undamaged structures.

Structures undergo certain deficiencies which reduces its ability to carry the original design loads. Deterioration (corrosion of steel reinforcement and loss of concrete section), structural damage (vehicular impact, excessive wear, excessive loading and fire), or errors in the original design or construction (misplaced or missing reinforcing steel and inadequate concrete strength) are some examples for structural deficiencies. Impacts of these deficiencies are recovered by retrofitting structural elements.

Upgrading ability of structural elements to safely resist flexure, shear, torsion and axial loads or any other action is called structural strengthening. Strengthening is accomplished by either reducing the magnitude of these forces or by enhancing the member's resistance to them.

There are many situations that additional strength becomes essential to a structure.

When the use of structure is changed, it may require a higher load carrying capacity. This situation may also occur if additional mechanical equipment, filing systems, industrial plants or other items is being added to the structure. To withstand this new condition a structure requires strengthening.

It may need the structure to resist loads that were not anticipated in the original design. This includes loads resulting from wind and seismic forces or load blasting. To improve resistivity to these forces structural strengthening is required.

Strengthening systems can improve the resistance of the existing structure to internal forces in either active or passive manner. Passive strengthening systems engage only when additional loads are applied to the structure rather than those existing at the time of installation. Bonding steel plates or Fiber reinforced polymer (FRP) composites on the structural members are belonging to passive strengthening. Active strengthening systems engage instantaneously and may be accomplished by introducing external forces to the member that counteract the effect of external forces. As examples, external post tensioning systems or jacketing the members are used to relieve or transfer existing loads.

1.2 Available techniques of strengthening concrete structures

There are many techniques used to upgrade concrete structures. Concrete jacketing, steel jacketing, precast concrete jacketing, prestressed concrete jacketing and application of composite materials are some of the existing strengthening techniques. Structures such as historical buildings, bridges and buildings located in earthquake prone areas are improved with these techniques in order to achieve better performance in them.

1.2.1 Concrete Jacketing

This involves addition of a thick reinforced concrete layer in a form of a jacket. Longitudinal bars and transverse ties are used as reinforcement. Strength gaining is done by additional concrete and reinforcement. The minimum allowable thickness of a jacket is 100 mm. This method is mostly used for columns in existing structures. Construction of a concrete jacket for a wall is shown in Figure 1.1.

There are some drawbacks in the method as well. Huge dead mass is added to the structure due to the new concrete jacket. Sizes of the sections are increased and thus free available usable space is reduced. Stiffness of the building is highly increased. Adequate dowelling is provided for the existing columns. Longitudinal bars are anchored to the foundation. Longitudinal bars should be continuous through slabs as well. It requires drilling of holes in existing columns, beams, slabs and footings. It is not practically feasible to place tie bars at beam column joints. As a whole, the speed of implementation is very low. Larger amount of surface preparation is required.

Figure 1.1: Concrete jacketing (Hamara Kuwait commercial division,
Viewed December 21 2014)

Therefore, concrete jacketing cannot be named as a good strengthening method for concrete structures.

1.2.2   Steel Jacketing

This involves enhancing existing RC elements with steel plates (Figure 1.2). Steel plates are used to strengthen RC elements in order to control flexural deformations and crack widths, and increase load carrying capacity of the member under service load for ultimate conditions. The gap between plate and the element is filled with a non shrink grout. It provides passive confinement to concrete core. Thickness of grout is about 25mm. Cylindrical steel jackets are used in circular columns. However rectangular steel jackets for rectangular columns are not recommended. They should be strengthened with elliptical jackets. In that case high amount of grout filling is required.

Although this method was recognized to be an effective, convenient and economic method for strengthening structures, there are some drawbacks in the technique in practice. Resistance provided in axial and hoop direction in steel jacketing cannot be optimized. Steel take large portion of axial load due to its high Young's modulus. Sometimes it may result premature buckling of the steel. This may cause the steel plates to be detached from the element and fail the system.

Steel is not protected as much as internal reinforcement. Thus the steel jacket is vulnerable to corrosion. It could adversely affect the bond strength and since it may lead to failure of strengthening system. Due to effect of corrosion and impact with floating materials, it cannot be used for columns in water such as river and oceans. This effect can be controlled through careful surface preparation, storage and application of resisting priming systems.

Figure 1.2: Steel jacketing (Reinforced concrete buildings, Viewed December 28 2014.)

Weight adding and size increment is considerably high, especially for rectangular columns. This may cause the structure to be distorted.

Installation of steel plates in site is not an easy task because of difficulty to shape in order to fit complex profiles, their higher weight, and requirement of expensive false work during bonding. Generally the available plate lengths remain between 6 m and 8 m. Since the spans of structural elements are usually longer than that of plates, the

system requires joints. Large amount of drilling is required in this method and it has complicated the installation process.

Therefore the method is considered as time consuming and labour intensive.

1.2.3 Precast concrete Jacketing

In this method new longitudinal reinforcement is set around the existing column and pre cast concrete segments are set around the new reinforcement. Then all segments are tied together by strands. Non shrinkage mortar is injected between the existing concrete and pre caste concrete segments. Pre stressed force is then introduced in the strands to assure the contact of the segments.

Figure 1.3: Precast concrete jacketing (Dash 2009)

It helps in faster construction than concrete jacketing and steel jacketing. Figure 1.3 shows a picture of precast concrete jacketing.

1.2.4 Pre-stressed concrete Jacketing

Existing columns are pre-stressed by external strands to provide active confinement. Installation of such a system can be less disturbing to the building occupants. The technique is very recently developed and on-site implementation is not known yet. Shear strength increase is only due to increase in concrete strength against the jacketing where the jacket contributes significantly towards shear strength.

It does not increase weight of the structure. Size is increased only by 5mm. Surface preparation required is very low. Thus it is an efficient method and it can be more economical than steel jacketing.

1.2.5 Externally applied Pre-stressed steel

Figure 1.4: Strengthening of a rectangular column with
pre-stressed steel (Yarandi et al 2004)

Structures which the appearance does not important, can be retrofitted using external pre-stressed steel. Usually, bridge decks, tunnels and beams are strengthened with this method. The external reinforcement is applied along the longitudinal direction and pre-stressed in order to close existing cracks while providing additional compression capacity to the member (Figure 1.4). A higher efficiency is achieved with special profiles of reinforcement.

Apart from that columns and other exposed elements are also strengthened in urgent situations such as seismic damage (Miyagi et al 2004). In that case, the steel is used in transverse direction of the column. They are supposed to provide a better confinement to the element and bare the axial load transferred from upper floors. This technique is more beneficial due to advantages like active confinement as well as passive confinement and shear capacity (Miyagi et al 2004). However the appearance and disturbance at the implementation limit the applicability of the technique.

1.2.6 External strengthening using composite materials

With the invention of composite materials, they become a very good alternative to steel jacketing and pre-stressed steel. Avoiding the problem of corrosion of steel is the main advantage with this technique. Although the high strength composite materials are very expensive compared to steel, positive features like light weight, easy handling in construction sites, reduction of labor cost and less disturbance to existing functions can compensate the effect of cost (David et. al. 1998).

1.2.6.1 External strengthening using FRP

FRP stands for fiber reinforced polymer. It is a composite made of high strength fiber and an adhesive compound. Commonly used fiber types are, Aramid, Carbon and Glass. Basalt fibers are also used in civil engineering industry. Epoxy resin is the mostly used adhesive. Cement-based bonding materials are also used. The epoxy adhesive and the fiber becomes a plastic composite on the concrete surface. Then the old structure and the newly bonded material create a structural relationship that has a greater strength than the original structure.

FRP is a high strength, low weight material. It was originally developed for aircrafts, ships and high-speed trains.

1.2.6.2 Usage of FRP's in Civil Engineering Structures

Since 1980s, FRP has used to strengthen civil engineering structures (Sveinsdottir 2012). FRP strengthening technique is suitable for structural repair and retrofitting of existing structures that are facing durability problems, such as environmental factors, increased load and corrosion. FRP is more beneficial due to its features like high durability, low thermal expansion, good fatigue performance, damage tolerance, non-magnetic properties and environment resistivity. FRP is available in the forms of sheets, bars and mesh. Commonly used type in civil engineering structures is sheets. FRP sheets are available in different shapes, surface texture and configurations. Due to the flexible nature of FRP sheets they are found to be a good retrofitting alternative for concrete structures in earthquake areas as well as in the normal applications.

Research studies that have been conducted on flexural strengthening of reinforced concrete structures indicated a significant strength increment with use of CFRP sheets as an external reinforcement (Shahawy *et al* 1995). It also improves serviceability of structures (Chaallal, Nollet and Perration 1998). Failure of a CFRP strengthened beam can be due to flexure, shear or de-bonding. To improve the serviceability of a structure, it should be made sure that either the failure of the beam is not due to shear or failure is more ductile. Flexural failure of un-strengthened RC beams is normally ductile. Failure of FRP strengthened beams in flexure is observed to be similar to the failure mode of normal RC beam (Mohamed 2002). Therefore flexural failure is more preferred in structural elements.

1.3   Problem statement

1.3.1   Failure modes

Failure modes of beams with FRP external reinforcement in flexure can be categorized in to two main types; (a) classical failure and (b) premature failure (Chaallal, Nollet and Perration 1998). Failure of an element due to failure of steel bars, tensile failure of FRP sheets or crushing of concrete in compression zone is known as classical failure. When classical failure occurs, the strengthened system has achieved its ultimate capacity. Failure of the element in any method other than classical failure modes is known as premature failure. As indicated by the name, this mode of failure occurs before achieving full capacity of the system. Failure modes such as de-bonding of FRP, peeling off of FRP and concrete cover separation are under premature failure. Premature failure is the mostly experienced mode of failure and among the sub methods. FRP de-bonding is the most common failure mode which has been observed in practice (Xiong, et. al., 2007, Wu, et al., 2011).

1.3.2   De-bonding failure

This mode of failure limits the capacity to 60% to 80% of ultimate capacity of the system (Mostofinejad and Moghaddas, 2014). Another drawback of de-bonding failure is that it causes a sudden failure which does not give any prior warning. It affects the safety of strengthened buildings. Ultimately the system becomes an ineffective way

of usage of FRP materials due to de-bonding. Therefore de bonding is a critical issue which should be avoided in the strengthened systems.

1.3.3   De-bonding Delaying

End debonding is very critical when compared with other debonding failures. Different methods have been proposed in literature to delay end de-bonding. These methods are divided in to four main categories depending on the mechanics used to delay de-bonding. They are (a) Mechanical fasteners, (b) FRP pin and pan shape anchors, (c) Near Surface Mount reinforcement and (d) End wrap (Wu, et al. 2011). Mechanical fasteners are based on exerting a lateral pressure on the FRP layer towards the concrete surface. Then FRP/Concrete interfacial friction is increased and higher energy is required to initiate de-bonding. As far as pin and pan shape anchors are concerned, fibres in the pan acts like tensile members and transfer peeling stresses to the pin shaped portion. Thus de-bonding is delayed by reducing peeling stresses in the FRP strip. Near surface mount reinforced systems prevent de-bonding by increasing the bonded area. FRP strips are immersed in to groves in this method and thus the bonded area for a certain length of the FRP material is almost three times as normal situation. End wraps can distribute stresses concentrated at the edges of CFRP strips and transfer them to concrete element (Sawada et al. 2003). Then failure mode can be shifted from de-bonding to a classical failure mode (Kalfat et al. 2011).

The use of wire mesh–epoxy composite constitutes a new technique to significantly enhance the performance of concrete in flexure. The wire mesh absorbs energy stored in the FRP sheet due to loading. Therefore the failure load can be increased (Qeshta et al. 2014, Srisangeerthanan 2013).

All the five techniques mentioned above are good methods of delaying de-bonding. However end wraps have more advantages over the other three methods. According to Spadea et al. (2001), end wraps are capable of improving ductility of the strengthened element. End wraps also contribute to increase shear capacity of the element. Therefore, investigations on end wraps are much important. However, there

is no proper study carried out to investigate the interaction between resistance to de-bonding and strength gain (Grelle and Sneed 2013).

1.3.4 Design guidelines

As mentioned earlier, de-bonding failure is the most common failure mode that has observed in many applications. There are some efforts taken to overcome the problem. Anchorage using end wraps is found to be a good technique to delay end de-bonding. However this method cannot be extensively used in practice due to lack of design guidelines. Therefore this investigation is objected to figure out the behavior of end anchored flexural elements with CFRP transverse wraps and propose a theoretical model to predict the behavior.

As far as available models are concerned, FIB guidelines have provided different approaches to resist the effect of premature failure on the ultimate capacity. The first method is anchorage verification and FRP strain limitation. It is based on predicting the maximum load that can be resisted by the anchorage zone. The code has proposed to limit the ultimate tensile strain in FRP in to a certain value in order to prevent peeling-off. Then, the required anchorage length (Equation 1.1) and the maximum force that can be resisted by the anchorage zone are verified (Equation 1.2). The code states that, if the maximum anchorage requirement is provided by any other means of end anchorage, the bonded length can be reduced and anchored force can be improved.

$$l_{b,max} = \sqrt{\frac{E_f t_f}{c_2 f_{ctm}}}$$ ....Equation 1.1

$$N_{fa,max} = \alpha c_1 k_c k_b b \sqrt{E_f t_f f_{ctm}}$$ ....Equation 1.2

The second approach is calculation of the envelope line of tensile stress. In this calculation, the maximum possible increases in tensile stress within the externally bonded reinforcement (EBR), which can be transferred by means of bond stresses between two subsequent flexural cracks, are calculated. When the tensile stress in the EBR exceeds the value that can be transferred by bond stresses, debonding and peeling-off is predicted to be initiated at flexural cracks.

Third method is verification of anchorage and of force transfer between FRP and concrete. It first determines the anchorage and the limits the interfacial shear stresses in order to prevent debonding.

ACI guidelines have also provided a multiplication factor to the ultimate strain in FRP, in order to prevent debonding. In addition to that the code has specified an anchorage length of 150 mm extending from the point where existing moment equals to cracking moment. Apart from that, there is no any detailed calculation has provided to address the anchorage effect in flexural reinforcement. The flexural capacity depends on material properties and cross section of the element. Equation 1.3 shows the expression for flexural capacity as per ACI. Anchorage length is only specified for transverse end wraps in shear strengthening. For end wraps, active bond length is given by Equation 1.4. The guidelines also specify that, edges of flexural FRP reinforcement should be anchored with transverse wraps when the required anchorage length cannot be satisfied.

$$M_n = A_s f_s \left(d - \frac{\beta_1 c}{2}\right) + \varphi_f A_f f_{fe} \left(h - \frac{\beta_1 c}{2}\right) \dots\dots\dots\dots \text{Equation 1.3}$$

$$L_e = \frac{23,300}{(n t_f E_f)^{0.58}} \dots\dots\dots\dots\dots\dots\dots\dots\dots\dots\dots \text{Equation 1.4}$$

The above two approaches are strength based approaches. However energy based approaches has also been suggested by different authors to predict flexural capacities of the systems. According to Chen, et al. (2012), interfacial fracture energy can be expressed as in Equation 1.5, assuming a linear bond slip model. He has conducted pullout tests for FRP U-wraps in shear. The tensile force that can be resisted by the bond is as in Equation 1.6 (Chen, et al. 2012). Effective bond length is derived by Equation 1.7 in the same study.

$$G_f = \tau_{max} \delta_f / 2 \dots\dots\dots\dots\dots\dots\dots\dots\dots\dots \text{Equation 1.5}$$

$$P = {\tau_f b_f}/{\lambda} \dots\dots\dots\dots\dots\dots\dots\dots\dots\dots\dots \text{Equation 1.6}$$

$$a_u = \frac{\pi}{2\lambda} \dots\dots\dots\dots\dots\dots\dots\dots\dots\dots\dots\dots \text{Equation 1.7}$$

However when end anchorage is provided, the system may carry higher load than what is predicted in the above mentioned equations. At the same time, required

anchorage length may also reduce. Therefore, design equations should be generated to represent the behaviour of end anchored flexural elements.

1.4   Scope of the study

This study is carried out to investigate the behaviour of beam elements, flexural strengthened with externally bonded CFRP reinforcement and end anchored at FRP end-wraps. Since the inclined wraps can contribute to shear capacity of the system and thus more effective, end wraps are applied perpendicular to the predicted path of shear crack.

Main objective of this investigation is to contribute to the knowledge area by developing a theoretical model to predict behaviour of end anchored, flexural strengthened beams. After conducting the experimental program, the behaviour can be closely scrutinized and the effects of end wraps can be recognized. As the outcomes of experimental and theoretical study, a new theoretical model and guidelines can be proposed. It is then being validated with the experimental results available in literature. Ultimately, author's aim here is to propose a theoretical model which can predict the behaviour of flexural strengthened and end anchored beams accurately and utilize it as a design guideline.

Another objective of this research is to study the stress distribution throughout flexural FRP sheet and in anchors. It is helpful to verify the stress transfer mechanism in the system. Then interaction between anchorage length and strength gain can be studied. Based on these observations, further improvements can also be proposed to the system.

Apart from the above mentioned objectives, there is a set of sub objectives which is to be achieved in this study.

1.5.1 Sub objectives

> ➢ To gather knowledge on FRP composites and their applications in the industry
> ➢ To study the interaction between increment of flexural capacity of concrete beams with end anchorage

- ➢ To develop a theoretical model, that can be utilized for further studies in the research area.
- ➢ To propose design guidelines for FRP strengthened and end anchored beams

1.5 Methodology

A literature survey was conducted, to get knowledge about the research area. After getting a sound knowledge, the reading topics were narrowed down in order to identify a research gap. Once the research gap was identified, the methodology was developed considering the availability of resources, objectives of the study and time frame.

Of the developed methodology, there are two main sections namely; experimental program and theoretical study. Experimental program is the main section of the research program. Scaled down physical models are made for the experiments. A new model is proposed based on the observations of experimental investigation. The experimental results are utilized to validate the model. Then the theoretical model is applied to further specimens taken from literature. The predictions and experimental results are compared in order to prove the validity of the proposed model.

Need of theoretical models in this research program is to develop design guidelines. First of all, behaviours of test specimens are predicted with the available theoretical models. New guidelines or modifications can be proposed based on the outcome of theoretical study.

After all the sections are completed, final conclusions and recommendations are made. As the ultimate goal, the work will be published in a journal or a conference in order to make a contribution to the research area.

```
                    ┌─────────────────────┐
                    │  Literature review  │
                    └──────────┬──────────┘
                               │
                               ▼
                    ┌─────────────────────┐
                    │ Identify research gap│
                    └──────────┬──────────┘
                               │
              ┌────────────────┴────────────────┐
              ▼                                  ▼
    ┌─────────────────────┐          ┌─────────────────────┐
    │ Experimental program│          │   Theoretical study │
    └──────────┬──────────┘          └──────────┬──────────┘
               │                                 │
               │                                 ▼
               │                      ┌─────────────────────┐
               │                      │ Study      proposed │
               │                      │ Theoretical Models  │
               │                      └──────────┬──────────┘
               │                                 │
               ▼                                 ▼
    ┌─────────────────────┐          ┌─────────────────────┐
    │ Testing and Results │          │   Predict Results   │
    └──────────┬──────────┘          └──────────┬──────────┘
               └────────────────┬───────────────┘
                                ▼
                     ┌─────────────────────┐
                     │   Compare results   │
                     └──────────┬──────────┘
                                ▼
                     ┌─────────────────────┐
                     │  Propose Guidelines │
                     └──────────┬──────────┘
                                ▼
            ┌──────────────────────────────────────┐
            │   Conclusions and Recommendations     │
            └──────────────────────────────────────┘
```
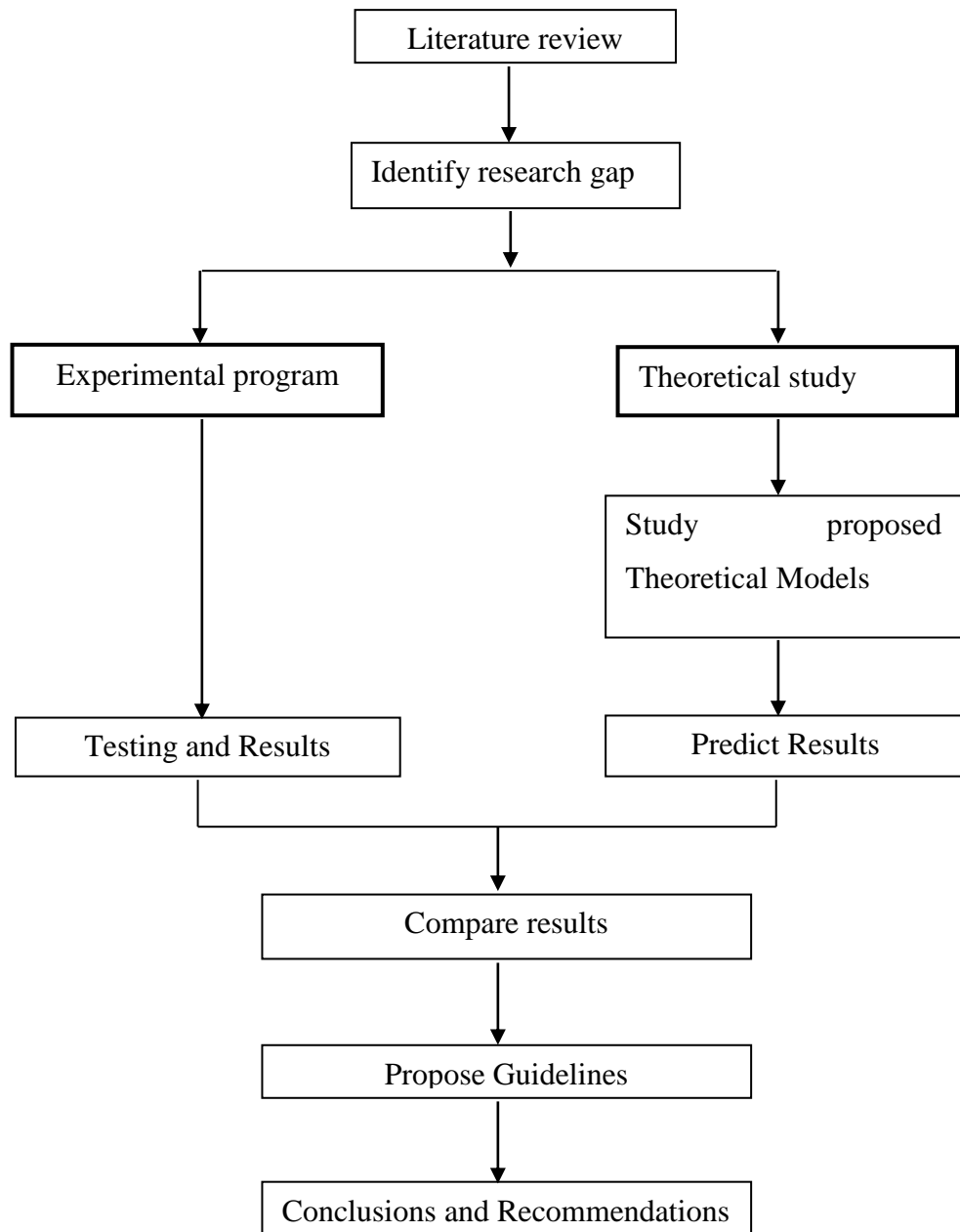
Figure 1.5: Methodology flow chart

1.6   Dissertation outline

Chapter 1   Presents the background and the research gap. It also describes
Introduction   the scope of the study, research methodology, main results
                       included and outline of the theses.

Chapter 2   An extensive literature review starting from the history of FRP

Literature review	application technique to the present stage of the industry is included. The review then describes another axis of literature beginning from material behavior up to composite behavior of flexural strengthened and end anchored beam elements. Finally it addresses the research needs concluding the review.
Chapter 3 **Experimental investigation**	Core of the study is presented here. The test program, observed parameters and the adopted testing procedure are described clearly with the aid of sketches and photographs. Outcomes of the experimental program are described in this chapter. Discussions on the experimental behaviors and analysis of results are also included.
Chapter 4 **Theoretical study**	In this study, an effort was taken to identify the parameters affecting to strength gain of end anchored, flexural strengthened beams and developed a relationship among them. In order to initiate the model, available design equations proposed by several authors were assessed.
Chapter 5 **Proposed theoretical model**	A theoretical model was proposed to predict the behavior of beams flexural strengthened with CFRP sheets and end anchored with CFRP wraps. The model was validated with experimental results of current study and results of five other studies. The proposed model, a design example and model validation, are presented in this chapter.
Chapter 6 **Conclusions and recommendations**	This chapter gives a summary of the study. It also recommends potential future research works which are related to current study.

1.7 Conclusions

Improvements done in the structures of existing buildings are mainly in two types; repair and strengthening. Repair means recovering the deficiencies occur in structures due to seismic loads, vehicular impacts, fire etc. Strengthening is upgrading structures to withstand the effects of increased in loading, poor material quality, design, computation or construction faults.

There are many techniques available to rehabilitate the structures as well as upgrade existing structures. Concrete jacketing, steel jacketing, precast concrete jacketing, prestressed concrete jacketing, externally applied prestressed steel and external strengthening with composite materials are some of them.

Strengthening using fibre reinforced polymer composites has been very popular method of retrofitting structures. It has extensive material properties such as light weight, high tensile strength, high elastic modulus, corrosion resistance etc. Therefore FRP strengthening has become a widely using strengthening technique in civil engineering industry, compared to other strengthening techniques. However, it has been difficult to achieve full capacity increment of the strengthened element due to premature failure. FRP debonding, concrete cover separation and peeling off of FRP are all belong to premature failure modes.

Several remedies have been proposed to overcome the premature failure. They can be divided in to five main categories, namely; mechanical fasteners, FRP pin and pan shape anchors, near surface mount reinforcement, FRP end wraps and application of mesh between FRP and concrete surfaces. Among the five, FRP end wraps are found to be more advantages because they can contribute to shear capacity whereas any of the other four, cannot improve the shear capacity.

Although there are very good techniques have been proposed to delay end debonding, the design codes do not provide any guidelines to predict the behaviour of strengthening system consist of end anchorage. Therefore current study is aimed to investigate the interaction between amount of end anchorage and strength gain of beams flexural strengthened with externally bonded CFRP and anchored with CFRP end wraps.

CHAPTER 2

2 Literature Review

2.1 Introduction

External strengthening of structures using FRPs is a popular technique in whole world. However detail design guide lines for this technique are still at a developing stage. There are many research works going on regarding the topic worldwide. An extensive review on research work carried out to investigate de-bonding failure of CFRP/ concrete interface is presented in this chapter.

2.2 Strengthening of structures

The aim of strengthening is to improve load carrying capacity of the whole structure or some of the structural elements. It can address issues such as increased traffic load in bridges, service load increments in buildings, weakening due to inadequate maintenance, damage due to seismic loads, defects in design or construction etc. A wide variety of structures all over the world namely; bridge decks, beams, girders and columns, buildings, parking structures and tunnels have been treated for above mentioned issues and are being utilized safely.

There are lots of advantages of strengthening; no cost of demolition, less waste products, no cost of rebuilt, less time consuming, better option for buildings in congested areas and structures with historic value can be protected. In contrast, most of strengthening techniques may cause reduction of working space in the building due to increased sizes of elements. Since working space is more important factor for buildings, rebuilding of structures was selected over rehabilitation regardless of all the advantages of strengthening. However renewal of structures is now becoming popular throughout the world and efforts are always taken to improve retrofitting techniques.

2.3 History of usage of FRPs for structural strengthening

In early reinforced concrete designs the structures were supposed to have very long life time. However with the development of industry and transportation, the atmosphere got polluted gradually. This situation badly affects the durability of

concrete due to corrosion of steel reinforcement. Since then, engineers concern more about using non-metallic reinforcement in concrete structures.

Idea of Glass Fibre Reinforced Polymer (GFRP) reinforcement instead of steel reinforcement in concrete structures has already appeared in the 1950s (Rubinsky 1959). The idea immersed again in the 1970s, in Germany, Japan and some other countries. In 1980s glass fibre reinforced polymer reinforcement has used in several bridges in the countries such as Sweden, Soviet Union, Japan and USA. As a result of experimental work done in 1980s Aramid and Carbon fibre were developed. At the beginning they were only used to military purposes and aerospace researches due to their high price. The product spread in civil aircraft, helicopters, spacecrafts, satellites, ships, submarines, automobiles, electronics, chemical processing equipment and sport equipment applications with the gradual reduction of price.

Concept of usage of FRPs for construction purposes runs back to 1930s. It took about 50 years to convert the idea to a real application. A direct application of FRPs for strengthening of a civil engineering structure has been recorded only after early 1980s (Sveinsdottir 2012). In 1981 Fardis and Khalili have used FRP systems as an additional reinforcement for reinforced concrete columns which can improve confinement. A similar kind of study has been carried out in 1987 by Katsumata et al. In the same year Meier and Rostasy (1995) have used externally bonded FRP to a reinforced concrete bridge to increase flexure. Since then FRP has used to strengthen civil engineering structures for structural repair and retrofitting of existing structures that are facing durability problems, such as environmental factors, increased load and corrosion.

2.4   Present applications of CFRP

At present strengthening using FRP is much popular. It is now applied for steel, masonry and timber structures apart from concrete structures. There are also wide variety of FRP products, namely FRP bars, sheets, strips and plates. At the same time FRP products are used for variety of structural purposes. Figure 2.1 presents how FRPs are applied for flexure, shear, confinement etc.
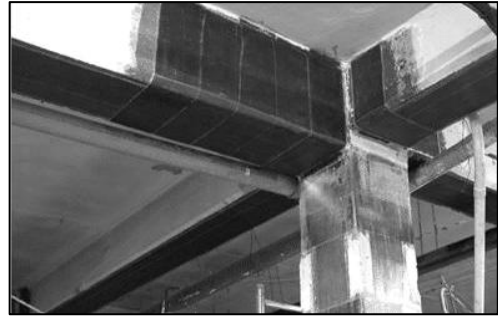
<div align="center">(a)</div> <div align="center">(b)</div>
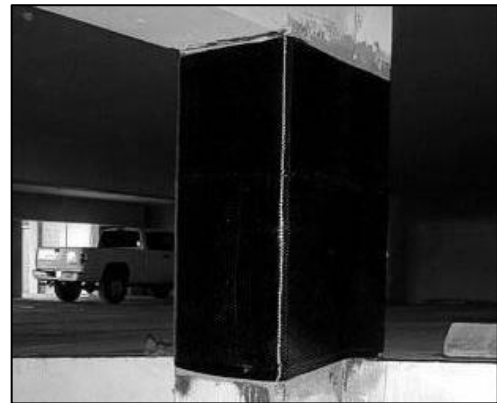
<div align="center">(c)</div> <div align="center">(d)</div>

Figure 2.1: Applications of FRP (a) Flexural strengthening of slab (civil construction retrofitting, n.d.), (b) Flexural strengthening of beam (Carbon Fibre Strengthening, n.d.), (c) Shear strengthening of beam (Structural Retrofit, June 2011), (d) Confining of column (Structural Retrofit, June 2011)

Research works and practical applications of FRPs are now being carried out all over the world. Development of design guidelines for industrial purposes of the technique is ongoing in different countries such as Europe (FIB), Japan (JCI), Canada (CSA) and United states (ACI).

2.5 Material behaviour

A reinforced concrete element with FRP external strengthening is a composite system of four major components. They are; concrete, reinforcing steel, FRP and adhesive. Each of these materials has different stress-strain diagrams. Therefore when they act as a composite, the behaviour will be highly nonlinear. Analyzing of

this complicated behaviour is challenging and understanding each component separately is important. This section describes the behaviour of each material of the composite separately.

2.2.1 FRP / Concrete composite

The basic theory behind FRP strengthening is providing additional tensile reinforcement to structural element. The composite action of existed element and externally added reinforcement will change the element's behaviour. There are three main materials which contribute to structural behaviour of the composite; concrete, steel and FRP. In a strengthened system, both fibre and steel carry tension and concrete bare compression. Stress distribution over the cross section of a flexural strengthened concrete element is shown in Figure 2.2.

In an un-strengthened element, steel reinforcement is the only material which carries tension. Once it is strengthened, fibres too contribute to tension capacity. Since FRP has very high tensile capacity, neutral axis goes down while increasing the contribution of concrete in compression, in order to comply with increased tensile capacity. Therefore flexural capacity of the element increases significantly. If the composite action is well established in the system the element can be loaded up to the limit of shear failure, FRP rupture or concrete crushing. Furthermore, achievable strength gains depend highly on the adhesive substance used, as well. The adhesive helps to bind the composite to the concrete substrate and acts as a shear load path between the two surfaces.
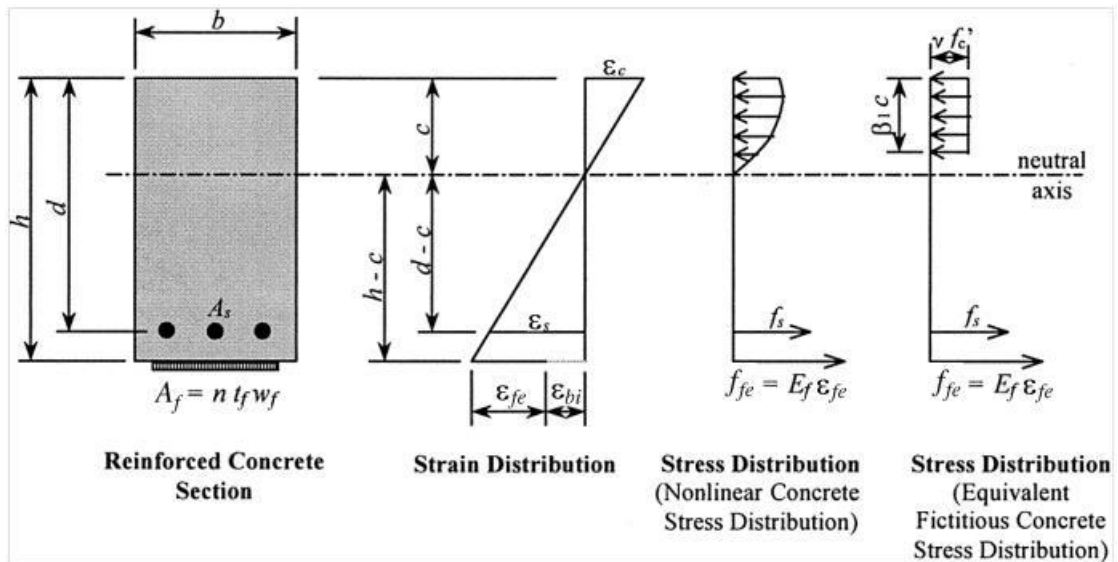
Figure 2.2 Internal strain and stress distribution for a rectangular section under flexure at ultimate stage (ACI 440.2R-02)

2.5.1 Concrete

Concrete is the most common construction material all over the world. It is a mix of four ingredients; cement, aggregate, water and admixture. Hydrated cement particles act as a bonding agent between the aggregates and bind them together. After hardening the mix become a strong building construction material; concrete.

Concrete is considered as a homogeneous material. It has a great compression capacity. However its strength in tension is comparatively less. Concrete can be designed to have a range of properties such as characteristic strength, elastic modulus, compressive strength etc. Stress – strain relationship of concrete under compression is shown in Figure 2.3.

As indicated in Figure 2.3 , the initial portion of the stress- strain curve can be considered as linear. The behaviour becomes non linear after that. Therefore calculation of E value is not straightforward. For normal weight concrete, equation for elastic modulus is given in Equation 2.1, (BS 8110: Part I: 1997) where γ_m is the material safety factor and f_{cu} is the concrete cube strength. For concretes up to about 6,000 psi, value of elastic modulus can be approximated as in Equation 2.2, (BS 8110: Part I: 1997), where w is the unit weight (pcf) and f'c is the cylinder strength (psi).

$$E = 5.5\sqrt{\frac{f_{cu}}{\gamma_m}} \quad \text{...Equation 2.1}$$

$$E = 33w^{1.5}\sqrt{f_c'} \quad \text{................................Equation 2.2}$$
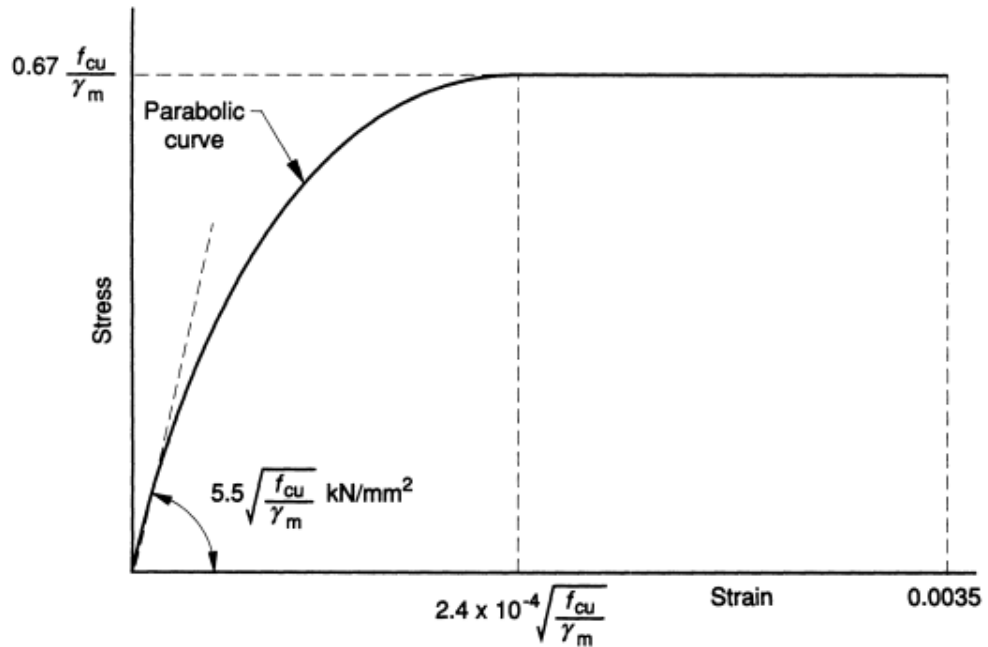
Figure 2.3 : Stress – Strain curve for normal weight concrete (BS 8110)

Tension behaviour of concrete is sketched in Figure 2.4. The ultimate tensile strength is very low compared to ultimate compressive strength. Therefore concrete is considered as a material which has insignificant tension capacity. At the same time it is brittle in tension. When concrete is using as the construction material of flexural member, its tension faces should be reinforced with a material which has higher tensile capacity.
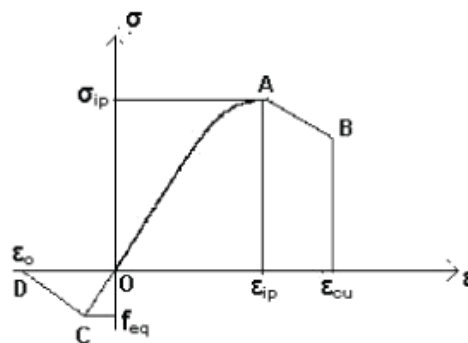
Figure 2.4 : Stress strain curve for concrete (Madureira and Ávila, 2012)

22

2.5.2 Reinforcing steel

Steel is an alloy. Depending on the consistency, different types of steel have different mechanical properties. Parameters such as yield strength, ductility, stiffness, toughness and hardness define the material. As far as the stress strain curve is concerned, the behaviour is linear elastic up to yield stress. The curved portion after yield stress represents the plastic region of steel (Figure 2.5). The point where behaviour changes from elastic to plastic is known as yield strength.

However the behaviour has simplified for the ease of design processes and the graph is shown in Figure 2.6. The simplified behaviour is a bilinear curve with two lines representing elastic region and plastic region.
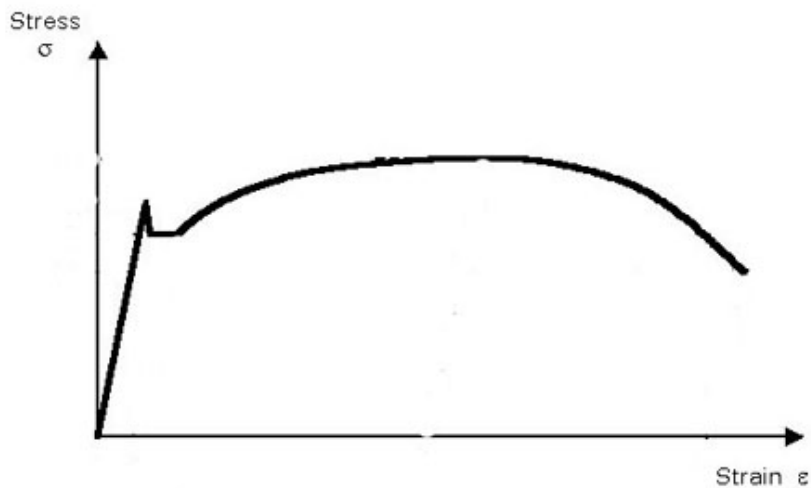
Figure 2.5 : Stress- strain relationship for steel (The mechanical properties of steel, n.d.)
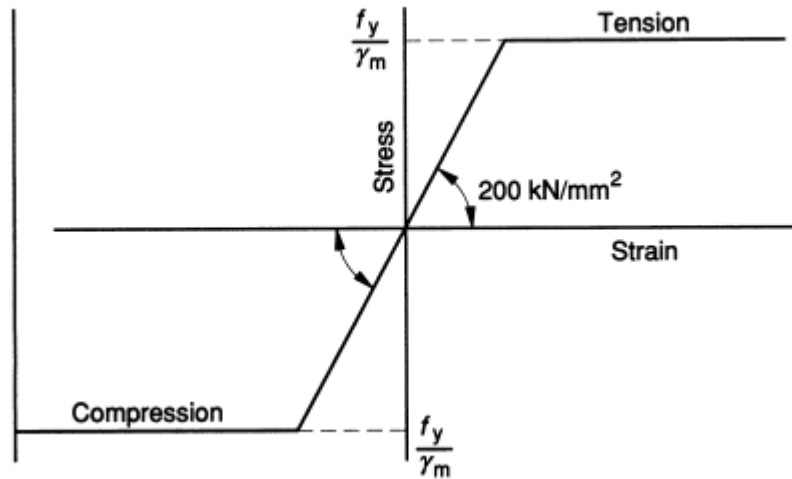
Figure 2.6 : Idealized Stress – Strain curve for steel for design purposes (BS 8110 : Part I: 1997: Clause 2.6.2)

2.5.3 Carbon fibre

The composite, CFRP is made up of carbon fibres and epoxy resin. There are several carbon fibre types. Quality of carbon fibres depends on precursor fibre material and heat treatment temperature. Accordingly a fibre produced by PAN (Pyrolysis of organic precursor fibres) which consumes more energy and more processing time is in good quality than fibres made of coal tar pitch base (Kopeliovich, n.d.). The fibre itself has also a composite structure because not the whole carbon content is present in the form of graphite crystals in the fibre. Graphite fibres are the fibres that have carbon more than 99%. The higher the amount of graphite crystals contains in fibre, the Young's modulus of fibre is also higher (Borosnói, 2002). Usually CFRP materials are made of graphite fibres which have higher strength. Based on final heat treatment temperature, carbon fibres have classified in to three types. They are; Type-I, high-heat-treatment carbon fibres (HTT), Type-II, intermediate-heat-treatment carbon fibres (IHT) and Type-III, low-heat-treatment carbon fibres (LHT). Type-I carbon fibres have high elastic modulus, Type-II carbon fibres have high-strength and Type-III carbon fibres have low modulus and low strength materials.

Carbon fibres have high modulus of elasticity, 200-800 GPa while that in Glass fibre is 70-85 GPa and Aramid fibres is 70-200GPa (Sveinsdottir 2012). The ultimate elongation in carbon fibres is 0.3-2.5% and it is lower than other fibre types. It also

has higher stiffness over the other fibre types. Carbon fibres are resistant to water and to many chemical solutions. They withstand fatigue excellently, do not stress corrode and do not show any creep or relaxation. Carbon fibre is electrically conductive and therefore might give galvanic corrosion in direct contact with steel. (Carolin,2003). A comparison of mechanical properties of each fibre type is tabulated in Table 2.1.

Table 2.1: Materials used as fibres for FRP systems and their properties (Meier 1995)

Criterion	Carbon	Aramid	E-Glass
Tensile Strength [N mm^{-2}]	Very Good [2860]	Very Good [1280]	Very Good [1080]
Compressive Strength [N mm^{-2}]	Very Good [1875]	Inadequate [335]	Good [620]
Modulus of Elasticity [GPa]	Very Good [177]	Good [87]	Adequate [39]
Long Term Behaviour	Very Good	Good	Adequate
Fatigue Behaviour	Excellent	Good	Adequate
Bulk Density [kg m^{-3}]	Good [1600]	Excellent [1380]	Adequate [2100]
Alkaline Resistance	Good	Good	Inadequate
Price	Adequate	Adequate	Very Good

Based on mechanical properties of carbon fibres there are five categories defined. They are; Ultra-high-modulus (UHM), High-modulus (HM), Intermediate-modulus (IM), Low modulus and high-tensile (HT) and Super high-tensile (SHT). Mechanical properties of each fibre type are different and they are shown in the Table 2.2 below.

Table 2.2: Mechanical properties of different carbon fibre types (Sveinsdottir 2012)

Fiber type	Elastic Modulus	Tensile Strength
Ultra-high-modulus (UHM)	540-640GPa	2.6-4.0GPa
High-modulus (HM)	290-330GPa	2.7- 5.4GPa
Intermediate-modulus (IM)	200-350GPa	
Low modulus and high-tensile	< 100GPa	> 3.0Gpa

(HT)		
Super high-tensile (SHT)	230-240	> 4.5Gpa

2.5.4 Fibre reinforced polymer

FRP is a composite consist of fibre and a matrix. The materials used for fibres are generally glass (E-Glass or S-Glass), Aramid or Carbon (low modulus or high modulus) which are commonly known as GRFP, AFRP and CFRP. Mechanical properties of the composite depend on the fibre type, matrix used, amount of fibre and fibre direction (Setunge et al. 2002). Volume or size of the composite may affect the mechanical properties in certain occasions. Since the matrix substance is of considerably low strength to that of the fibres, overall gains are greatly limited to that of the composite strength where it is moderated between the strengths of individual fibres and that of the matrix substance.

Orientation of fibre in the composite can govern the type of application. According to the pattern of woven, the composite can be categorized as unidirectional, bi-directional or multi-directional (Figure 2.7). Unidirectional composites are used for specific strengthening purposes. Multi directional type is mostly used for multipurpose applications.
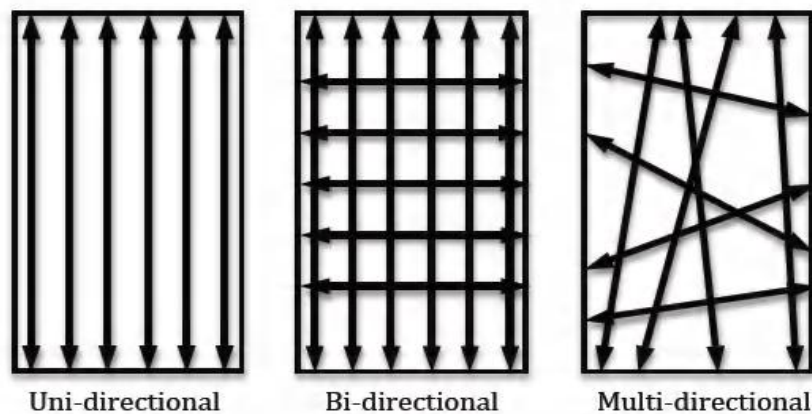
Figure 2.7 : Fibre directions in composite materials (Sveinsdottir 2012)

2.5.4.1 Mechanical properties

CFRP has extensive mechanical properties compared to other reinforcing materials such as steel, GFRP and AFRP. Figure 2.8 shows the stress strain diagram for different reinforcing materials including CFRP. When compared to steel, Young's modulus of CFRP is very high. Uni-axial tensile strength is also very high in CFRP. However CFRP does not give a unique stress strain curve like steel. Its behaviour varies in a range of stress strain relationships, depending on the parameters which defines the composite.
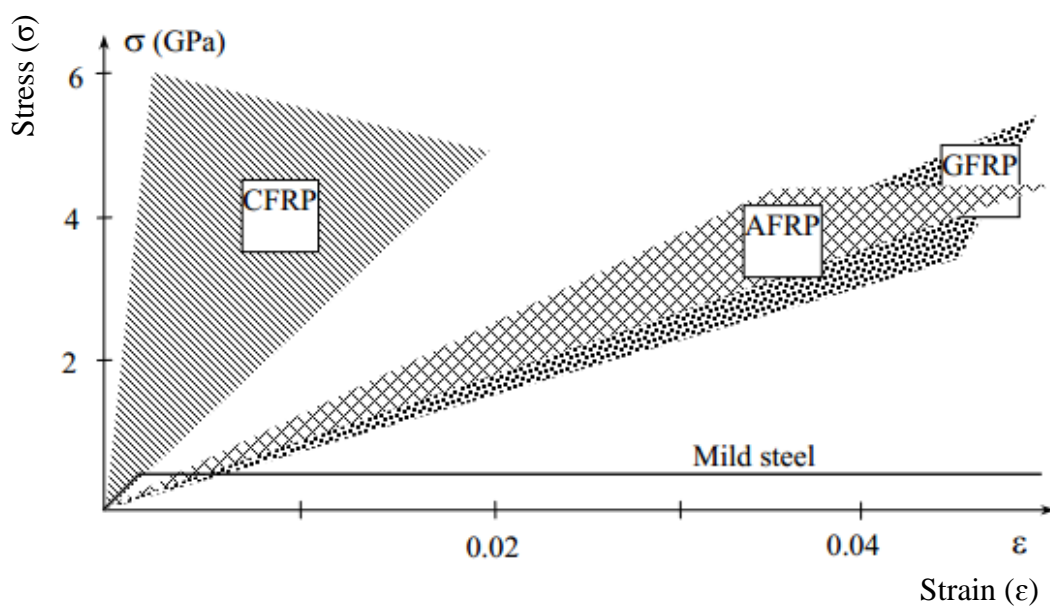
Figure 2.8 : Uni-axial tension stress-strain diagrams for different unidirectional FRPs and steel. (FIB technical report 2001)

CFRP = Carbon FRP, AFRP = Aramid FRP, GFRP = Glass FRP

Mechanical properties of CFRP are described below.

- High Strength to weight ratio
  This is also known as specific strength (Strength to weight ratio of CFRP). FRP composites are light weight and so as CFRP. However their strengths are higher than strength of steel.
- Good Rigidity
  CFRP is high in stiffness than aluminum, pine and other FRP composites such as glass and aramid. For an example, CFRP is four times stiffer than GFRP. (Gite. Suvidha and Margaj 2011)

27

- Corrosion resistant

  If pure carbon fibres directly contact with steel reinforcement, there may be a risk of galvanic corrosion. Since the matrix is intact, there are no problems of contacting with composite and steel.

- Electrically Conductive

  Carbon fibre conductivity can facilitate Galvanic Corrosion which may occur in fittings due to electrical conductivity of carbon fibres. Therefore Careful installation is needed to reduce this problem.

- Good Fatigue Resistance

  Fatigue resistance of CFRP is greatly influenced by orientation of the fibres and the different fibre layer orientation (Sveinsdottir 2012). CFRP has higher fatigue resistance, when cyclic stresses coincide with the fibre orientation. Failure limit also varies with the type of forces applied; tension, compression or shear. However the problem with fatigue failure of carbon fibres is that, they fail without warning.

- Good tensile strength but Brittle

- Fire Resistance/Not flammable

  Polymeric materials can be flammable or can be deteriorated in fire (Borosnyi, 2002). Therefore, in CFRP, the resin determines the fire resistance. Resins may soften, melt or catch fire above 150 to 200 ^{0}C. Fibers themselves are more or less able to resist higher temperatures: aramid to 200 ^{0}C, glass 300 to 500 ^{0}C while carbon up 800 to 1000 ^{0}C (Borosnyi, 2002). Therefore if there is a risk of fire, special protection measures should be taken.

- Low Thermal Conductivity - 24 W/(m.K)

  Steel plates become detached after a matter of minutes of exposure, to high temperatures. CFRP laminates lost its cross sectional area gradually when exposed to a burning at surface. It takes about an hour of time to lose its stiffness and final detachment. This behaviour exists due to its low thermal conductivity. However some forms of CFRP have high thermal conductivity.

- Low coefficient of thermal expansion

  Linear coefficient of thermal expansion is very low or even negative in CFRP in the fibre direction. In uni-directional CFRP, the value varies from minus 1 to +8 Inch / inch degree F. Coefficient of thermal expansion is less than 2 Inch / inch degree F, when carbon fibres are woven.

- Non poisonous
- Biologically inert
- X-Ray Permeable

- Self Lubricating
- Excellent EMI (Electromagnetic Interference) Shielding Property
- Better resistance to moisture, solvents, bases and weak acids
- Durable

  > Durability problem is mostly connected with the matrix. Epoxy, which is the matrix used in CFRP is capable to withstand deterioration in most cases.

When compared with structural steel (Table 2.3), Elastic modulus of FRP is of the same order of magnitude as steel. However tensile strength of CFRP is comparatively very high. As far as strain at failure is concerned, it can be observed that steel can achieve very high strains compared to CFRP. This indicates a brittle failure in CFRP whereas steel undergo a ductile failure.

Table 2.3 : Typical properties of Prefabricated FRP strips and comparison with steel
(FIB technical report 2001)

Material	Elastic modulus (GPa)	Tensile strength (MPa)	Ultimate tensile strain (%)
Prefabricated strips			
Low modulus CFRP strips	170	2800	1.6
High modulus CFRP strips	300	1300	0.5
Structural steel	200	400	25 (Yield strain 0.2)

Even though FRPs have very good mechanical properties, FRP systems have a few adverse properties as well. Unlike steel, FRP does not have a plastic region in its stress strain diagram. Thus FRP strengthened elements fails suddenly without yielding and/or plastic deformation. This behaviour of FRP would not be of any significance, if the failure were due to concrete failure or failure of adhesive. However, ultimate failure of a FRP strengthened system would be at a loss of ductility although it will have an enhanced capacity.

2.5.4.2   Advantages and disadvantages of CFRP strengthening

There are so many advantages of using FRP materials for external strengthening of structures over conventional strengthening techniques like steel plate bonding and concrete jacketing. Although the material properties of FRPs, containing different fibre types vary, there advantages and disadvantages are almost similar.

2.5.4.2.1 Advantages

- The main advantages of FRP materials are their excellent mechanical properties; lightweight, high strength, high stiffness, resistance to corrosion and flexibility.
- The original size, shape and weight of the members are unaltered, thus not attracting higher seismic forces. This feature cannot be achieved in any other jacketing method. Therefore this method is particularly useful for strengthening historic and artistic masonry structures. No change of dimensions is particularly important for bridges and other structures with limited head room and for tunnels.
- No drilling of holes is required as in concrete and steel jacketing.
- The FRPs have extremely good corrosion resistivity. Thus it is highly suitable for marine and coastal environments.
- FRP wraps prevent further deterioration of concrete and inside reinforcement.
- Ease of installation, which is similar to putting up wall papers, makes the use of FRP sheets a very cost-effective and efficient alternative in the strengthening of existing buildings.
- Provides minimal disturbance to existing structure and generally the strengthening work can be performed with normal functioning of structure. Once it has been rolled on carefully to remove entrapped air and excess adhesive it may be left unsupported and no need to damage existing structure to place bolts.
- Simplified installation.
  Fibre composite materials are available in long lengths. Thus there is no need of laps and joints. The material can take up irregularities of the shape of existing surface. It can follow curved profile and can be readily used behind existing services. Overlapping is required only when strengthening in to two directions and it is not a problem because material is thin.
- FRP is a durable material and requires minimal maintenance. If damaged in service, it is simple to repair it by adding an additional layer.
- There is less environmental impact of FRP materials. Energy required to produce FRP materials is less than that for conventional materials. Because of their light weight, energy required to transportation is also less.

When comparing with steel, the FRP materials have extensive mechanical properties. Ultimate strength of CFRP is 2-3 times greater than tensile strength of steel. Density of FRP materials is very low comparing with steel. Therefore obviously, the specific weight or the strength to weight ratio of CFRP is superior to steel. Handling and installation of FRP materials is very easy whereas using steel requires heavy machineries, high amount of labour and significant time. Steel is highly corrosive. However FRP materials do not corrode and they can protect steel from corrosion as well. FRPs Requires little maintenance, they have excellent durability and good flexibility whereas steel is wise versa.

2.5.4.2.2 Disadvantages

- High cost.
  Fibre composites are between 4-20 times as expensive as steel in terms of unit weight. Although the material cost is high, the cost of overall strengthening exercise is less than that of steel plate bonding in certain cases.
- Risk of fire or accidental damage unless the FRPs are protected.
  Damage to the plate strengthening material only reduces the overall factor of safety and it is unlikely to lead to collapse.
- Experience of long term durability is not yet available.
  This can be a disadvantage for structures expecting very long service life. However they can be overcome by appropriate monitoring.
- Low modulus of elasticity.
- The transverse strength is low.
- Require experienced and qualified staff and it is hard to find them in the industry.
- Lack of accepted design standards.
- Non plastic behaviour. Thus CFRPs undergo a sudden failure.
- Susceptibility to stress-rupture.

2.5.5 Adhesive

Adhesive is used to connect two materials each other so that full composite action can be developed among them. It glues the two materials together and provides a load path between those two materials (Sveinsdóttir, 2012). It also affects the mechanical properties of composite in transverse direction to the fibres. An adhesive should meet certain requirements like high elastic modulus, high strength, bond quality, workability and durability. Thus it should exhibit certain properties; low

creep, thermal stability, resistance to moisture, alkaline nature and fire resistivity. Most widely used structural adhesives are epoxies. Their properties like high surface activity, high cohesion and adhesion, low shrinkage and low creep are very beneficial for the structural industry. However they have three major disadvantages; high cost, long curing time and lower resistance to fire.

Cement based material can also be used as an adhesive. They provide strong bond, good workability, better fire resistance to the composite and low health hazards in the installation phase (Dawood and Rizkalla 2008). As shown in Table 2.4 epoxy resins have more desirable properties than polyester resin.

Table 2.4 : Mechanical properties of adhesives (Borosnyi, 2002)

	Polyester resin	Epoxy resin
Tensile strength (MPa)	450-800	600-800
Elastic modulus (GPa)	20-30	30-40

2.6 Application techniques

Selection of a proper application technique is very important to possess the properties of the system. There are three modes of application and it has categorized as in Figure 2.9.
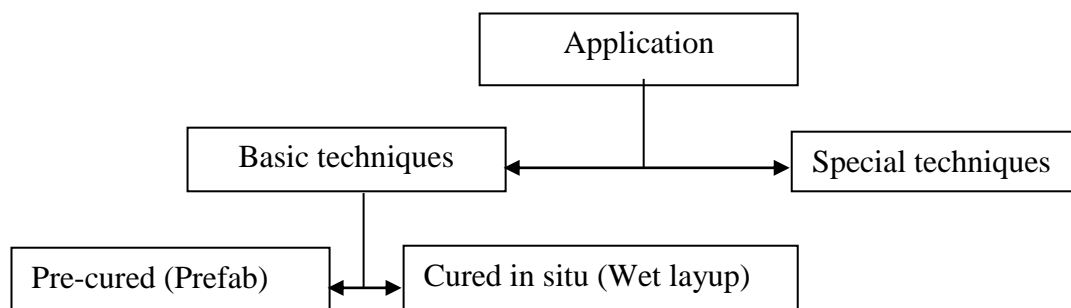
Figure 2.9: FRP application techniques

2.6.1 Basic techniques

This is the most widely used application technique. It involves manual application of FRPs; wet lay up or pre-fabricated systems. As per the ACI Committee 440 (2002) design guidelines, wet layup system is the most general form, where dry fibre sheets

or fabrics are bonded to concrete substrate and cured at site. In this method, application of adhesive is required to both bind the sheet to the concrete and to impregnate the sheet. Thus, low viscosity resins are used. FRP products with thickness of 0.1mm to 0.5mm are suitable to this method. The other method of basic application technique is pre-cured system. It is also known as Prepreg system or Prefab system. Prepreg systems may contain either unidirectional or multidirectional FRP sheets or fabrics which are converted to strips or laminates by pre-impregnating with a saturating resin. Thicknesses of FRPs are within the range of 1 mm to 1.5 mm. At the site, FRP is directly applied on to the concrete surface without any additional application of a saturant. It is then cured on site. The precured systems have pre cured fibres and are generally bonded with an adhesive inclusive of a primer and putty.

2.6.2 Special techniques

Special techniques are the methods of application using machineries. Some of the special techniques are, automated wrapping, pre-stressed FRP, Fusion-bonded pin-loaded straps, In-situ fast curing using heating device, Prefabricated shapes, CFRP inside slits and FRP impregnation by vacuum (FIB technical report 2001). Quality controlling is very easy with this type of methods.

2.7 Failure mechanisms

Various experiments have shown that, flexural strength of reinforced concrete structures can be enhanced up to a significant level by using CFRP sheets as an external reinforcement. It also improves serviceability of the structure (Chaallal. 1998). Flexural failure of un-strengthened RC beams is normally ductile. Failure of FRP strengthened beams in flexure is observed to be similar to the failure mode of normal RC beam (Mohamed, 2002).

Failure modes of beams with FRP external reinforcement in flexure can be categorized in to two main types; (a) classical failure and (b) premature failure (Chaallal. 1998).

2.7.1 Classical failure

Failure of an element due to

     a)   FRP rupture

     b)   Concrete crushing

     c)   Shear failure

are known as classical failure (Figure 2.10). When classical failure occurs, full capacity of the strengthening system has reached.

(a) FRP rupture

(b) Crushing of compressive concrete
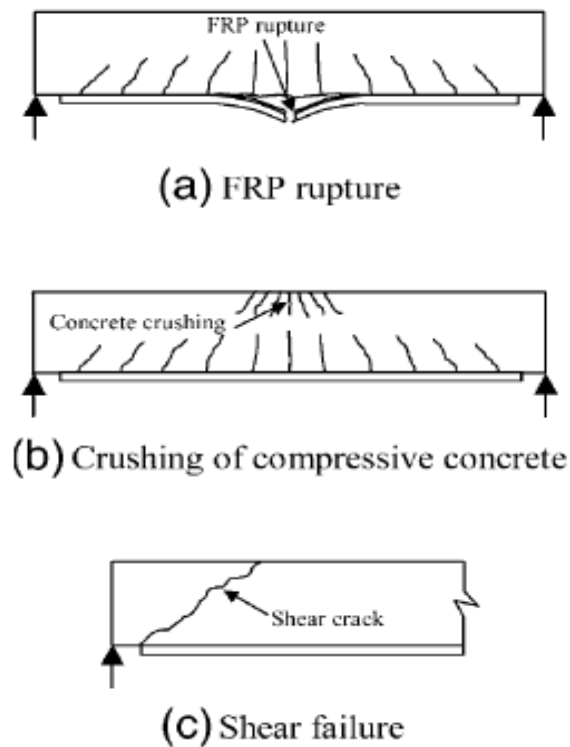
(c) Shear failure

Figure 2.10: Classical failure modes of FRP-strengthened RC beams. (a) FRP rupture; (b) Crushing of compressive concrete; (c) Shear failure; (Smith and Tang, 2002)

Concrete crushing occurs when the compressive stress of concrete is reached before achieving the yield strength of concrete, ultimate bond strength and FRP rupture strain. This mode may more common with low strength concrete.

Failure may also occur due to FRP rupture. This mode is known as a classical failure mode since it has achieved the ultimate tension capacity of FRP.

When concrete crushing strength and FRP rupture strength is very high, the system may not fail in flexure. In this situation, the enhanced flexural strength is greater than shear strength. Then the system fails in shear.

2.7.2 Premature failure

If a different failure mechanism other than classical failures, governs the failure of the beam, the phenomena is known as premature failure. There are two sub modes in premature failure namely; cover separation and FRP debonding (See Figure 2.11) (Smith and Tang, 2002).

(a)

(b)

(c)
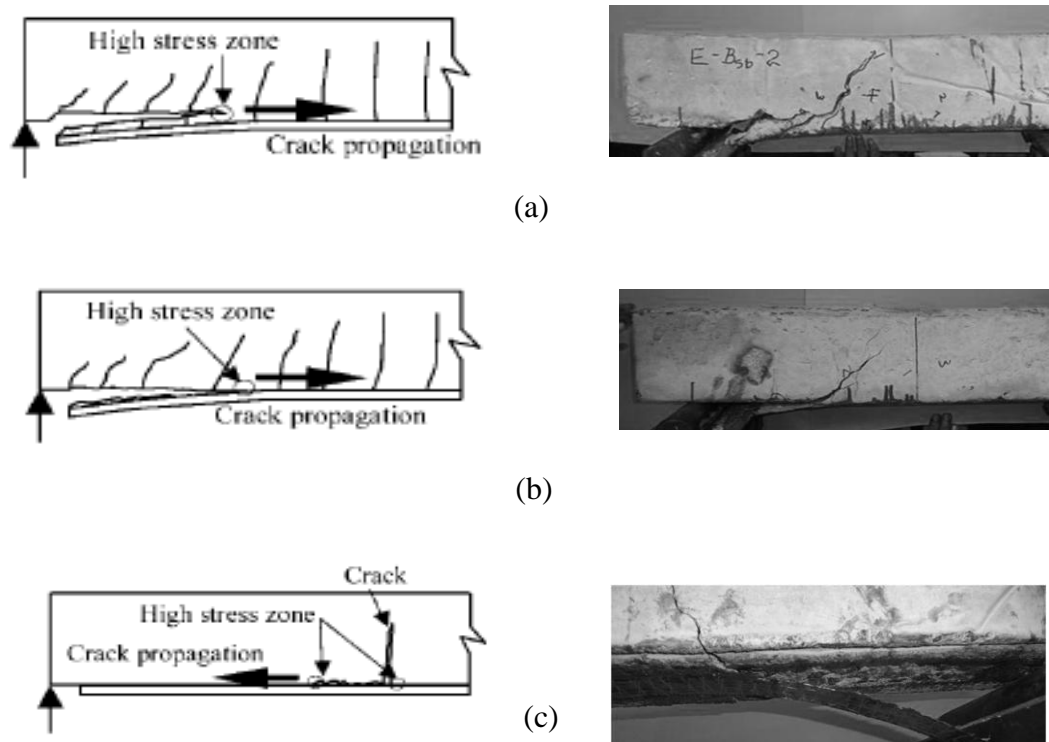
Figure 2.11: Premature failure modes of FRP-strengthened RC beams (a) Concrete cover separation; (b) Plate end interfacial debonding; (c) Intermediate crack induced interfacial debonding. (Smith and Tang, 2002)

The most common premature failure mode of flexural strengthened beams is debonding failure (Ramanathan, 2008). Debonding initiates at the locations where

there are high stress concentrations in the FRP sheet, such as at ends of the sheet and near cracks in concrete (Amery and Mahaidy, 2006). According to Aram et. al. (2008), there are two modes of debonding failure; end debonding and mid span debonding (Figure 2.11).

2.8 Debonding failure

2.8.1 End debonding failure

Plate end debonding occurs due to cracks induced by high interfacial shear and normal stresses caused by the abrupt termination of the plate. Debonding process initiates closer to ends of the FRP sheet and propagates towards the middle of the beam. The failure can be in two modes; plate end shear failure and anchorage failure at last crack. Once a shear crack occurs near to the plate end, it propagates until it meets tensile reinforcement. Then it finds a new path weakened by high stresses between steel-concrete interface, and thus the crack follows the track along the tensile steel reinforcement. Therefore plate end shear failure will ultimately end up in cover separation failure.

Anchorage failure at last crack, as in the name, is induced by the cracks occur in the anchorage zone. When a crack occurs on the tension face of concrete, de-bonding occurs up to a small distance around the crack. Then there is a discontinuity of the bonded length of FRP. If the remaining bonded length towards the edge of the FRP plate is less than required anchorage length, the system fails. This phenomenon is known as anchorage failure.

2.8.2 Mid-span de-bonding failure

Mid span debonding starts from flexural or shear cracks closer to middle of the beam. This mode of failure is named as shear crack debonding or flexural crack debonding, according to the type of crack at which debonding is started. In this failure, delamination occurs closer to middle of the beam and propagates towards the end of the plate. Figure 2.12 shows a descriptive picture of debonding failure modes.
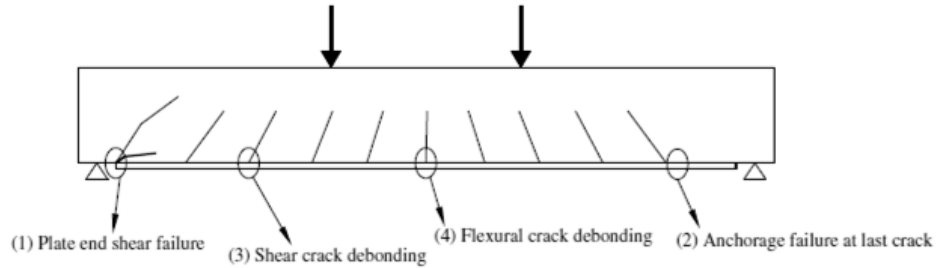
Figure 2.12: Possible debonding failure modes (Aram et. al., 2008)

Plate end debonding will initiate at a discrete shear crack. There are high shear and normal stresses at the end of the plate in order to maintain zero strain at the pale end. Once a crack is formed at the plate end, both the stress components will come down to zero (Leung, 2006). During experimental works done by many researchers (Buyukozturk et al., (2004), Aram et al.,(2008)) have observed that, a thin layer of concrete generally remains attached to the plate upon the delamination. It suggests that failure is normally occurred within the concrete, which is the weakest element in the system.

Buyukozturk et al. (2004) has conducted an experimental investigation on simply supported beams strengthened with different lengths of CFRP sheets and has revealed that, debonding failure load and ductility reduces with decreasing lengths of CFRP reinforcement.

In general, debonding of the FRP plate from the concrete is due to these high stresses. Concrete is unable to resist high tensile stresses. When the tensile force in CFRP sheet is transferring to concrete, it is highly vulnerable to undergo tensile cracks and therefore delamination occur at the cracked points.

Debonding can also occur as a consequence of steel yielding. When steel reinforcement yields, all shear force has to be taken only by FRP- concrete interface. Thus there can be sudden strain increments in FRP causing debonding due to high slip (Faella et al.2008).

2.9   De-bonding delaying techniques

Prevention of debonding is much important since it influence several drawbacks of the system including loss of ductility and inefficiency. Many researchers have carried out studies to investigate debonding delaying techniques (Spadea et al. (2001), Sagawa et al. (2001), Antonopoulos and Triantafillou (2003), Kotynia (2005)). Prestressing of FRP and provision of anchorage are the two main options which have proposed in literature. Provision of anchorage is found to be a good solution for FRP debonding where lack of development length or inadequate bond strength is the cause (Ceroni et al. 2008). Not only for prevent debonding, anchorage systems are also used to provide a ductile failure mode for the structural member instead of the sudden and brittle failure caused by debonding or FRP rupture.

2.9.1 Effects of anchorages

According to Mostofinejad and Moghaddas (2014), debonding failure limits the flexural strength gain of the system to about 30% over an unstrenghtened beam, whereas the system inherits the ability to give a strength gain of 52% under classical failure. Another study done by Xiong et al (2007) has reveled that the specimens can achieve 86% strength increment from the CFRP strengthened system, if the debonding failure is prevented. Without end debonding delaying strategy, the beams could achieve only 52% strength gain. Therefore, an effective technique to prevent debonding failure is much essential.

2.9.2 Different mechanisms of anchorages

Reinforced concrete flexural elements strengthened with externally bonded FRP plates or sheets are highly vulnerable to debonding failure. This failure mode leads the element to a more brittle failure, which is not good for safety under serviceability conditions. Therefore researches have tried various methods to delay debonding failure.

According to Wu et al. (2011), available end debonding delaying techniques can be divided in to four main categories depending on the mechanism used to prevent debonding (See Figure 2.13). The four methods are,

1. End wraps
2. Mechanical fasteners

3. Near surface mount reinforcement
4. FRP pin and pan shape anchors.

(a)

(b)

(c)

(d)
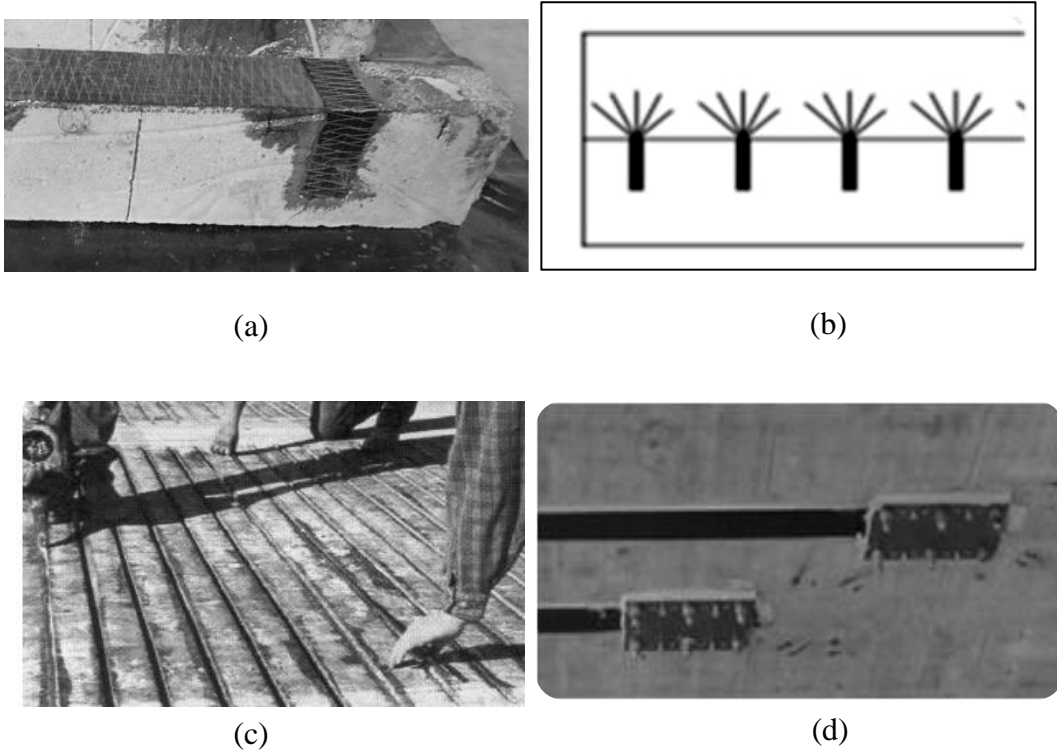
Figure 2.13: Debonding delaying techniques (a) End wraps, (b) Pin and pan shape anchors (Ceroni et al., 2008), (c) Near surface mount reinforced systems (Lorenzis et al., 2000), (d) Mechanical fasteners (Julien et al., 6 January 2004)

Technique of providing additional anchorage using FRP end wraps is based on avoiding stress concentrations. Transverse FRP wraps distribute stresses which are concentrated at the edges of CFRP strips. It also provides a safe path for transfer of the stresses to concrete element. End wraps which are used to prevent debonding failure are in form of U-jackets, Combined L-Wraps, X-wraps and inclined wraps. End wraps can also improve the shear capacity of the system. Research works have revealed that, about 6% strength gain can be achieved with end U-wraps, over non-anchored beam and that of combined L-wraps is 8.5% (Siddiqui 2009, Gunes et al. 2009)

Anchorage provided by steel rivets, bolts, anchoring steel plates and interlocking anchorages etc are known as mechanical fasteners (Figure 2.13 d). They exert a lateral pressure on the FRP layer towards the concrete surface. As a result FRP/Concrete interfacial friction is increased. Then external work done required to initiate debonding is increased and debonding delays. In literature, an average 33% and 30% (Antoniades et al. 2003) of flexural strength gain over non anchored beams have recorded for different types of mechanical anchorages.

The third anchorage type is Near Surface Mount Reinforcement systems (NSMR) (Figure 2.13 c). In this method, a grove is cut along longitudinal direction of the flexural member and FRP strips are inserted in to those groves. FRP is bonded to the element by filling the grove with an adhesive. Since both sides of the FRP strip are bonded to concrete element bond area is about twice as conventional externally bonded FRP. The increment of bond area results rise in bond strength and thus delay end debonding.

Pin and pan shape anchors are made with FRP. A bundle of fibres are glued together to make a pin and pan shape anchor. After FRP flexural reinforcement is applied, the anchor is installed so that the pin portion is anchored to a hole drilled to concrete element and the pan is spread on flexural FRP around the hole. These anchors are supposed to collect peeling stresses and shear stresses through the pan shaped portion and transfer them along fibres. All these concentrated stresses are then anchored to concrete element by the pin.

Another method which does include to the above four techniques has been proposed by Qeshta et al. (2014). A wire mesh is included in between the concrete substrate and FRP sheet and bonded with epoxy as shown in Figure 2.14. The wire mesh can absorb the energy which are concentrated to the edges of CFRP plate and transfer them to the concrete element after distributing stresses throughout the mesh (Qeshta et al. 2014). Then, the magnitude of stresses reduces and therefore the system can remain un-bonded in higher loads. Experiments have shown that the use of wire mesh–epoxy composite increases flexural strength up to about 123% over the plain concrete control specimen (Qeshta et al. 2014).
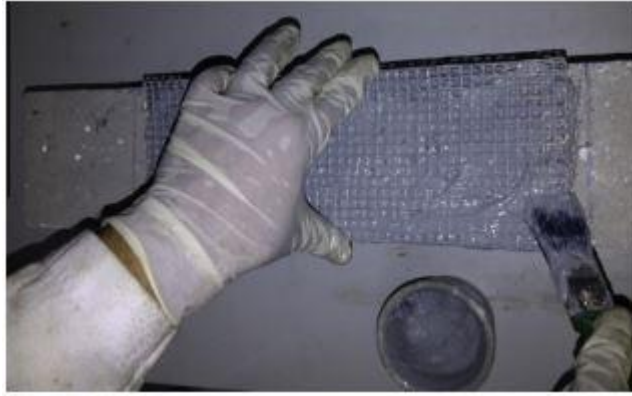
Figure 2.14: Application of wire mesh as end anchorage (Qeshta et al. 2014).

Srisangeerthanan (2013) has also pointed out a similar behaviour of beams with a wire mesh bonded between concrete and the CFRP sheet. His specimens indicated more than 60% strength gain for two different arrangements of wire mesh.

2.9.2.1 End wrap anchorage

Apart from increasing ultimate load carrying capacity, end wraps have more advantages compared to other anchorage techniques. In fact, Spadea et al. (2001) have found that U-shaped anchors provide a more ductile failure compared to an un anchored, flexural strengthened member. FRP transverse wraps can provide a clamping effect to FRP flexural reinforcement (Sawada et al. 2003) facilitating a better anchorage. Therefore, effectiveness of longitudinal FRP reinforcement is increased (Antonopoulos and Triantafillou 2003). In 2005 Kotynia have revealed that efficiency increases because, U and L- shaped transverse wrapping helps in developing a greater percentage of the flexural FRP's rupture strain. Another important advantage of end wraps is that they can contribute to shear resistance of the strengthened member (Amery and Mahaidi 2006). It results in gain of overall load carrying capacity of the system. So, it is worthwhile to investigate more on FRP end wraps.

As far as end wraps are concerned, different wrapping configurations have proposed in previous studies (Figure 2.15). Inclined wraps can provide high shear resistance to element. Therefore effectiveness of the system is much higher when inclined wraps are used for anchorage.
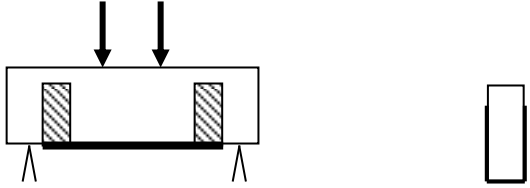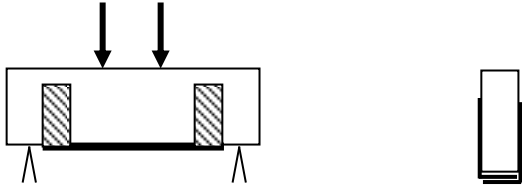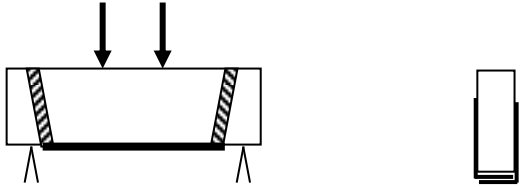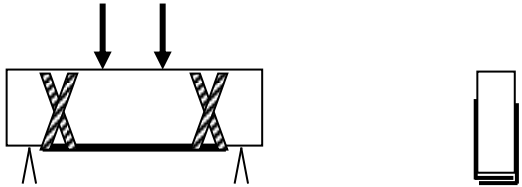
Form of Wrap	Schematic Diagram
U – Jackets	
Combined L – Wraps	
Inclined Wraps	
X - Wraps	

Figure 2.15: Configurations of FRP wraps

2.10 Experimental studies

Studies on strength gain of end anchored, external FRP flexural reinforcement has been conducted by many researchers (Xiong et al. 2007, Amery and Mahaidy 2006, Mahaidi and Kalfat 2011). They have observed the strain profile along the beam. Strain values were then utilized to work out bond stress vs. slip curve for the specimens.

Experimental studies can be divided in to two categories, depending on the method of testing; bending tests and pullout tests. In bending tests, a transverse load is

applied so that the beam subjects to a bending moment. For these tests, force is exerted by three point bending, four point bending or distributed loading. Pullout tests are the testing of specimens done by application of direct tensile force. Shear strength of the bond between FRP/concrete surfaces can be assessed with this test.

2.10.1 Bending tests

Amery and Mahaidy (2006) in their studies, they state that debonding can be prevented by introducing CFRP straps. They have conducted investigations on the coupled behaviour flexural CFRP and end wraps. Details of the beams they have tested are summarized in Table 2.5.

Table 2.5: Specimen details of tests conducted by Amery and Mahaidy (2006)

Beam number	Description	Loading	Failure mode
RR1	No strengthening	Four point bending	Shear
RR2	CFRP straps at constant spacing	Three point bending	Flexure (steel yielding)
RR3	CFRP flexural strengthening	Four point bending	Shear
RR4,RR5,RR6	Coupled reinforcement (CFRP straps + sheets)	Three point bending	Flexure (FRP rupture)

RR3 specimen is strengthened with three layers of longitudinal CFRP sheet. The coupled configuration is consisting of three layers of CFRP longitudinal strips and CFRP straps located at 200mm centre to centre spacing throughout the beam. The strain distribution of RR3 and RR5 specimens are shown in Figure 2.16 and Figure 2.17 respectively.

According to the figures it is clear that strain levels has reduced significantly with the provision of straps. Amery and Mahaidy (2006) conclude that interface slip between

the CFRP sheets and the concrete surface reduces considerably due to the provision of u-wrap anchorage. It proves that the composite action between the concrete beam and the CFRP sheets is well established by straps.

A similar kind of strain reduction has been observed by Garden and Hollaway (1998) by providing anchorage with steel fasteners at two ends.
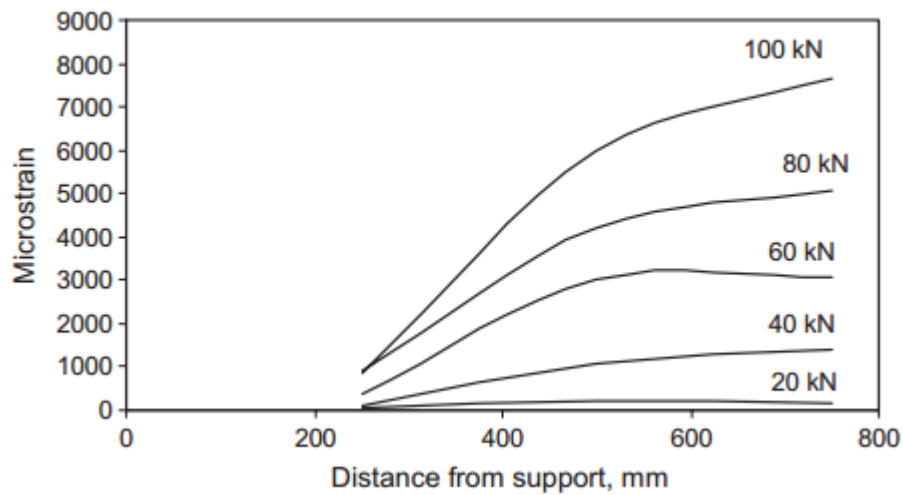
Figure 2.16: Longitudinal strain in the third (outer) CFRP layer, beam RR3 (Amery and Mahaidy 2006)

44
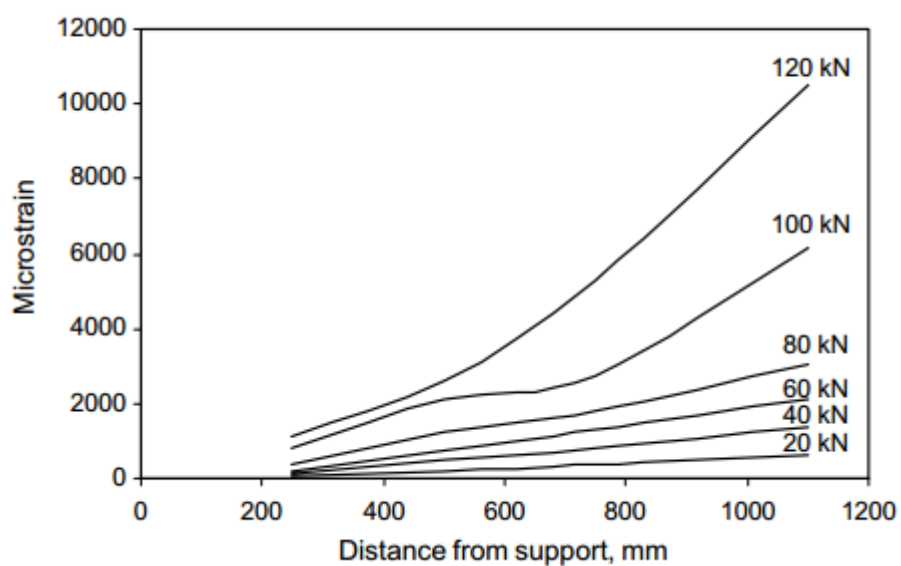
Figure 2.17: Longitudinal strain in the third (outer) CFRP layer, beam RR5 (Amery and Mahaidy 2006)

2.10.2 Pullout tests

Mahaidi and Kalfat (2011) has investigated the effect of end U wraps by conducting pullout tests. They have prepared 600mm × 300mm × 250mm blocks and strengthened them with 120mm wide FRP sheets. The unloaded edge was anchored by 250mm wide CFRP end strap. Figure 2.18 shows the resulted longitudinal strain throughout the length.
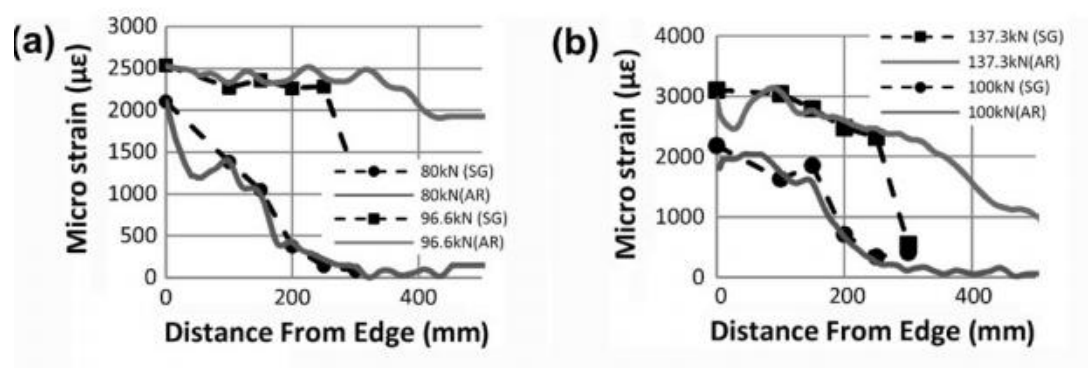
Figure 2.18: Strain vs. distance along laminate: (a) No anchorage (control), (b) anchored with CFRP transverse U-wrap (Mahaidi and Kalfat 2011)

Note: The distance is measure from the loaded edge.

Similar to the results of bending tests, this study too reveals that strain levels reduce when the flexural reinforcement is anchored at the end with CFRP strap.

As far as Bond stress vs. Slip diagrams are concerned (Figure 2.19), area below the curve is high in case of the specimen with end anchorage (type2). It suggests that the fracture energy is high for type 2 blocks meaning that a higher load can be resisted by the specimen.

Mahaidi and Kalfat (2011) conclude that, FRP straps can increase the failure load on average 39%-43%.
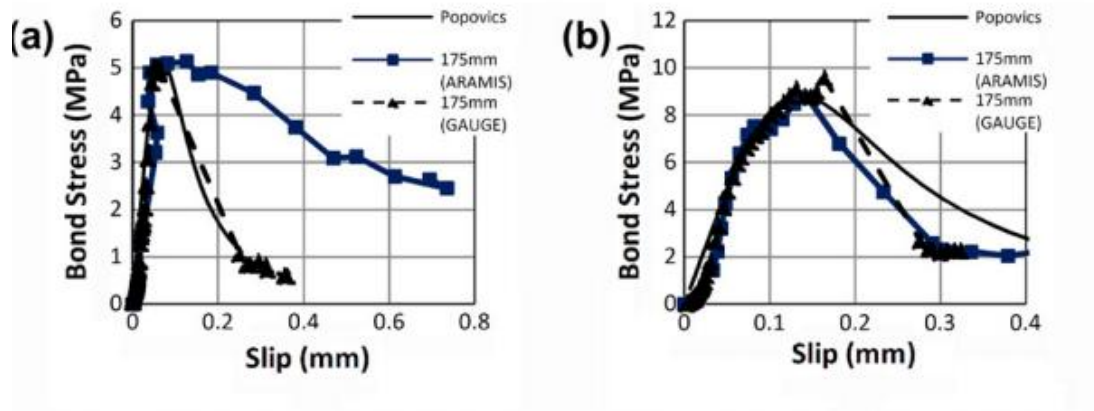
Figure 2.19: Bond–slip curves fitted with Popovics equation – anchorage type 2: (a) No anchorage (control), (b) anchored with CFRP transverse U-wrap (Mahaidi and Kalfat 2011)

2.11 Theoretical studies

Externally bonded CFRP sheets provide additional flexural capacity to concrete elements. When the flexural reinforcement is anchored with end wraps, they further increase the flexural capacity and contribute to shear capacity as well. Therefore, reviewing existing theoretical studies on flexural strengthening and shear strengthening is important before considering the combined effect. Although many calculation procedures are proposed by several authors (Ghandour (2001), Ahmed et al. (2001), Shahbazpanahi et al. (2015)) design guidelines can be named as a good reference where all the reliable studies are concluded. In this section, ACI 440 R and FIB-bulletin-14 design guides are referred for flexural strength and shear strength predictions.

2.11.1 Flexural strengthening

ACI-440-R design guide have proposed Equation 1.3 in section 1, to predict flexural capacity of the FRP flexural strengthened members. Since debonding occurs due to inadequate strength of substrate to sustain the force in FRP, they have introduced a bond-dependent coefficient (K_m), to address the issue. K_m multiplied by rupture strain of FRP is the failure criteria for debonding according to ACI-440-R, provided that the effective anchorage length is satisfied.

FIB-bulletin-14 guide propose different sets of equations to predict failure under different sub categories of premature failure. Equation 2.3 is the basic equation for moment capacity under full composite action. Definitions of certain parameters in the equation vary depending on the sub failure mode considered.

$$M_{Rd} = A_{s1}f_{yd}(d - \delta_G x) + A_f E_f \varepsilon_f (h - \delta_G x) + A_{s2}E_{s2}\varepsilon_{s2}(\delta_G x - d_2)$$

<div align="right">Equation 2.3</div>

2.11.2 Shear strengthening

In both ACI-440-R and FIB-bulletin-14 guides, total shear capacity of the member is given as the summation of shear capacity of concrete (V_c), steel (V_s) and FRP (V_f) (see Equation 2.4), where φ_f is additional FRP strength-reduction factor. However the way the two design guides define the shear contribution of FRP is different.

$$\boldsymbol{V_n = (V_c + V_s + \varphi_f V_f)} \dots\dots\dots\dots\dots\dots\dots\dots\dots\dots\dots\dots\dots\dots \text{Equation 2.4}$$

According to ACI guidelines, contribution of FRP reinforcement to shear capacity is expressed as in Equation 2.5. It simply calculates the total shear resistance generated by the FRP straps or wraps, in the form of stresses in the material.

$$\boldsymbol{V_f = \frac{A_{fv}f_{fe}(\sin\alpha + \cos\alpha)d_f}{s_f}} \dots\dots\dots\dots\dots\dots\dots\dots\dots\dots\dots\dots\dots \text{Equation 2.5}$$

When predicting shear capacity provided by end U wraps, the ultimate strain is generally limited to 0.004 in order to address delamination (ACI-440-R).

Shear contribution of FRP external shear reinforcement V_{fd}, according to FIB method is given by Equation 2.6. This calculation is a quite complex assessment, where FRP reinforcement ratio ρ_f , exact angle between principal fiber direction and alignment of diagonal crack and effective depth of cross section (d), are also taken in to consideration.

$$V_{fd} = 0.9\varepsilon_{fd,e}E_{fu}\rho_f b_w d(\cos\theta + \cot\alpha)\sin\alpha \dots\dots\dots\dots\dots\dots\dots\dots\dots\text{Equation 2.6}$$

2.11.3 Combined effect of CFRP flexural reinforcement and end wrap anchorage

Li et al. (2013) have conducted an experimental investigation on the flexural behaviour of low-strength reinforced concrete beams strengthened with externally bonded carbon fibre sheets and end anchored with FRP U-wraps. The relationship for the effective shear force in the FRP/concrete interface was developed using fracture mechanics based approach. They have further studied the effects of u-wraps on the bearing load of the system by conducting parametric studies in a brace-arch model (Li et al. 2013).

As a result of Li et al. (2013) study, they have proposed a theoretical model to predict the behaviour of low strength concrete elements externally strengthened with CFRP and end anchored with U-wraps. According to their investigations, effective bond length (L_e) can be expressed as a function of elastic modulus of CFRP (E_f), thickness of CFRP sheets (t_f) and tensile strength of concrete (f_t) as indicated in Equation 2.7. Since this study deals with low strength concrete, debonding has always occur within the concrete substrate. Therefore, they have equated the ultimate bond strength between CFRP and concrete (τ_u) to tensile strength of low strength concrete.

$$L_e = \frac{F_u}{b_f \tau_u} = \sqrt{\frac{0.4 E_f t_f}{f_t}}$$ .... Equation 2.7

According to Li et al. (2013) flexural capacity of unanchored beam (M_u) is calculated as in Equation 2.8.

$$M_u = f_y A_s \left(h - a_s - \frac{x}{2} \right) + F_d \left(h - \frac{x}{2} \right)$$ ....Equation 2.8

When the beam is anchored with U wraps, tensile force in FRP (F_d) in Equation 2.8 is modified as the minimum of tensile force before sheets debonding (F_{e1}) and tensile force when concrete cover separation occurs in presence of end U wraps (F_{e2}). Once F_d is modified, the flexural capacity of the end anchored beams can be calculated with the same equation used for the case of beams with flexural strengthening only.

However, the above equations are proposed to elements made up of low strength concrete where concrete strength is less than 15 MPa and applicability of these equations on normal strength concrete (25 Mpa to 50 Mpa) should be further investigated.

2.12 Conclusions

FRP strengthening has been used for structural strengthening since few decades. At present it has become more popular due to its special advantages. Although extensively used, there are some drawbacks of the system which does not have an exact precaution yet. The main issue with CFRP external strengthening system is premature failure. As far as premature failure is concerned, debonding is the more common mode of failure. Debonding may begin either at the end of the CFRP layer or from mid-span of the beam. The former one is known as end debonding and its origin can be a plate end shear crack or anchorage failure. Mid-span debonding, initiates at a flexural or shear crack in the span.

Many researchers have carried out studies to investigate measures to delay end debonding. Wu et al. (2011) have separated the available debonding delaying techniques in to four main methods. They are mechanical fasteners, end wraps, pin and pan shape FRP anchors and Near Surface Mount FRP reinforced systems. Application of a wire mesh is another method proposed by Qeshta et al. (2014) and Srisangeerthanan (2013) does not belong to the above mentioned categories.

Among all the debonding delaying techniques, U-strap anchorage is found to be more beneficial. Research works have proven that the strain values in flexural FRP can be significantly reduced with provision of U-jacket end anchorage. As far as theoretical models are concerned, guidelines are available for flexural strengthening and shear strengthening separately and there is no proper guideline to address the shear flexure interaction.

2.13 Research needs

As stated by Grelle and Sneed, (2013), there are no detail investigations carried out to investigate the debonding resistance and strength gaining of end anchored flexural

elements. Although the available studies address the behaviour qualitatively, design guidelines cannot be developed without quantitative conclusions. There are many research works which propose equations to model the behaviour of conventional FRP retrofitting systems. Little research is carried out to investigate the relationship of strength gain Vs end anchorage. Therefore a theoretical model to predict behaviour of FRP flexural strengthened, end anchored beams is much important.

CHAPTER 3

3 Experimental Investigation

3.1 Experimental programme

The current experimental investigation consists of eight reinforced concrete medium scale beams strengthened with CFRP. The experimental results was utilised to study the contribution of end anchorage on strength gain of the system in flexure. This chapter provides detailed description of the experimental programme, procedure and results.

3.1.1 Test configuration

Specimens were prepared with Grade 30 concrete. All the beams were in the size of 150 mm×100 mm cross section and 750 mm in length. Flexural reinforcement of, two 6mm diameter mild steel bars were provided to each beam as shown in Figure 3.1. Another two 6 mm diameter bars were used at the top surface of beams for hanging shear links. Shear reinforcement was consisted of 15 number of shear links made of 4 mm diameter GI bars, spaced at 50 mm intervals. Reinforcement arrangements used in test beams are shown in Figure 3.1. Other parameters engaged with the test configuration are shown in Annex A.1.
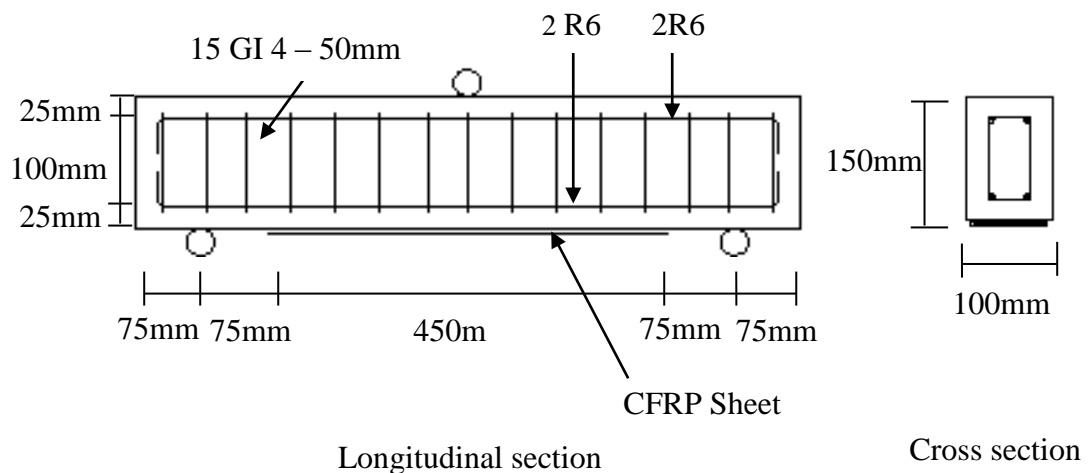
Figure 3.1: Geometry and reinforcement arrangement of specimens

The specimens were strengthened using 90 mm wide and 450 mm long CFRP strip which is applied to the tension side of each concrete element. Inclined end wraps are

placed perpendicular to the expected shear crack, which is assumed as the line matching two subsequent loading points. The aim is to make the transverse wraps more efficient in shear resistance. The beams strengthened with end anchorage are schematically presented in Figure 3.2.
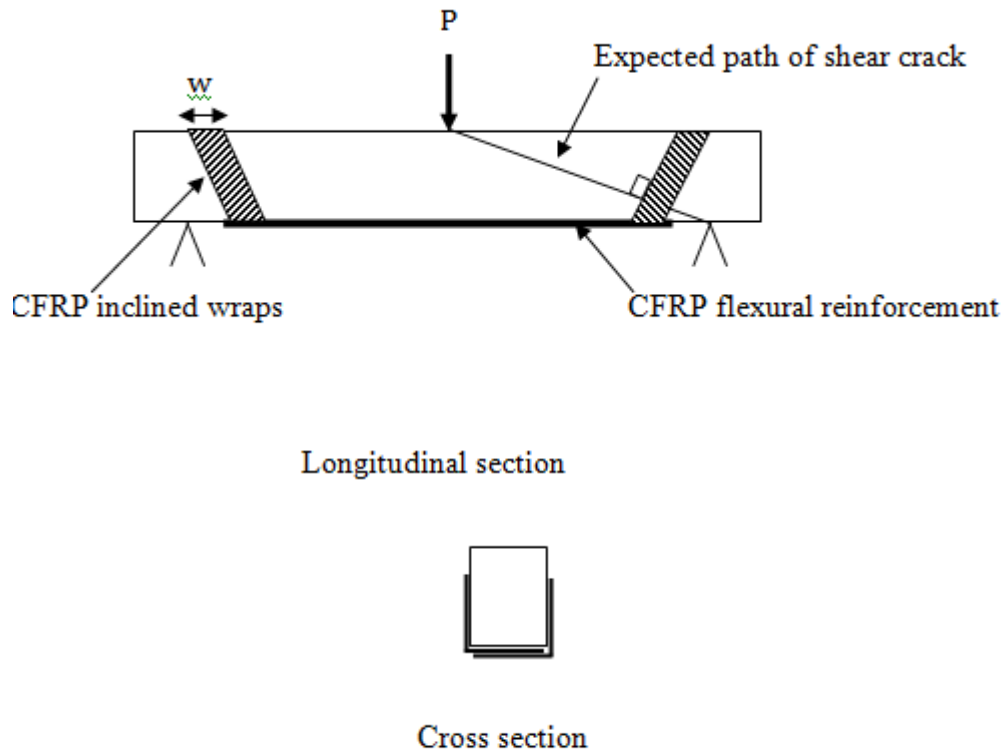
Figure 3.2 : FRP external reinforcement with end anchorage

The specimens were consist of two control beams, two flexural strengthened but not end anchored beams and three sets of flexural strengthened beams with varying quantities of end anchorage. Different anchorage amounts for the specimens were achieved by increasing the width of end wraps. Test beam details are summarised in Table 3.1 and

Table 3.1: Details of test beams

Specimen	Beam designation	Description	External flexural reinforcement	Width of inclined end wrap	Width of mid span U-wrap
1,2	C(1), C(2)	Control beams (Unstrengthened beams)	-	-	-
3,4	F(1), F(2)	Flexural strengthening only	90mm	-	-
5,6	FA1(1), FA1(2)	Flexural strengthening + inclined wraps as end anchorage	90mm	60mm	-
7,8	FA2(1), FA2(2)	Flexural strengthening + inclined wraps as end anchorage + mid span anchorage with U-wrap	90mm	60mm	60mm

3.1.2 Material properties

3.1.2.1 Concrete

Grade 30, normal grade concrete was used for specimen casting. The concrete mix (Figure 3.3) was prepared with ordinary Portland cement belongs to cement strength class 42.5. Course aggregate was metal, which is a crushed aggregate type with 20 mm maximum particle size. Fine aggregate was uncrushed river sand with particle size less than 4 mm.

BRE (Building Research Establishment) mix design method was adopted to determine the mix proportions (BRE 1197). The target slump value was 75 mm. No admixtures were added to the mix. The mix design data is included in Appendix A.2.

Compressive strength of concrete was determined by conducting cube testes, with size 150 mm × 150 mm × 150 mm. Four cubes from each concrete batch (0.03 m^3 volume) were casted. The cubes were tested at the same date of testing the specimens from the same batch in order to get the exact compressive strength. The measured mean compressive strength of cubes is 47.46 N/mm^2. The cube test results are given in Appendix B.1.1.

Material testing on concrete compressive strength and steel reinforcement characteristics were tested in the experimental program. According to the results, mean compressive strength of concrete on the day of testing the beams is 47.46 N/mm^2. The measured yield strength of flexural reinforcement is 218.04 N/mm^2 and yield strength of shear reinforcement is 277.66 N/mm^2. All the results and calculations of material testing are included in Appendix B.1.2. and B.1.3.
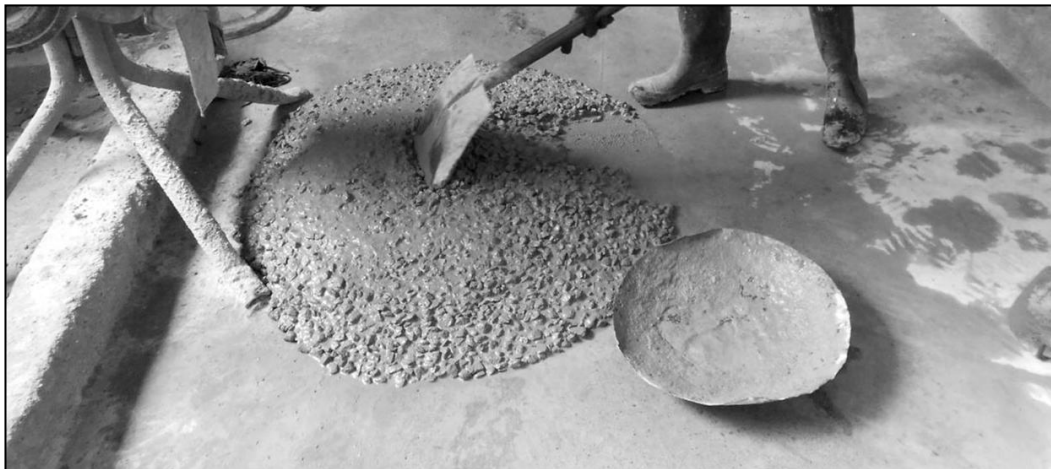
Figure 3.3 : Concrete for specimens

3.1.2.2 Reinforcement

Internal reinforcement was consisted of steel flexural and shear reinforcement. Four, 6 mm diameter mild steel bars were used as flexural reinforcement; two bars at the top and the other two at the bottom. Shear stirrups were made up of 4 mm diameter

50 mm

galvanized iron (GI) wires. Shear link and arrangement in the reinforcement cage are shown in Figure 3.4 and Figure 3.5 respectively.
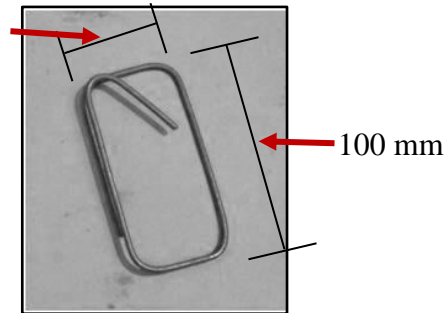
Figure 3.4: Shear Links (GI 4mm diameter bars)
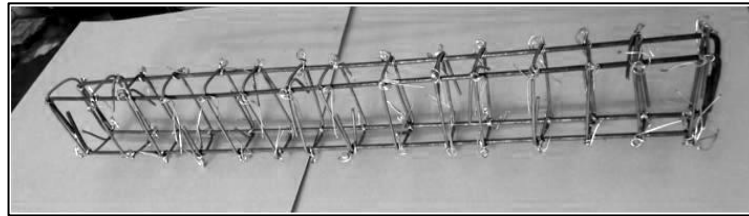
Figure 3.5 : Reinforcement cage of specimens

Uni directional CFRP fabric (Figure 3.6) was used as external reinforcement for flexural strengthening and for the purpose of end anchoring. MBrace CFRP fabric with 640 000 N/mm^2 elastic modulus and 2600 N/mm^2 tensile strength is the utilized product in this experimental programme (BASF, MBrace fabric, May 2009).

Properties of external reinforcement and steel reinforcement according to manufacture specifications are given in Table 3.2.

Fiber direction
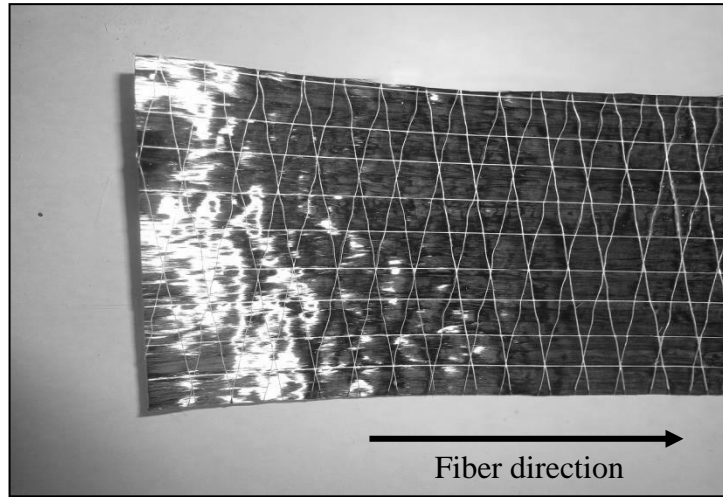
Figure 3.6: Uni directional CFRP fabric

Table 3.2: Properties of reinforcing materials (BASF, MBrace fabric, May 2009)

Material	Property	Value
CFRP Laminates	Tensile strength	$2600 \ \text{N/mm}^2$
	Thickness	0.146 mm
	Elastic modulus	$640\ 000 \ \text{N/mm}^2$
Steel reinforcement R6	Elastic modulus	$200\ 000 \ \text{N/mm}^2$
	Tensile strength	$218 \ \text{N/mm}^2$ *(Measured)*
Stirrups GI4	Elastic modulus	$195\ 000 \ \text{N/mm}^2$
	Tensile strength	$277.66 \ \text{N/mm}^2$ *(Measured)*

3.1.2.3 Primer and Adhesive

Priming is essential to apply on porous substrates such as concrete in order to improve substrate quality, before applying the adhessive. The primer product used for this study is MBrace primer. There are two parts of the product; epoxy resin and epoxy hardener. The mix proportions are shown in Table 3.3. The pot life of primer at 32 $^{\text{o}}$C is 25 minutes. It should be kept seven days at a temperature greater than 20 $^{\text{o}}$C to complete cure. Figure 3.7 shows the two components of MBrace primer.

Table 3.3: Properties of primer and saturant (BASF, MBrace specifications)

Parameters	Properties of primer	Properties of saturant
Mix proportions [Part A : Part B]	3 : 1 by volumes or 6.90: 3.10 by weights	3 : 1 by volumes or 100 : 30 by weights
Tensile properties		
Yield Strength	14.5 MPa	54 MPa
Strain at yield	2.00%	2.5%
Elastic modulus	717 MPa	3034 MPa
Ultimate strength	17.2 MPa	55.2 MPa
Flexural properties		
Yield Strength	24.1 MPa	138 MPa
Strain at yield	4.00 %	3.8%
Elastic modulus	595 MPa	3724 MPa
Ultimate strength	24.1 MPa	138 MPa
Glass Transition Temperature	-	163^0C

Component A : Epoxy resin   **Component B** : Epoxy hardener
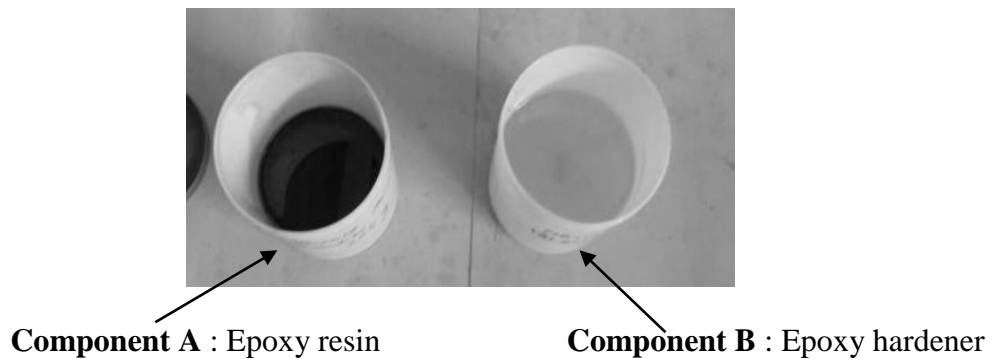
Figure 3.7: Two part primer

MBrace adhesive was used for bonding of CFRP sheet. It also consist of two components namely; saturant and hardener. As shown in Figure 3.8, the blue colour component is the saturent and the reddish semi liquid is the hardener. Their properties are shown in table Table 3.3. Two parts should be stored and mixed in temperatures below 20 ^{o}C and pot life at this temperature is 10 minutes (BASF,

MBrace saturant LTC specifications). Pot life includes the mixing time as well. Since the pot life is very short, small amounts of the mix should be prepared per one time so that all the mix can be utilized within the pot life. For the saturant, the full cure time period is seven days at 20 $^{\circ}$C temperature. The estimated coverage is 0.7 – 1.6 lt/m^2 per layer of FRP sheet.

Component A : Saturant   **Component B** : Hardener
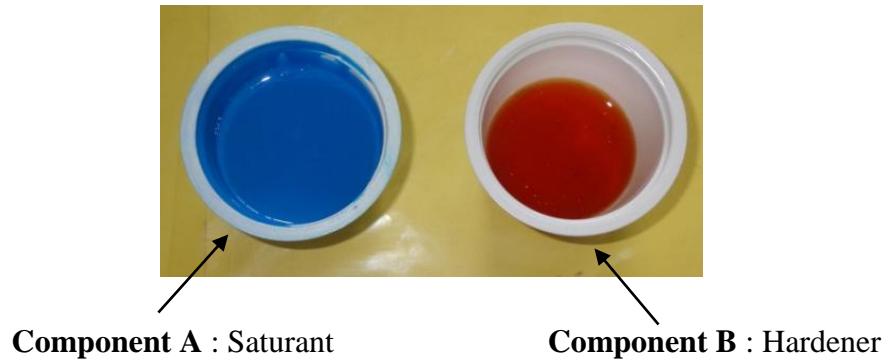
Figure 3.8: Two part epoxy adhessive

3.1.3   Preliminary design calculations

Since the experiment is based on flexural strengthening, failure criteria of control beams should be in flexure. Therefore, load carrying capacity under a flexural failure should be less than the capacity under shear failure. At the same time there should be a considerable gap in between the two values. Otherwise the enhanced flexural capacity of strengthened beams may become greater than the shear capacity of reinforced concrete beam. It may cause shear failure in the strengthened beams, whereas control beams fail in flexure. Then the exact gain of flexural strength cannot be determined by the experimental results. In order to avoid these complications, it is important to maintain the flexural capacity lower than shear capacity even after strengthening. Preliminary design calculations were carried in order to evaluate the capacities under two failure modes. It shows a likely mode of failure due to flexure before and after strengthening.

The calculations were done in accordance with to BS 8110: Part I, 1997, Clause 3.4. The stress strain profiles adopted for the calculations are shown in Figure 3.9. The ultimate compressive strain allowed for concrete in the latter standard was 0.0035. Material safety factors were discarded from stress distributions. Mechanical

properties of materials and other design parameters used for the calculations are given in Table 1 of Appendix A.
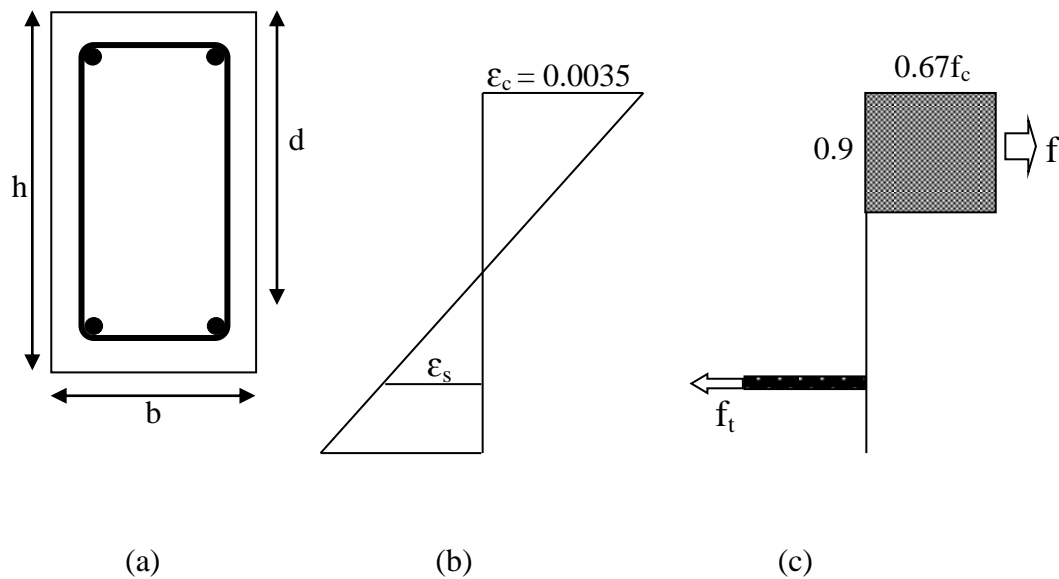
Figure 3.9 : strain and stress distributions across the beam. (a) Cross section, (b) Strain distribution, (c) Stress distribution

3.1.3.1 Evaluation of flexural capacity

The calculation of flexural capacity is given in Appendix A.1.1. For the calculations, it was assumed that the effect of top reinforcement on flexural capacity is negligible. For the considered cross section, depth to the neutral axis was 7.8 mm. It yields a lever arm of 114.5 mm. Consequently, the moment capacity of the beam is 1.62 kNm. Starting with the flexural capacity, a backward calculation was conducted to determine the applicable load before the beam fails. Effects of both central point load and self-weight were considered in order to be more accurate. The applicable load on the beam before flexural failure is 10.9 kN. The course for the failure will be yielding of flexural reinforcement.

3.1.3.2 Evaluation of shear capacity

Shear capacity of the beam is contributed by shear resistance of concrete and tension of shear reinforcement. They were evaluated according to BS 8110: Part I; 1997 and the calculations are given in Appendix A.1.2. According to the calculations, the total shear capacity of the beam is 2.6 N/mm^2. Contribution of concrete on the shear

capacity is 0.775 N/mm^2 and the remaining 1.825 N/mm^2 shear capacity is gained due to the presence of shear reinforcement. Shear force in the concrete beam is induced by external loads applied to the beam and the self weight of the beam. As a result, the applicable load on the beam under three point bending condition before achieving shear capacity is 81.39 kN.

3.1.3.3 Failure criteria

The expected failure load of test specimens in shear is about eight times higher than that in flexure. Therefore, it can be concluded that the control specimens will fail in flexure, due to steel yielding. The ACI-440-2R provides guidance on design and construction of externally bonded FRP systems, states that flexural strength increment of 10% to 160% can be achieved by application of FRP external reinforcement. Accordingly, the maximum capacity of the flexural strengthened specimens will be 160 times the failure load of control beams. Consequently, the failure load of strengthened beam is equal to 28.34 kN which is still less than the shear capacity. By means of that, the strengthened beams will also fail in one of the flexural failure modes. Therefore the selected specimen geometry and reinforcement details are suitable for the study.

3.1.4 Specimen Preparation

Specimen preparation includes all the steps starting from reinforcement preparation up to application of CFRP. A special attention was driven to maintain the quality of specimens throughout the experimental programme. Each and every step of the procedure was conducted according to available construction guides (ACI-440-2R).

3.1.4.1 Casting beams

The beams were casted in steel moulds. They were cleaned and oiled the inner surfaces before casting the beams. A steel mould ready for use is shown in Figure 3.10. Reinforcement cages were pre-prepared outside the moulds and they were placed in, with the help of 25 mm cover blocks. The concrete mix was prepared using a mechanical mixer. The mix was manually poured in to moulds and compacted with a poker vibrator (Figure 3.11).

Figure 3.10: Steel mould for beams

Figure 3.11: Compaction with poker vibrator

3.1.4.2 Curing

The beams and cubes were unmoulded after 24 hours of casting. They were kept fully immersed in a water tank until they were taken out for surface preparation. Figure 3.12 is a view of test beams while curing.
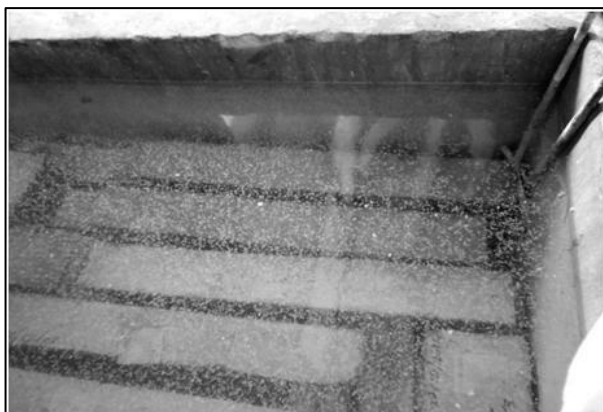
Figure 3.12: Curing of beams

3.1.4.3   Surface preparation

Sandblasting was the adopted surface preparation technique. Sandblasting was done on the 14th day after casting. Aggregate surfaces on the soffit of the beam were exposed while maintaining an even surface of less than one millimetre level difference. Ultimately, a uniformly rough surface was obtained. Figure 3.13 shows a sandblasted surface of a beam.
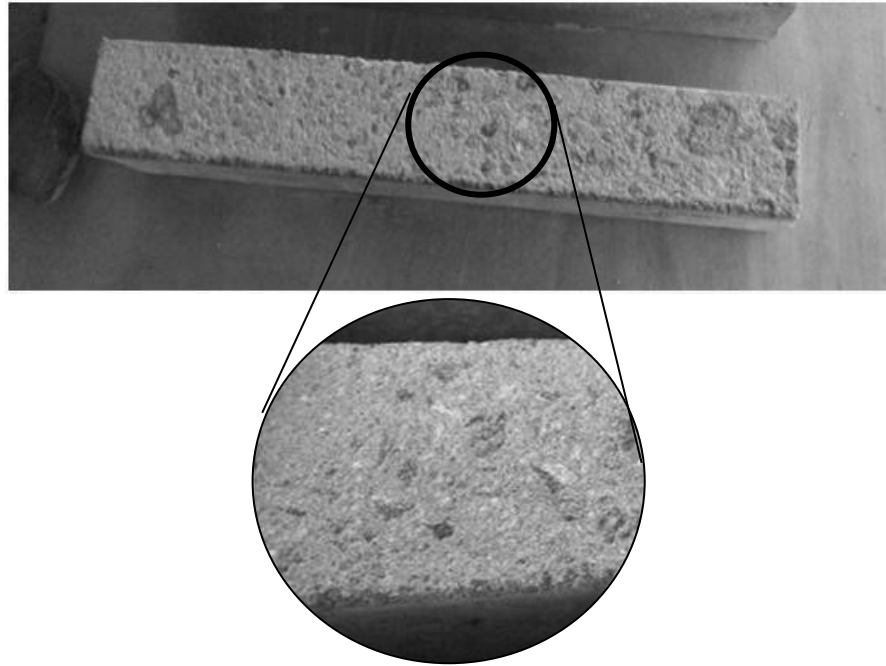
Figure 3.13: A beam after surface preparation

3.1.4.4   Application of primer

External strengthening was done after passing 28 days from the day of casting. As specified in the manufacturer's guidelines, the concrete substrate was brushed so that all the dust particles get removed and cleaned with acetone in order to remove any oils and greases remain. The two part primer was mixed in to the given weight ratios and a thin coat of primer was applied on to the roughened surface of beams. The primer applied beams were kept about 45 minutes for curing. Primer requires seven days to get fully cured. Since CFRP is applying in wet layup system, primer should be cured for minimum 40 minutes and less than 24 hours (BASF, MBrace Primer

MBT specifications). Figure 3.14 shows the application of primer to form a thin uniform coat.

Figure 3.14: Application of primer on beam soffits

3.1.4.5 Application of CFRP

Two-part saturant (base and hardener) was mixed in weight ratios until a uniform blue colour is obtained. The saturant was applied uniformly on adhering faces of beam and CFRP strip. When adhesive is applied on the CFRP sheet the fibre direction was considered carefully and the brush should be directed along the fibre direction as shown in

Figure 3.15 (a). Then the laminate was placed on the beam properly aligned with the marked reference lines. CFRP laminate was pressed using a hard rib roller so that all entrapped air is removed (

Figure 3.15 (a)). Another layer of adhesive was applied on top of the CFRP laminate and again forced with a rib roller. After application of CFRP, the specimens were kept seven days for curing.
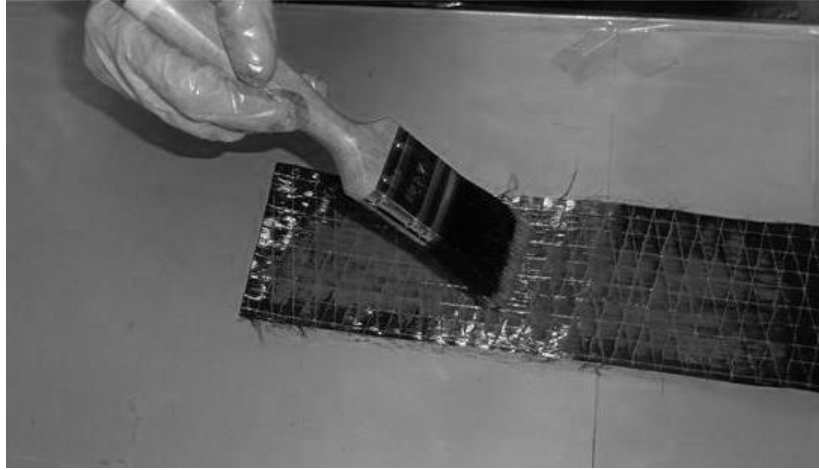
(a)

(b)

(c)

Figure 3.15: Procedure of application of CFRP (a) Apply adhesive on CFRP sheet, (b) Apply adhesive on concrete substrate, (c) Remove air gaps using a hard rib roller

3.1.5   Test programme

The test beams were kept to cure for more than 28 days before strengthening. After application of CFRP, they were cured for more than 7 days which is the adhesive curing period. When the curing is over, specimens were tested using three point bending test in accordance with ASTM C 293.

3.1.5.1   Applied load

The applied load was measured using a load cell attached in between the loading equipment and the beam as shown in Figure 3.16. Readings were obtained at each one second time intervals with the aid of a data logger TDS-530.Crack initiation load which is the load corresponding to 0.3 mm crack width and ultimate failure load were also recorded.
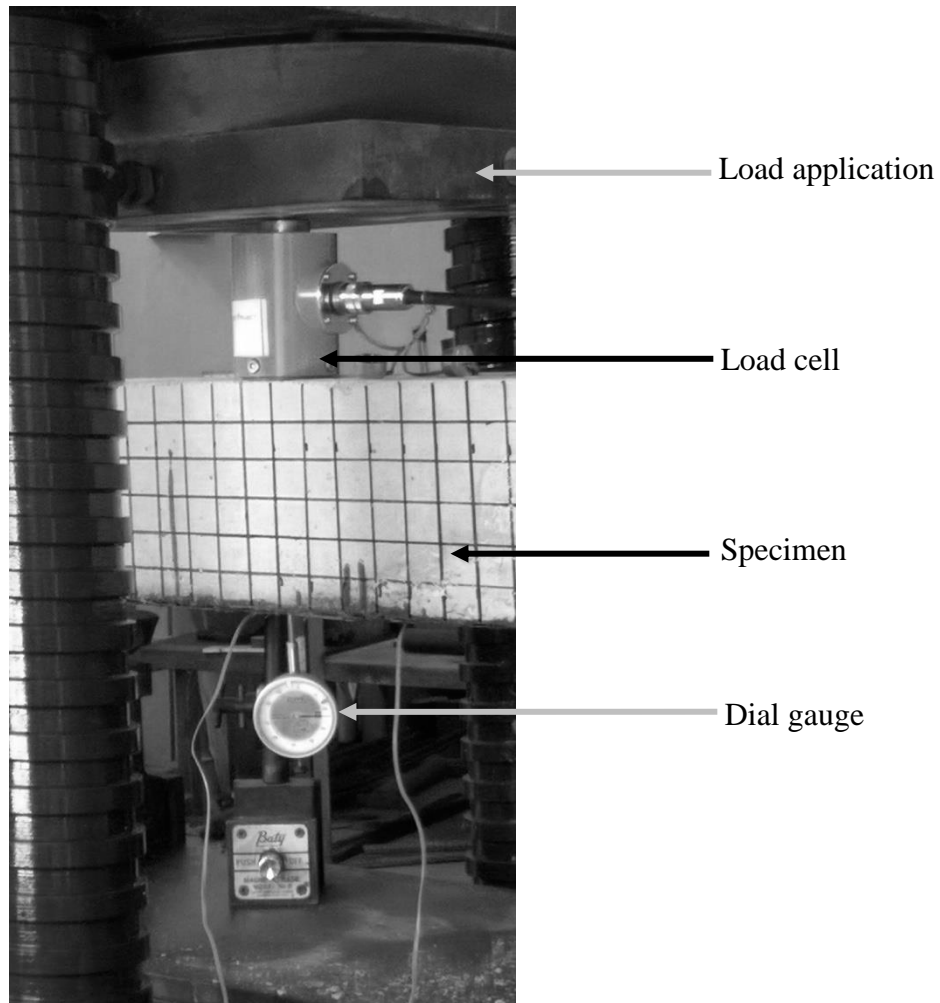
Figure 3.16: Load cell and dial gauge

3.1.5.2 Deflection at the centre of the beam

Central deflection of beams was measured using a dial gauge attached to the bottom surface of the beam. Readings were recorded at every 0.2 Mt load increment. Figure 3.16 shows the arrangement of a dial gauge in the test setup.

3.1.5.3 Strain in bottom fibres

PL-06 strain gauges were attached to the bottom surface of the elements in order to measure the strain levels. Length of a strain gauge was 60 mm and gauge resistance was 120 Ω. Locations of the strain gauges on the specimens are shown in Figure 3.17. Readings were always obtained with reference to a control strain gauge. The control was consisted of a similar strain gauge attached to a concrete beam, placed in the same environment, but without applying any load. Temperature effects and other

environmental effects could be detected and removed from the strain readings with this method. Strain gauge type utilized for the experiment is shown in Figure 3.18.

(a)

(b)

(c)
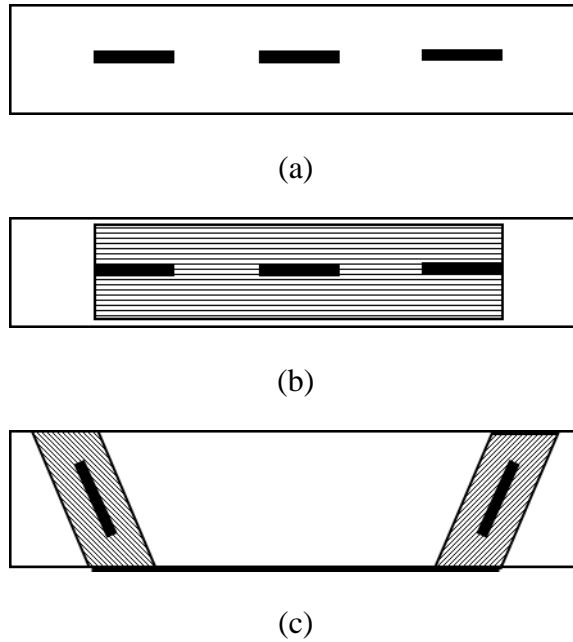
Figure 3.17: Positions of strain gages (a) Bottom face of un-strengthened beam (b) Bottom face of beams without end anchorage (c) Side view of end anchored beams
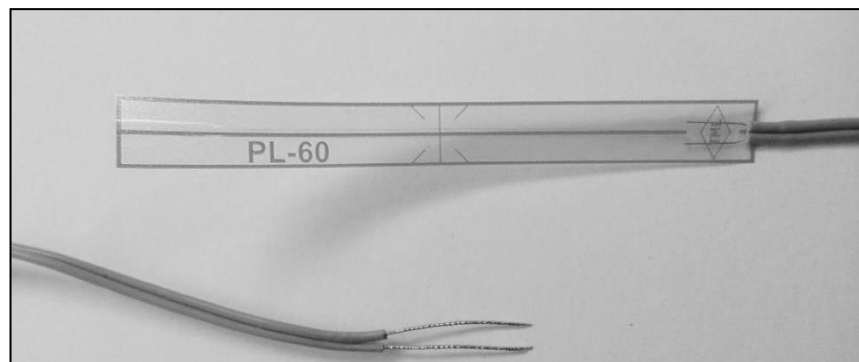
Figure 3.18: A sample of a strain gauge

3.1.6 Test setup

Specimens were loaded using Amsler Testing Machine at the mid of the span. Span between two supports was 600 mm. Dial gauges were placed at the middle of the beam soffit. Load was applied by increments of 2 kN. Central deflection, applied load and strain values were recorded. Failure mode, the load at initiation of crack, capacity under serviceability limits and ultimate capacity were noted. A schematic diagram of test set up is shown in Figure 3.19 and the test apparatus is shown in Figure 3.20.
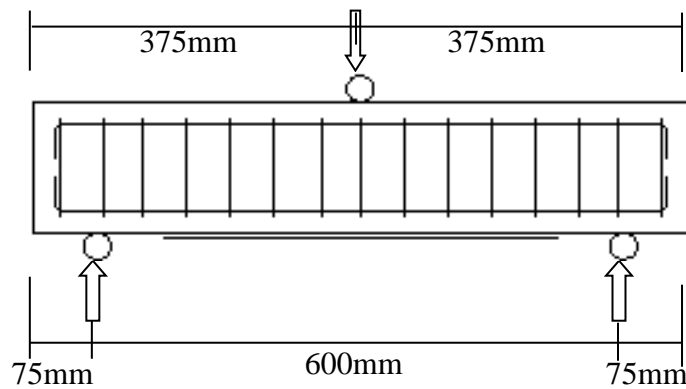
Figure 3.19: Schematic diagram of test set up (three point bending test)
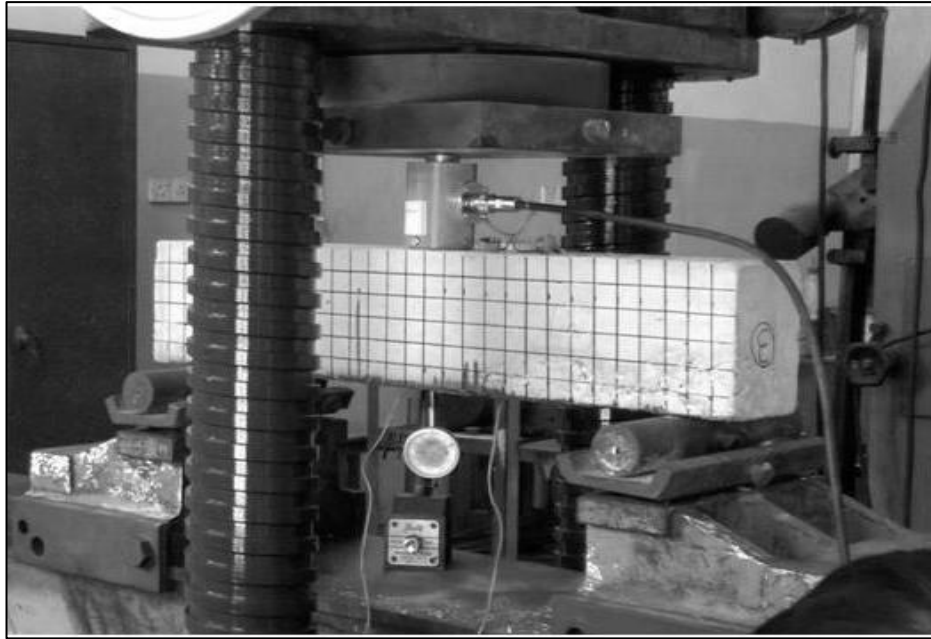
Figure 3.20: Test set up

3.2   Experimental results and analysis

This section presents the results of experimental study. It includes failure modes observed for each element, load deflection relationships and strain variation along the beam span. The results are compared with the theoretical predictions and a discussion is also included in this section.

3.2.1   Test results

The beams were loaded in a constant rate and deflection values were recorded at every 0.2 Mt intervals. Strain values were measured at a rate of 2 readings per second using a data logger.

3.2.1.1   Ultimate Failure Loads

Ultimate failure was account when the beam does not take any further load. The ultimate load values for each specimen are given in Table 3.4.

Table 3.4: Ultimate failure loads

Specimen designation	Ultimate failure load (kN)	Average failure load (kN)	Average Percentage strength increment	
			Compared to unstrengthened beam	Compared to beams without end anchorage
C(1)	20.01	20.79	-	-
C(2)	21.58			
F(1)	37.67	39.73	98.53 %	-
F(2)	41.79			
FA1(1)	50.81	49.05	145.1 %	23.45 %
FA1(2)	47.28			
FA2(1)	52.34	50.69	153.35 %	27.6 %
FA2(2)	49.05			

As shown in the comparison, an average strength increment of 98.53 % was achieved with flexural strengthening of concrete beams relative to un strengthened beams. When the end anchorage is provided and debonding is fully prevented, the average ultimate strength gain has increased up to 145.0 %. It is a 23.45% higher load carrying capacity compared to beams without end anchorages.

Flexural capacity of beams anchored at two ends and mid span did not show a very high strength increment over end anchored beams. The average failure load of end anchored beams is 49.05 kN whereas that of mid span anchored beams is only 50.69 kN. It indicates that the provision of mid span anchorage in addition to end anchorage has not become much effective. The reason is that the mid span U-wrap cannot prevent mid span debonding. Flexural cracks occur at the place where the U-wrap terminates, and the interfacial strains increase. Ultimately, the beam fails due to rupture of CFRP sheet.

3.2.1.2 Failure modes

Failure mode is very important in predicting the load carrying capacity. Therefore sequence of occurrence of failure modes in each test beam was carefully observed from crack initiation to ultimate failure. Table 3.5 summarizes the details on failure modes of the beams.

Table 3.5: Failure modes of the beams

Beam designation	Description of the failure mode
C(1), C(2)	Flexural failure due to steel yielding
F(1), F(2)	End delamination at concrete epoxy interface.
FA1(1), FA1(2)	Failure due to FRP rupture at the center of the span
FA2(1), FA2(2)	Failure due to flexural crack induced debonding initiated at mid span

3.2.1.2.1 Specimens C(1) and C(2)

Specimens C(1) and C(2) are the control beams. When load is applying, a single flexural crack was initiated at the middle of the span of both specimens as shown in Figure 3.21 and Appendix B.2. The crack was widened with increasing load and ultimately failed due to yielding of steel. Local crushing of concrete was observed at the load application point. The failure was a ductile failure.
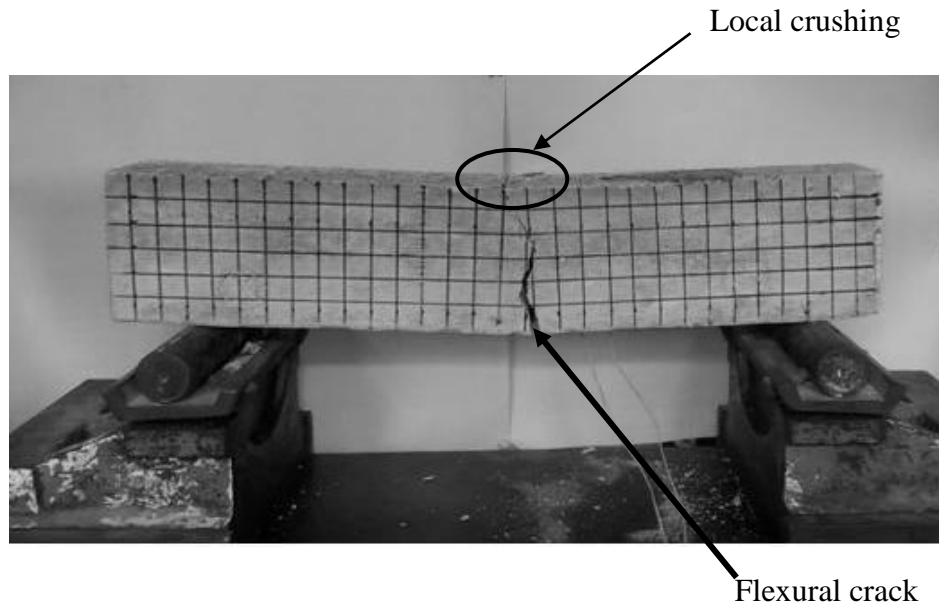
Figure 3.21: Flexural failure of specimen C(1)

3.2.1.2.2 Specimens F(1) and F(2)

Both the specimens failed due to concrete cover separation at concrete/epoxy interface. First, few small cracks were initiated closer to the mid span. Then, a shear crack occurred at the edge of the CFRP sheet approximately at about 45 degree angle, as described in Figure 3.22. It was extending towards the load application point. When the crack gets widened, the crack path suddenly changed to a horizontal profile which follows the track of internal flexural reinforcement. The crack path is shown in Figure 3.23. The bottom most line of the mesh drawn on the beam indicates the thickness of the cover and thus it is the same level of flexural reinforcement.

According to the behaviour of the beam the failure mode can be concluded as concrete cover separation which belongs to debonding type of failure. The reason for cover separation may be due to very high level of stresses concentrated at the plate ends.

No any local effects such as concrete crushing or debonding were observed. However in both the beams cover separation occurs at one edge and few very narrow shear cracks were marked at the other edge.
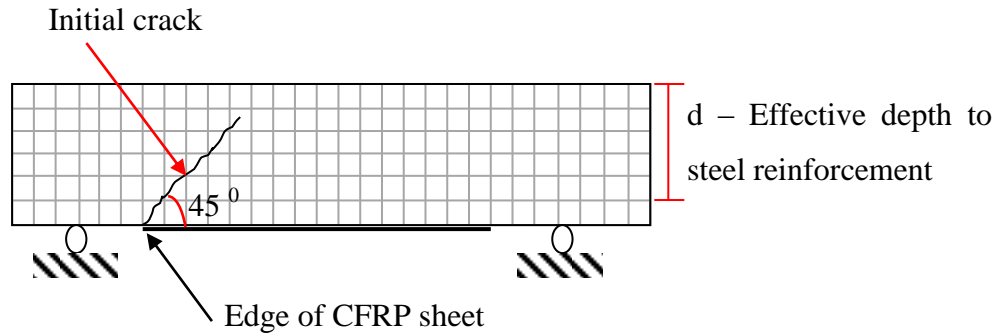
Figure 3.22: Schematic diagram of crack initiation in specimen F1
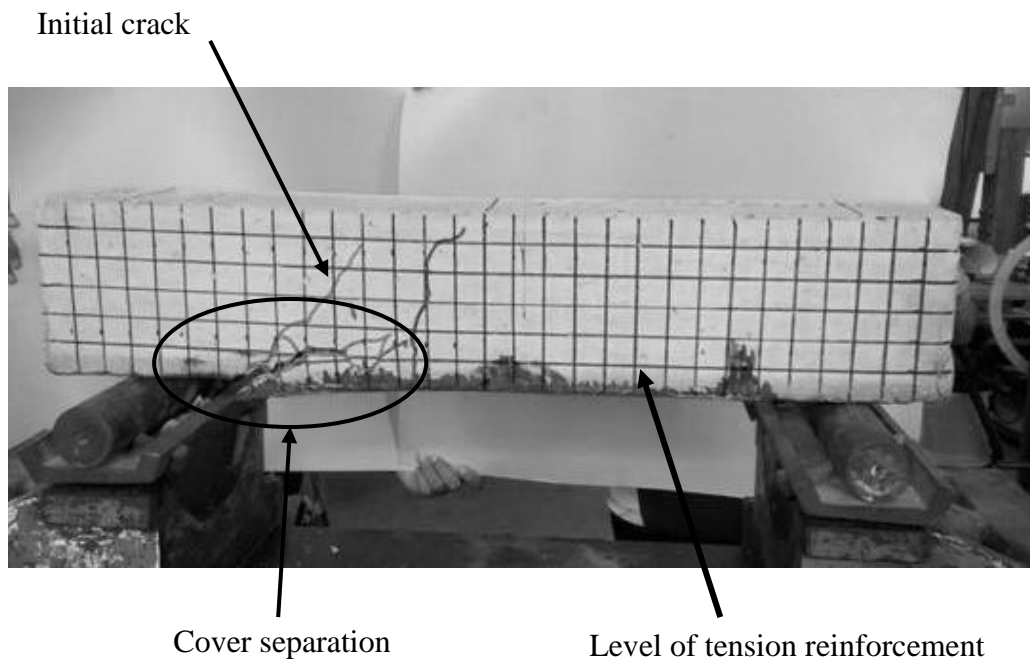
Figure 3.23: Speciman F(2) after failure

3.2.1.2.3 Specimens FA1(1) and FA1(2)

External reinforcement of these two specimens was end anchored with 60 mm wide CFRP inclined end straps. Therefore, the edges of the specimen remained more stable while loading. As far as sequence of failure is concerned, initial cracks were occurred from middle of the span. They were propagated with increasing load. As a result of large strain at the crack, flexural FRP reinforcement began to debond. Widening of the flexural crack became more faster after debonding and then, CFRP layer ruptured at the mid span.

In FA(1) specimen, debonding propagated towards the edges until the end wraps are met. Some damage to end wraps was also observed. In the specimen FA(2), the edges of the longitudinal CFRP sheet had not affected by the loading. No signs of rupture or delamination were shown. However, debonding had continued up to location of end wraps in this beam.

Non debonding of end straps indicates that sufficient amount of end anchorage had been provided to the flexural CFRP reinforcement.

Figure 3.24 indicates type of failure occurred in specimen FA(2) and Figure 3.25 shows rupture of FRP in the same specimen.
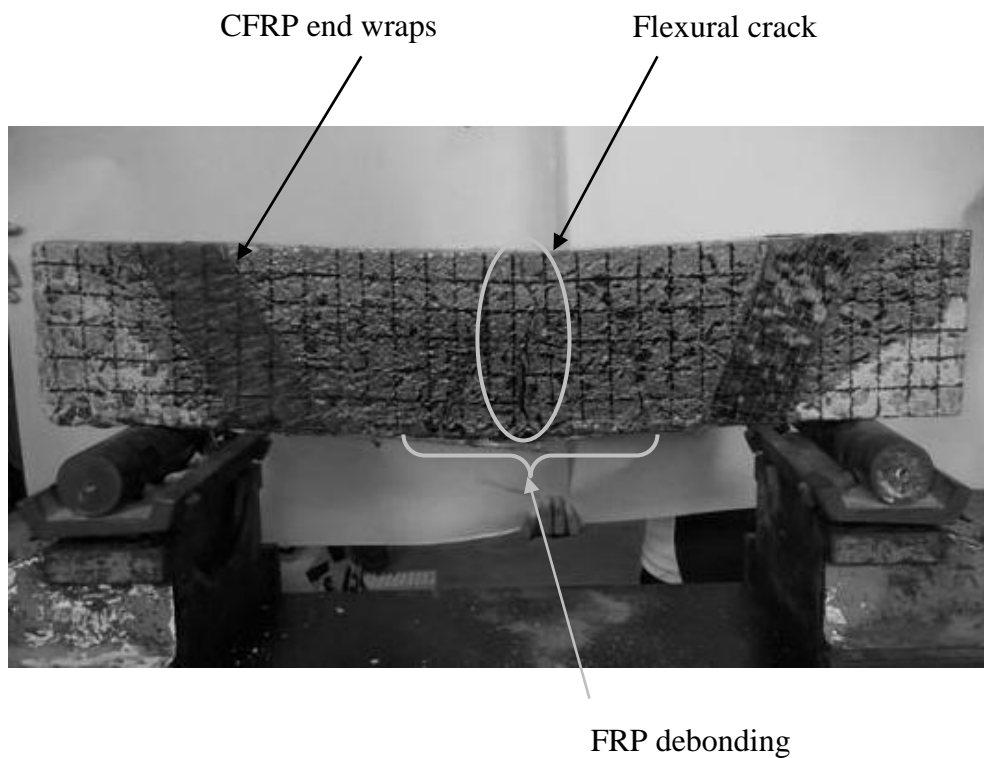
Figure 3.24: Specimen FA(2) after failure
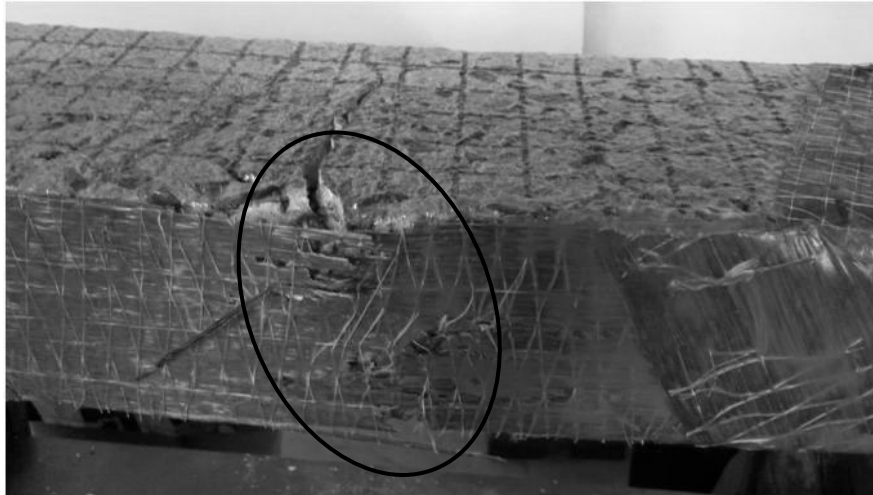
Figure 3.25: CFRP rupture occurred in specimen FA(2)

3.2.1.2.4 Specimens FA2(1) and FA2(2)

These beams had mid span U-wrap anchorage, in addition to the anchorage provide in FA1 specimen ends. Failure of these specimens was very complex. Initially, a flexural crack occurred along the border of the mid U-wrap. Then, debonding of concrete substrate began at the location of the crack and propagated towards the edge. In FA2(2) specimen, the end of the CFRP sheet debonded the end wraps. A thin layer of concrete has attached to the debonded CFRP sheet. Concrete crushing was also observed near the middle of U-wrap. Figure 3.26 and Figure 3.27 show pictures of FA2(2) beam after testing.
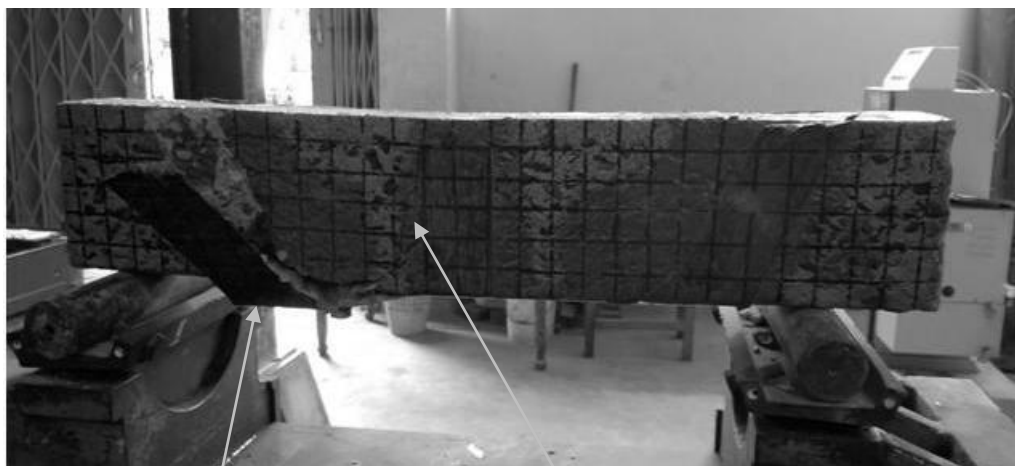
Debonding of end wrap   First crack at the mid span

Figure 3.26: Failure of specimen FA2(2)

Since the CFRP longitudinal reinforcement is anchored at both mid span and ends, a high energy is required to occur interfacial debonding. Flexural cracks occur in the concrete substrate at closer spacing, prior to interfacial debonding. These cracks are known as concrete tooth (Li, et. ai. 2013). When the stresses at the root of the tooth exceeded the tensile strength of the concrete, the concrete cover between two adjacent cracks broke (Li, et. ai. 2013). As a result, concrete tooth breakage takes place in the beam instead of interfacial debonding, which was observed in FA1 specimens.

Flexural cracks at the mid span   Concrete tooth breakage
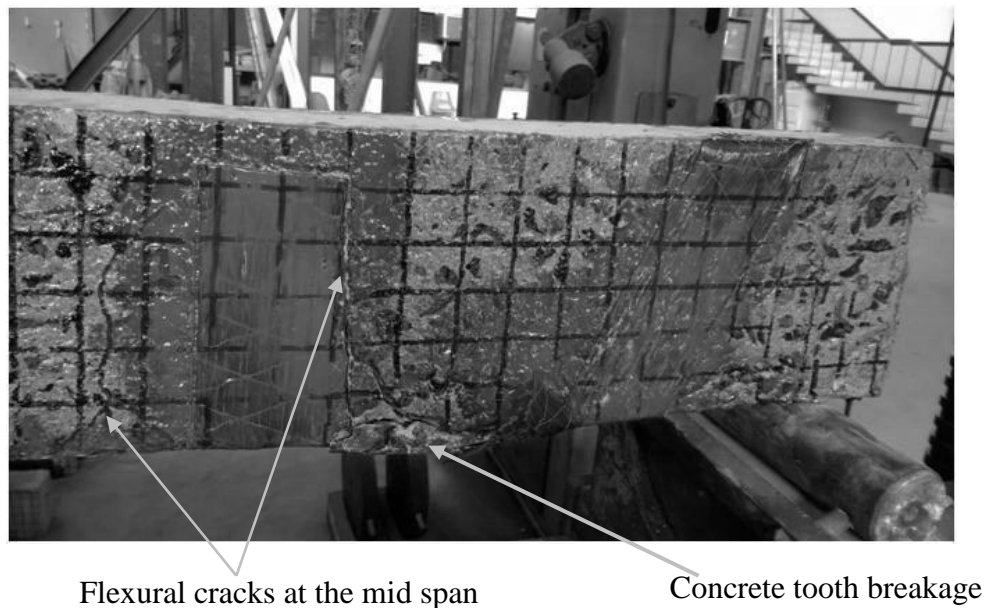
Figure 3.27: Concrete crushing in specimen FA2(2)

FA2(1) did not show concrete tooth breakage. However, its failure sequence was similar to FA2(2). The CFRP flexural reinforcement was detached from the element with a thin concrete layer attached to the strip. At the debonded edge, the end straps had ruptured along the edge of the beam instead of debonding (Figure 3.28).
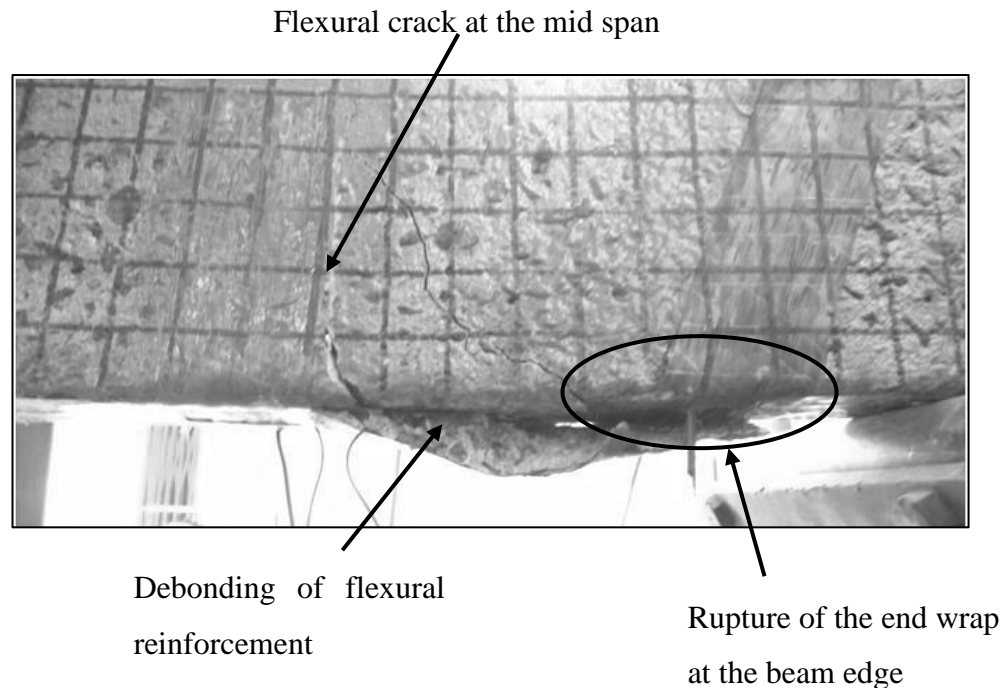
Figure 3.28: Failure of specimen FA2(1)

3.2.1.3   Serviceability failure

Occurrence of 0.3 mm wide crack or excessive deflection was considered as the limit for serviceability failure. Load corresponding to 0.3 mm wide crack was taken as the failure load. According to BS 8110: Part I: 1997, Clause 3.2.1, the noticeable deflection can be calculated as $L/250$ where L is the span length of the beam. The span of test specimens is 600 mm.

$$\frac{L}{250} = \frac{600\ mm}{250} = 2.4\ mm$$

Therefore the maximum allowable deflection for the beam in order to satisfy safety requirements is 2.4 mm. Figure 5.9 shows serviceability failure loads of specimens under the two criteria; occurrence of 0.3 mm wide crack and 2.4 mm deflection. For type C and type F beams, the failure criterion was visible cracks. For type FA1 specimens, achieving limiting crack width and 2 mm deflection happened coincidently. FA2 beams showed excessive deflection before reaching 0.3 mm wide crack.

	C(1)	C(2)	F(1)	F(2)	FA1(1)	FA1(2)	FA2(1)	FA2(2)
■ 0.3 mm wide crack	15.7	13.73	35.32	27.47	41.202	41.202	41.202	41.202
▨ 2.4 mm deflection	19	17.65	38	39.24	44.14	41.202	36.76	35.32
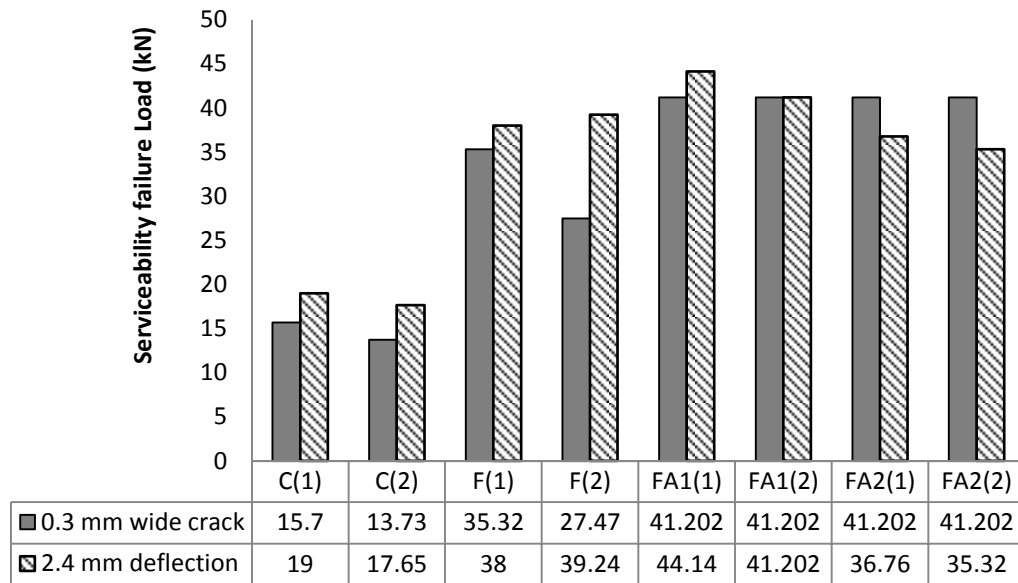
Figure 3.29: Serviceability failure loads of specimens

Table 3.6 shows the failure loads of specimens under serviceability limit conditions. The average strength gain of flexural strengthened beams is about 113.43 % compared to that of control beams. The end anchored beams showed a load increment of 180.10 %. Serviceability failure load of FA2 specimens is lesser than FA1 specimens. It shows only 15.53 % strength increment over type F beams whereas FA1 beams obtained 31.23 % strength gain. The trend of mid span deflections is also increasing with the increments of load capacities.

Table 3.6: Serviceability failure loads and deflections

Beam designation	Serviceability failure load (kN)	Average failure load (kN)	Mid span deflection corresponding to failure load. (mm)	Percentage strength increment %	
				With respect to control beam	With respect to CFRP strengthens beam (without anchorage)
C(1)	15.7	14.71	0.60	-	-

78

C(2)	13.73		0.72		
F(1)	35.32	31.395	1.60	113.43 %	-
F(2)	27.47		1.14		
FA1(1)	41.202	41.202	2.10	180.10 %	31.23 %
FA1(2)	41.202		2.40		
FA2(1)	36.76	36.27	2.40	146.57 %	15.53 %
FA2(2)	35.78		2.40		

3.2.1.4 Load Vs deflection relationships

Load deflection behaviour of a beam helps to determine its stiffness and ductility. Therefore the curves are very important when assessing the applicability of the proposed techniques in to practice.

Applied load vs. mid span deflection curves plotted for the specimens of current study, are shown in Figure 3.30. The deflection corresponding to 0.3 mm wide crack is marked on the relevant curve with a special mark, in order to assess the serviceability limit state performance.

As far as a simply supported beam loaded at the centre is concerned, the strain can be taken as a measure of deflection. Similarly, the stress becomes a measure of force in the elastic region. Therefore according to Hooke's low, the gradient of a load deflection curve indicates the stiffness of the beam and it is also named as elastic modulus. According to this theory, the gradient of the elastic region of the curve indicates the stiffness of the beam.
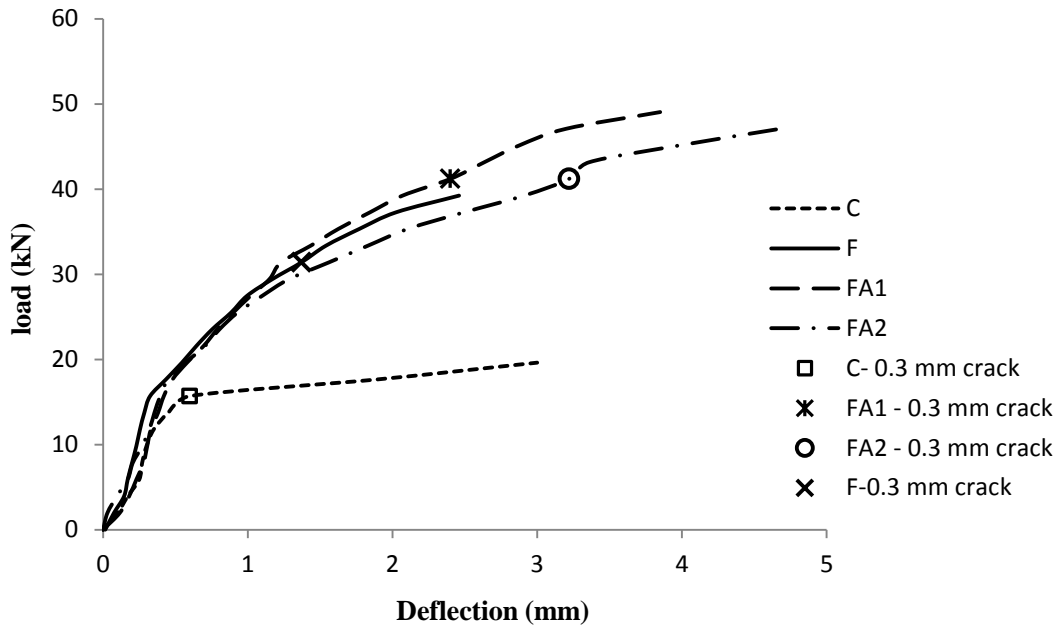
Figure 3.30: Load vs. mid span deflection

In the load vs. mid span deflection plot, it can be seen that the stiffness of control beam is lower than stiffness of the strengthened beams. All three strengthened beams have almost the same stiffness irrespective of their external reinforcement configurations.

Ductility is a very important parameter when determining the safety aspects of a structural member. If the ductility is large enough, the element will give an ample warning of an impending failure allowing sufficient time to take remedial actions. Ductility is usually quantified as a ductility factor or a ductility index (μ_Δ). It is mathematically defined as the ratio of maximum deflection (Δ_m) to displacement at yield (Δ_y).

$$\mu_\Delta = \frac{\Delta_m}{\Delta_y}$$ .... Equation 3.1 (Jayanath, 2013)

The ductility index was calculated using Δ_m and Δ_y values obtained from Figure 3.30. the results of ductility assessment are summarized in Figure 3.31.
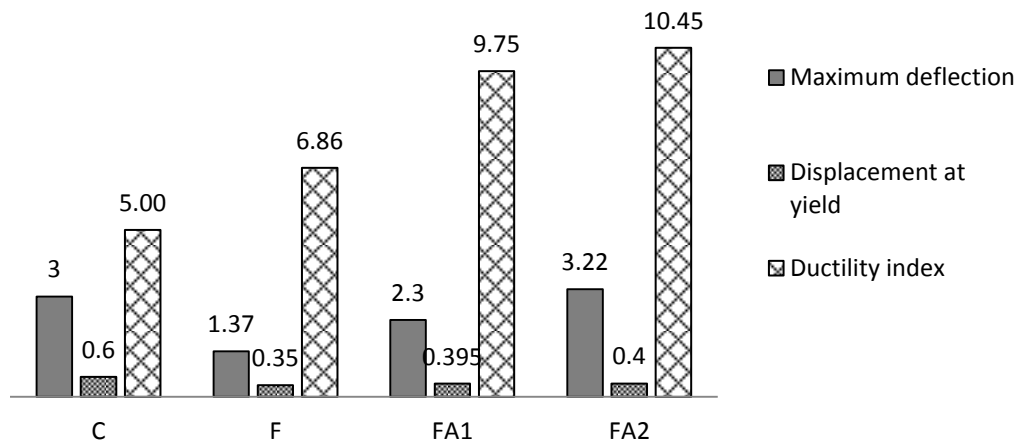
Figure 3.31: Ductility indexes of specimens

In the current study, the ductility has increased with provision of FRP external reinforcement. In most studies (Gunes et. al.2009, Dong et. al. 2013 Jayanath 2013), a reduction of ductility index have observed with strengthening using CFRP. In those experiments, yielding has occurred at a large displacement. However in current test program, displacement corresponding to yielding is small and therefore, ductility indexes have increased in strengthened beams. Reason for small deflection at yield is the low steel reinforcement ratio. A similar variation of deflection with respect to load has observed by Shou et.al. (2013).

3.2.1.5 Load - strain relationships

3.2.1.5.1 Specimens C(1) and C(2)

Variation of strains along the beam at different load increments is shown in Figure 3.32. The end strain is comparatively very smaller than the strain in the mid span. The difference of strains between mid-span and edge is increased while increasing the applied load.
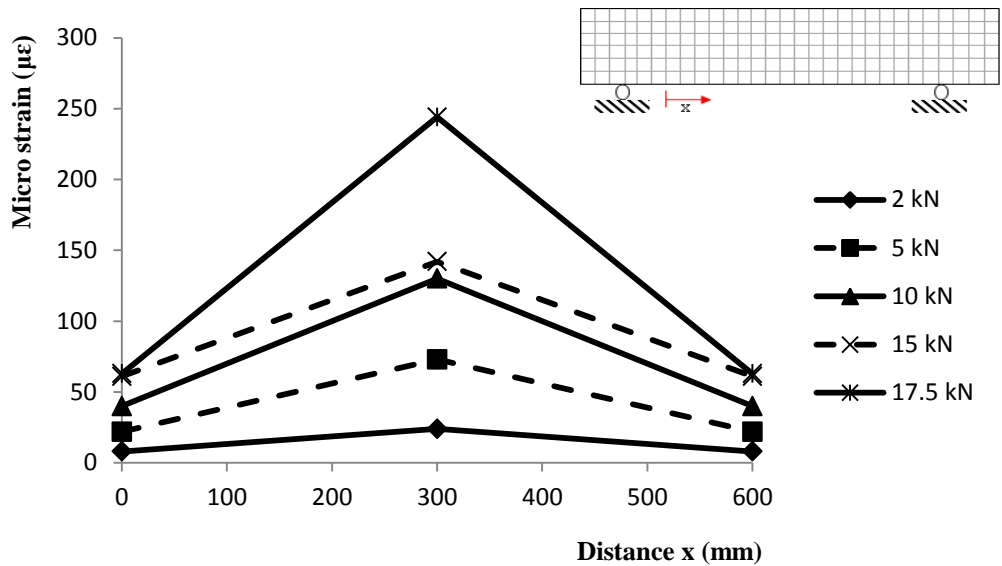
Figure 3.32: Strain distribution along type C specimens

As far as the applied load vs. micro strain plot is concerned, the initial region shows a linear strain increment with load (Figure 3.33). After about 14 kN, the strain shows very high increments for a small range of rise in load. This may be because of yielding of steel tension reinforcement.
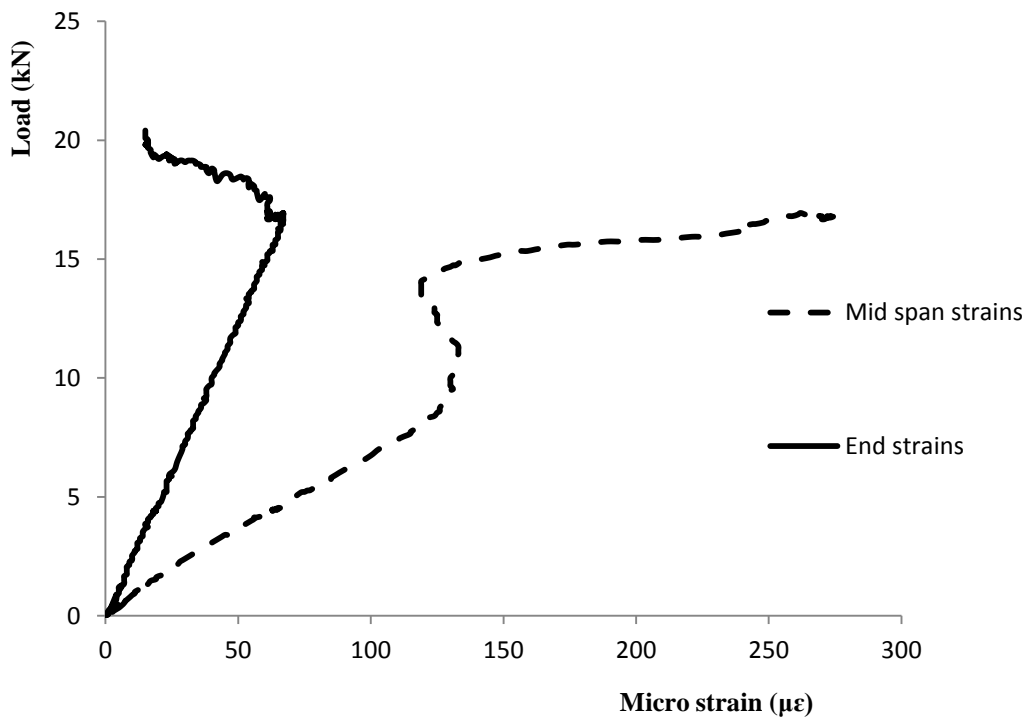
Figure 3.33: Applied load vs. Micro strain for type C specimens

3.2.1.5.2 Specimens F(1) and F(2)

The distribution of strain in CFRP along F(1) and F(2) beams are shown in Figure 3.34. Strain at the edge of CFRP laminate is zero for all the load values and end strain has increased greatly, compared to unstrengthened specimens.
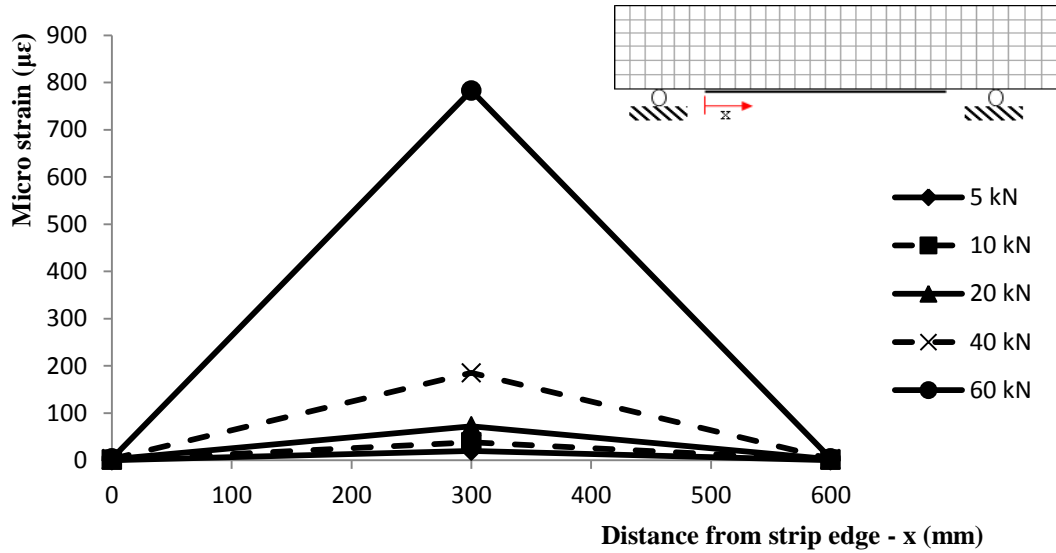
Figure 3.34: Micro strain vs. Distance curve for type F specimens
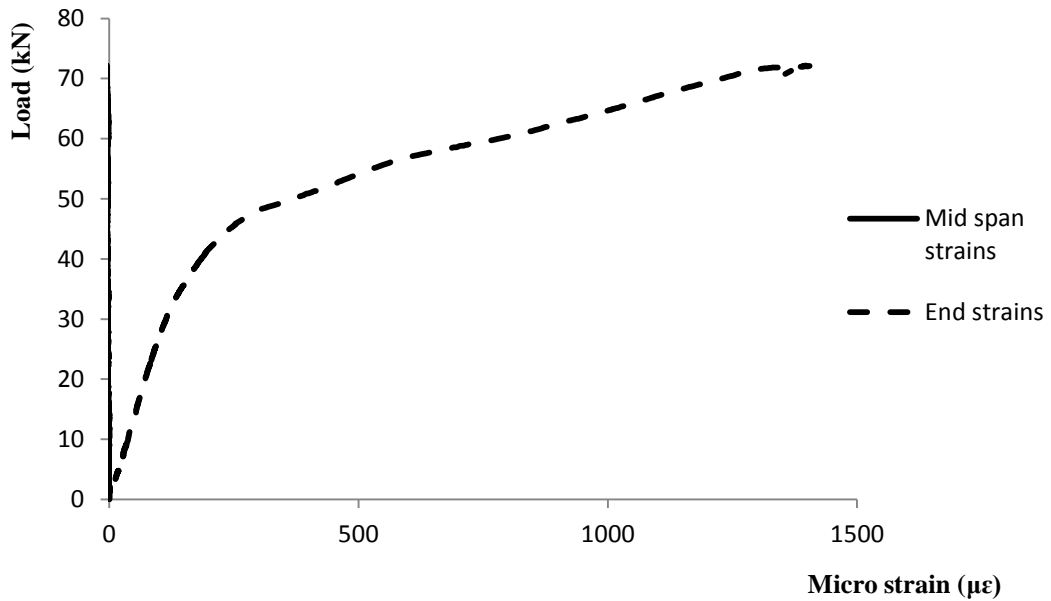
Figure 3.35: Applied load vs. Micro strain for type F specimens

Micro strain variation of type F specimens with applied load is almost similar to type C specimens. The initial region is liner and stiffness is large. The latter portion shows

a lower stiffness. This change of stiffness may be due to releasing stresses by the gradual delamination of concrete cover. The load vs. strain diagram is shown in Figure 3.35.

3.2.1.5.3 Specimens FA1(1) and FA1(2)

With the introduction of inclined wrap end anchorage in type FA1 beams, the strain levels have increased compared to type F beams. This indicates that the strength of CFRP reinforcement is effectively utilized when the edges are anchored with end wraps. The strain distribution is shown in Figure 3.36.
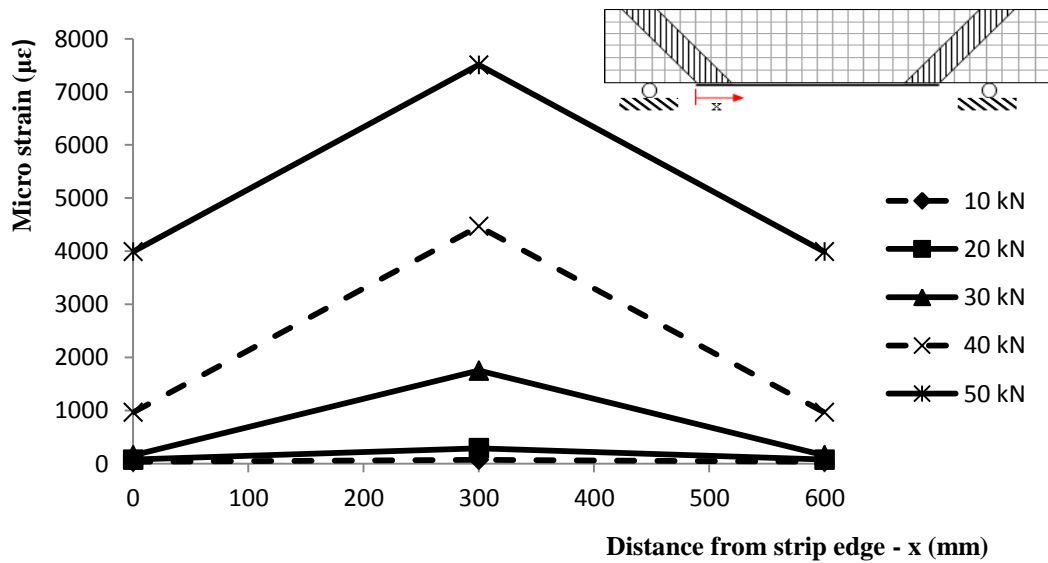
Figure 3.36: Micro strain vs. Distance curve for type FA1 specimens

In type F beams, cover separation has occurred at a strain of about 1400 με. FA1 beams have been able to withstand about 4000 με without debonding or cover separation. This is clear because of the presence of end wrap anchorages.
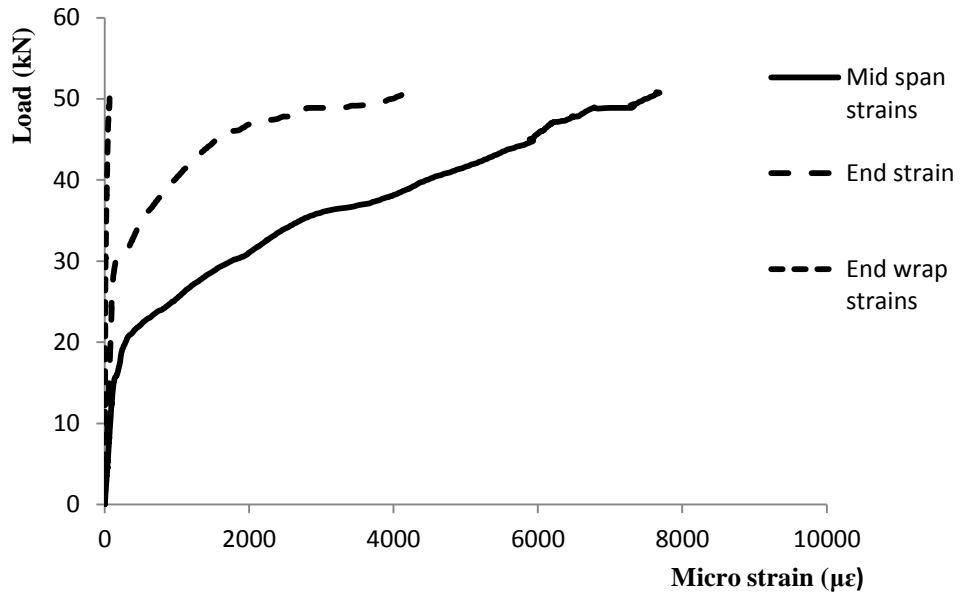
Figure 3.37: Applied load vs. Micro strain for type FA1 specimens

As shown in Figure 3.37, end wraps have not subjected to a considerable strain. The stiffness has further increased in FA1 beams. A change of stiffness can be seen in these specimens as in other two types. In this case, the reason may be steel yielding or gradual damage takes place in FRP sheet while achieving the rupture strain.

3.2.1.5.4 Specimens FA2(1) and FA2(2)
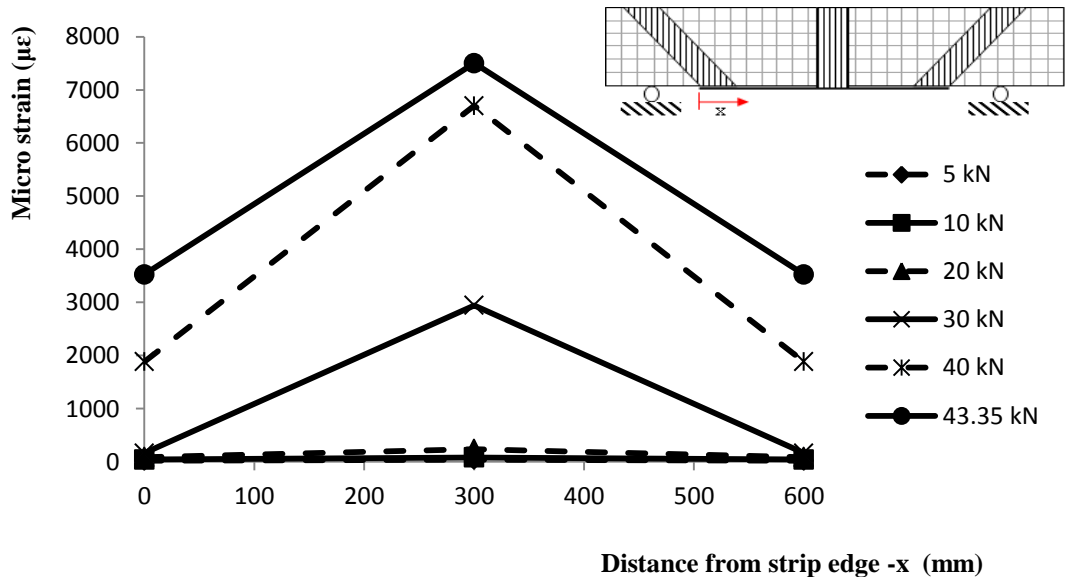
Figure 3.38: Micro strain vs. Distance curve for type FA2 specimens

Strain distribution for FA2 beams is shown in Figure 3.21. The variation is similar to FA1 beams. Ultimate failure loads of these two beam types were almost equal. Accordingly, magnitudes of the strains are also in the same range. These results indicate that the mid span wrap has not contributed to reduce longitudinal strain.
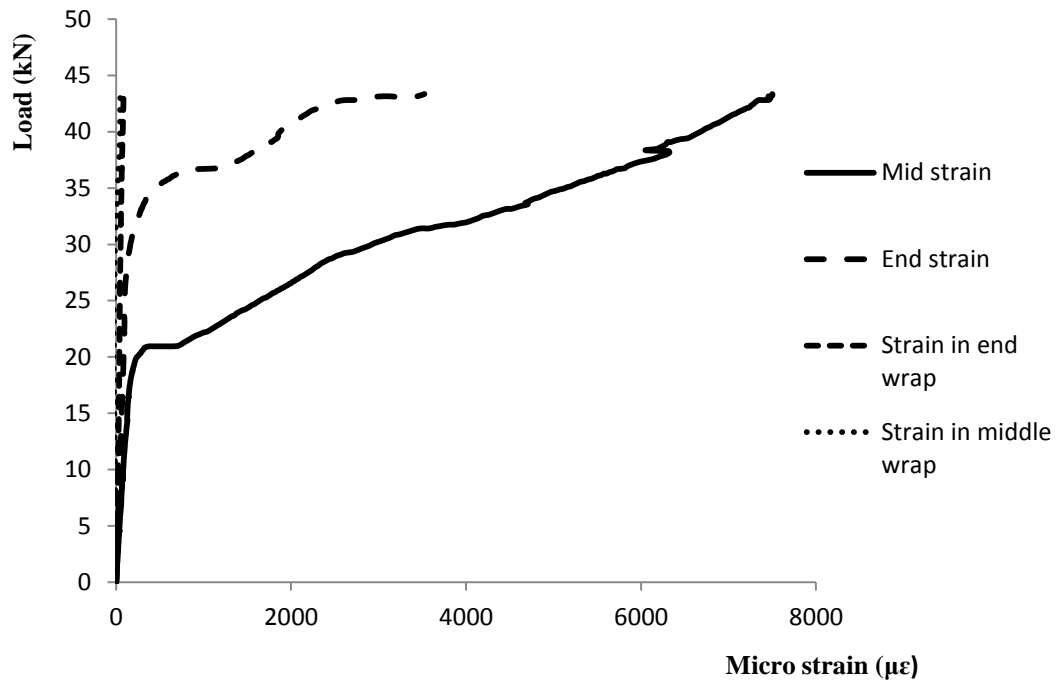
Figure 3.39: Applied load vs. Micro strain for type FA2 specimens

Applied load vs. micro strain plot is also very similar to FA1 specimens. Strain in end wrap is very small throughout the loading process. Strain in mid span U-wrap shows negative values up to about half of the applied load and it has become positive but very close to zero at the ultimate load. It suggests that initially, the mid span wrap has undergone compression.

3.2.1.6   Bond-Slip behaviour

Bond slip curves for each specimen was plotted in order to study the behaviour of interface in bending. Bond stress between two points of the beam was determined by dividing the difference of stresses at two given locations by the distance between them. Figure 3.40 elaborates the terms and Equation 3.2 mathematically represents this relationship.
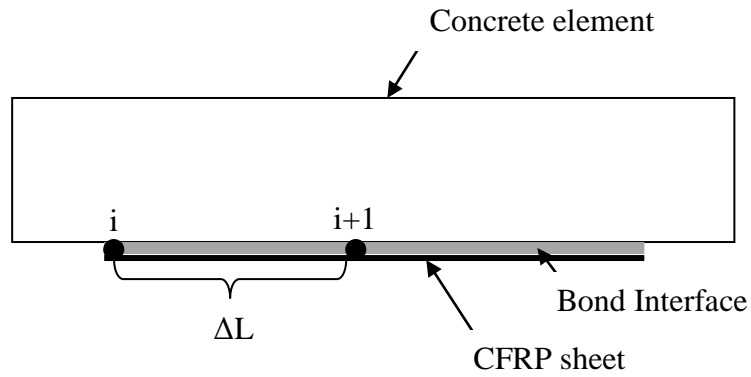
Figure 3.40: Schematic diagram of development of interfacial bond stress

$$\tau = E_f \frac{(\varepsilon_{f,i+1} - \varepsilon_{f,i})t_f}{\Delta L} \ \dots\dots\dots\dots\dots\dots \text{ Equation 3.2 (Achintha 2008)}$$

The average slip (S_i) is calculated as the mean value of displacement at the two points. The relationship is given in Equation 3.3.

$$S_i = \frac{(\varepsilon_{f,i+1} + \varepsilon_{f,i})}{2}\Delta L \ \dots\dots\dots\dots\dots\dots \text{ Equation 3.3 (Achintha 2008)}$$

Specimen calculation

Interfacial bond stress; $\tau = E_f \frac{(\varepsilon_{f,i+1} - \varepsilon_{f,i})t_f}{\Delta L}$

$$= 640000 \times \frac{(1-0) \times 10^{-6} \times 0.19}{250}$$

$$= 0.0004864 \frac{N}{mm^2}$$

Slip; $S_i = \frac{(\varepsilon_{f,i+1} + \varepsilon_{f,i})}{2}\Delta L$

$$= \frac{(1+0) \times 10^{-6}}{2} \times 250$$

$$= 0.000125 \ mm$$

Bond slip curves generated for each specimen are shown in Figure 3.41 – Figure 3.42.
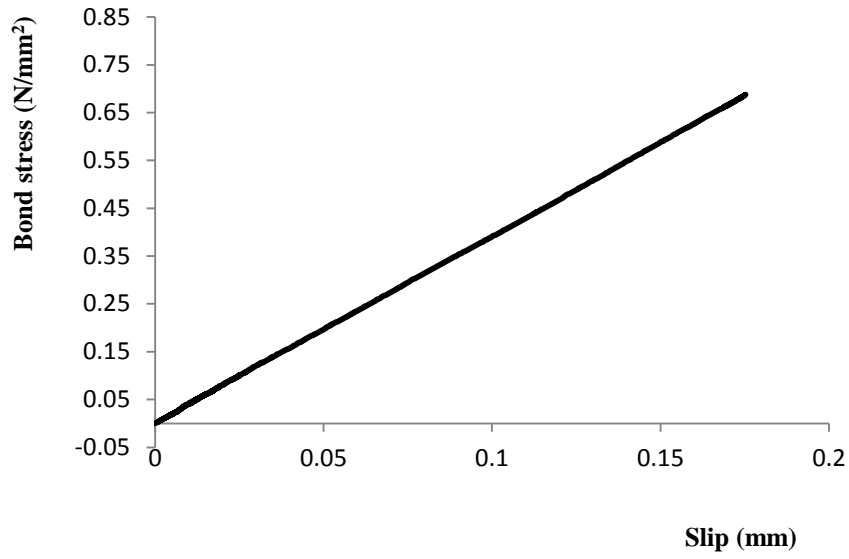
Figure 3.41: Bond Slip curve for type F specimens
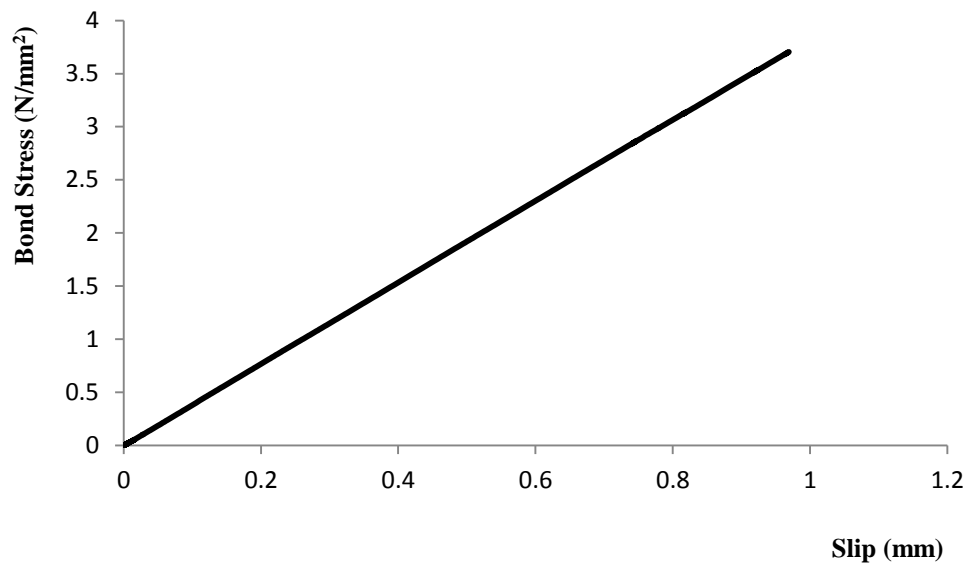
Figure 3.42: Bond Slip curve for type FA1 specimens
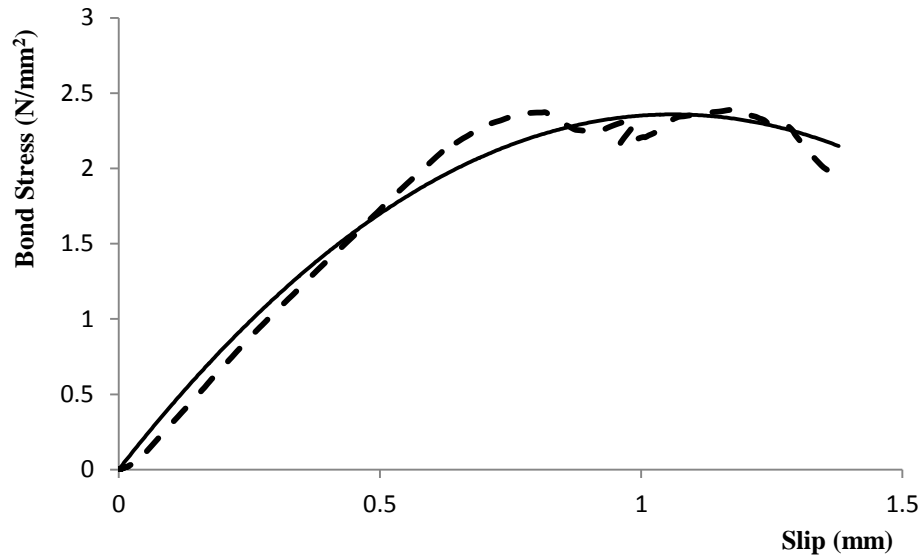
Figure 3.43: Bond Slip curve for type FA2 specimens

When the obtained bond slip curves are considered, they show only the initial portion of a normal bond-slip curve. This indicates that the interface have not reached its ultimate strength at the time of failure. The reason to this behaviour is because FRP rupture has occurred before the full bond strength is developed. However, in type FA2 specimens, the curve shows a greater portion of bond slip curve compared to Type F and FA1 specimens. The reason is that, FRP rupture in FA2 specimens has delayed due to the presence of mid span U-wrap. As a result, a greater portion of bond strength is developed in the interface of FA2 specimen. It proves that bond strength has more effectively used in FA2 specimens.

Fracture energy, G_f can be calculated from the bond slip curves. It is defined as area under the curve (Achintha 2008). It represents the amount of energy that should be excreted on the beam, in order to create fracture in it. Since energy is excreted by means of work done by externally applied load, fracture energy is an indirect representation of load carrying capacity.

According to Achintha (2008), there are two basic modes of occurrence of cracks in CFRP strengthened reinforced concrete beams, named as Mode I and Mode II. If the crack occurs at angle of 0° to the longitudinal axis, the failure mode is known as Mode I failure. When the alignment of crack is 90° to the longitudinal axis the failure

89

mode is Mode II. If the inclination of any crack is in between 0° and 90°, the failure is categorized as mixed mode. Normally, fracture energy of Mode I failure is less than 0.15 and that of Mode II failure is equal to 10-25 times Mode I fracture energy (Achintha. 2008).

As far as fracture modes of test specimens are concerned, type F specimens showed Mode I fracture and FA1 and FA2 specimens showed Mode II fracture.

Specimen calculation for type F specimens

Fracture Energy, G_f = Area under bond slip curve

$$= \frac{1}{2} \times 0.66199 \times 0.168875$$

$$= 0.0559$$

Fracture energy calculated for each specimen type is shown in Figure 3.43.

The figure shows that fracture energy increased with increasing anchorage.

$$G_{f,F} < G_{f,FA1} < G_{f,FA2}$$

These results indicate that, strengths of concrete beams are increasing with increasing anchorage amount. According to the results, fracture energy of type F specimens is equal to 0.05, which is less than the upper limit of 0.15 (Achintha 2008) for Mode I fracture. Fracture energy of FA1 and FA2 specimens are 1.77 and 2.4 respectively. It is respectively, 35.4 and 48 times the fracture energy of type F specimens.
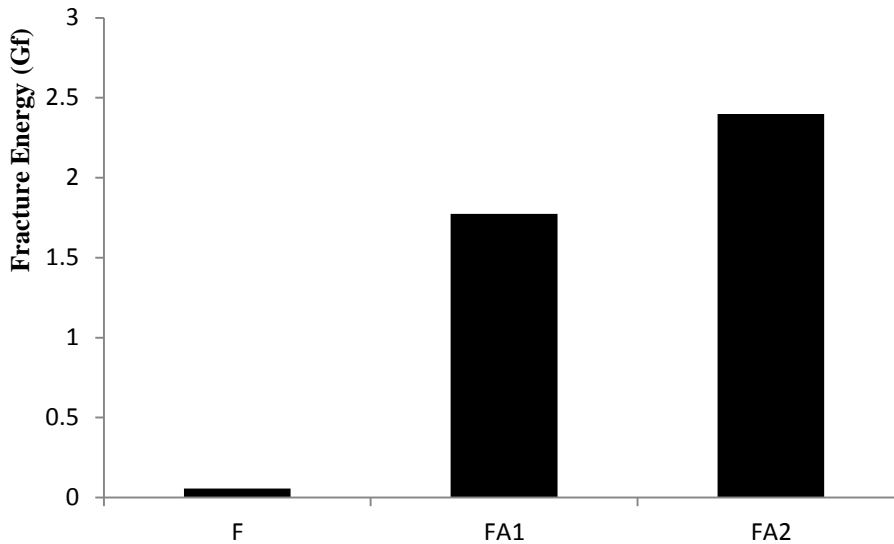
Figure 3.44: Fracture Energy of specimens

3.3   Conclusions

The experimental programme was objected to investigate the effect of inclined end wraps on the flexural capacity of externally strengthened reinforced concrete members. A total of eight small scale concrete beams were prepared and strengthened with four different external reinforcement configurations. The specimen types are;

1. Control beams with no external strengthening
2. Beams, externally strengthened for flexure with CFRP sheets
3. Flexural strengthened members with external reinforcement anchored at edges
4. Type 3 specimens anchored at mid span with CFRP u-wrap.

Specified characteristic strength of concrete for specimens was 30 N/mm^2. According to the mix design, the target mean strength of concrete was 43.12 N/mm^2. However, the actual mean strength of concrete was 47.46 N/mm^2. Since the actual mean strength is greater than target mean strength, the concrete mix can be recommended as a proper quality mix. They were consisted of internal flexural and shear reinforcement out of steel. According to the preliminary design calculations, the control beam had a capacity of 10.9 kN in flexure and 81.39 kN in shear.

The experimental results were analyzed for ultimate failure loads, failure modes, serviceability failure loads, load deflection relationships, ductility, load-strain relationships, bond slip behaviour and fracture energy.

When the control beams are concerned, their failure mode is flexural failure due to steel yielding. The beams indicated an average ultimate failure load of 20.79 kN. According to serviceability limit criterion, the failure load was 14.7 kN.

Type F beams failed due to concrete cover separation with an average strength gain of 98.53 % over control beams. Specimens of FA1 category showed a strength gain of 145.1 % relative to un-strengthened beams. Both type FA1 and FA2 beams showed almost the same strength increments under serviceability limit failure criteria. Failure mode for end anchored beams and the beams with combination of end and mid span anchorage was FRP rupture. As far as serviceability failure is concerned, FA2 beams showed excessive deflection before occurring wider cracks whereas most of the other beams behave in the opposite way. However, 0.3 mm crack and 2 mm limiting deflection was coincided in FA1 beams.

Stiffness values of FRP strengthened beams were higher than that of control beams. The variation of load and strain diagrams also provides further evidence. The strengthened beams showed large ductility indexes compared to that of control beams. This is because of small steel reinforcement ratio used in the specimens.

About 60 mm wide end anchors could totally prevent cover separation failure. The provision of end anchorage yielded high strength increments and mid span U-wrap was not effectively contributing to strength gain in the presence of end anchorage.

When the strain along the beams is concerned, the CFRP sheet achieved larger strains in presence of end anchorage. It is an indication of more effective use of CFRP.

The Bond Vs Slip curve has not fully developed in any of the test specimens. Type F and FA1 specimens showed only a linear portion of the usual bilinear bond – slip curve. The reason for partial development of bond slip curve is occurrence of CFRP rupture before the bond strength is completely developed. This inefficiency of

utilization of bond strength can be prevented by proper matching of rupture strength of CFRP and bond strength of epoxy adhesive. It is also observed that effectiveness of bond strength is increasing with increasing anchorage.

As far as fracture behaviour is concerned, type F beams failed on Mode I fracture, where the crack is parallel to longitudinal axis. The fracture energy was 0.05. When it comes to FA1 and FA2 beams, the fracture mode was Mode II fracture. The fracture energy is 1.77 and 2.4 respectively.

CHAPTER 4

4 Theoretical Analysis

4.1 Introduction

A theoretical model which can predict behaviour of structural elements is the key to develop design guidelines. When the existing models are concerned, there are design guidelines available to predict flexural and shear enhancement independently. However, predicting combined effect of flexural reinforcement anchored with end wraps is still in research. In this study, an effort was taken to identify the parameters affecting to strength gain of end anchored, flexural strengthened beams and a relationship among them was also developed. In order to initiate the model, available design equations proposed by several authors were assessed. The new model was proposed after quantifying the strength gain by end anchorage and it was validated using experimental results. The calculation procedure and the comparison of theoretical results with the experimental results are included in this chapter.

4.2 Analysis of FRP strengthened concrete beams

Load carrying capacities of strengthened beams were predicted using three methods given in the literature namely ACI-440-R design guide, FIB-bulletin-14 design guide and Li et al. (2013) design method.

The beam geometry, reinforcement details selected in the calculations are shown in shown in Figure 4.1. Clear span of each beam was 600 mm and shear span was 300 mm. Flexural steel reinforcement was consist of two 6 mm diameter mild steel bars in tension similar arrangement for compression reinforcement. Shear reinforcement was 4 mm galvanized iron wires spaced at 50 mm intervals.

External flexural reinforcement of the strengthened beams was a 90 mm wide and 450 mm long CFRP strips symmetrically bonded along the beam soffit. End wraps were 60 mm wide and inclined with inclination of 63.43^0 to the horizontal plane, so that the fiber direction is perpendicular to the expected shear crack path.

All the calculations were conducted according to the aforementioned geometry and reinforcement details. When the design guides does not provide specific equations

for inclined wraps, the methods specified for U-wraps were followed in the calculations.
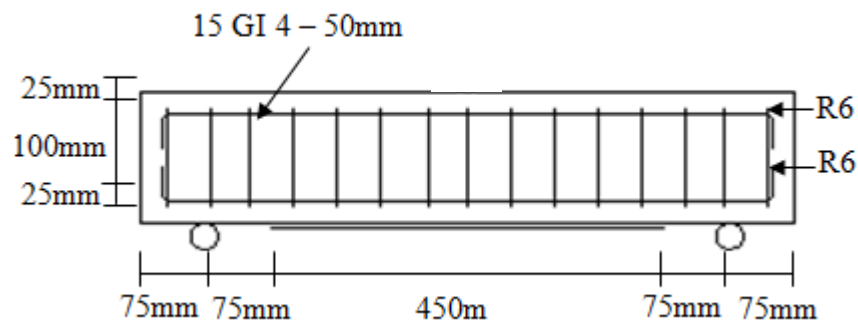
Figure 4.1: Schematic diagram of Geometry and reinforcement arrangement of test beams

Load carrying capacities of unstrengthened concrete specimens were calculated according to BS 8110 design guidelines (Appendix A). The calculated flexural capacity is 10.9 kN and shear capacity 81.39 kN. Therefore the control specimens will fail under flexure which is the lower capacity of member. The predicted failure mode is steel yielding.

4.2.1 ACI-440-R design guide

ACI guide is produced by the American Concrete Institute which is a leading authority and resource worldwide for concrete design. The institute has founded in 1904 and since then, it has involved with the development and distribution of consensus-based standards, technical resources, educational programs, and proven expertise for individuals and organizations involved in concrete design, construction, and materials, who share a commitment to pursuing the best use of concrete. Currently it is a well developed organization consists of 99 chapters, 65 student chapters, and nearly 20,000 members spanning over 120 countries (American concrete institute, n.d.). The mission of ACI is to provide knowledge and information for the best use of concrete.

ACI-440-R is the design guide for the design and construction of externally bonded FRP systems for strengthening concrete structures, published by the ACI committee.

It provides guidelines to predict flexural capacity of CFRP flexural strengthened concrete members using CFRP, shear capacity of CFRP shear strengthened concrete members and axial load carrying capacity of concrete members confined with CFRP. In addition to design equations, it has recommended the construction requirements and material quality requirements.

4.2.1.1 Stress distribution adopted for the design
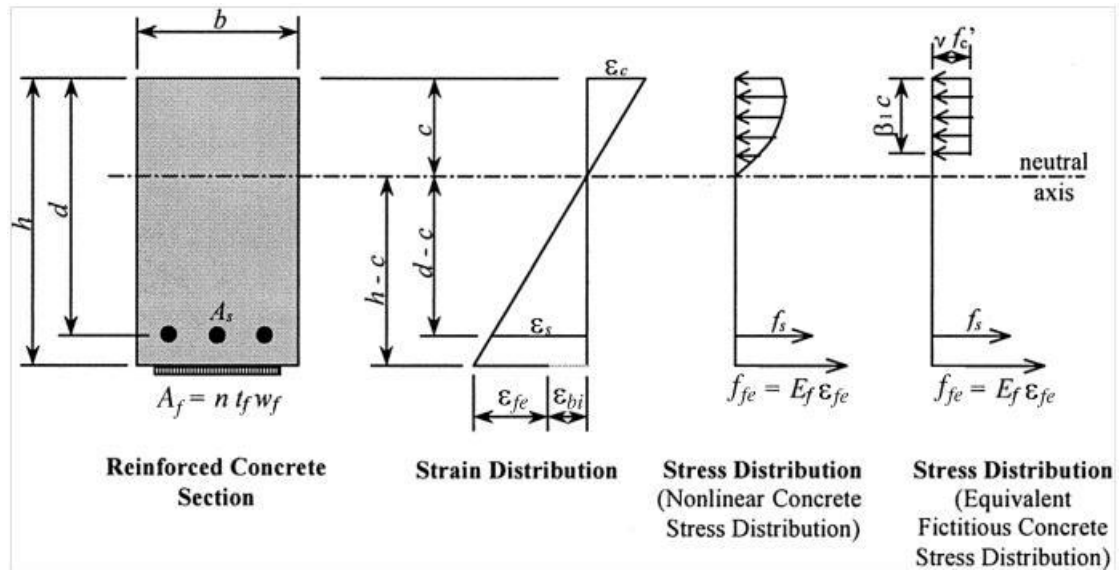
Figure 4.2: Internal strain and stress distribution for a rectangular section under flexure at ultimate stage (ACI 440.2R-02)

The assumed stress distribution over the cross section of FRP strengthened member, for design purposes in ACI-440-2R is shown in Figure 4.2. The code has idealized concrete stress in the compression zone in to a rectangular area. Compression capacity of top reinforcement and tension capacity of concrete below neutral axis are neglected. Tensile stress in FRP and bottom steel reinforcement is simplified in to two point loads acting at the centre of each reinforcement. All the safety factors given in the design guide were discarded in the current series of calculations.

4.2.1.2 Prediction of load carrying capacity and failure mode

ACI-440-2R has provided design equations to predict the capacity under premature failure. The calculations are shown in Appendix C.1.1. According to the predictions, the ultimate moment capacity is 5.32 kNm and applicable load is 35.53 kN. The system will fail due to FRP debonding. The calculations indicate that steel tension reinforcement have already reached its yield stress at the time of failure. If the premature failure is fully prevented, a flexural capacity of 7.44 kNm can be achieved by the system. The corresponding failure load is 49.69 kN (Appendix C.1.2.) and the failure is due to FRP rupture. Shear capacity of the concrete beam is still higher than the enhanced flexural capacity. Therefore the flexural strengthened concrete member will fail due to FRP debonding with an ultimate load of 35.53 kN.

With the provision of end wrap anchorage, the shear capacity and debonding load increase. If 100% prevention of debonding is assumed, failure can be either due to FRP rupture or due to shear failure. As calculated in Appendix C.1.3, ultimate load under shear failure is 106.98 kN whereas FRP ruptures at a load of 54.40 kN. In conclusion, the end anchored beam will fail due to FRP rupture if the provided anchorage is sufficient enough to fully prevent debonding.

4.2.1.3 Comparison

As far as experimental results are concerned, the specimens with 60 mm wide end straps could fully resist debonding. As a result, the system failed due to FRP rupture. Therefore, for this particular scenario, the predictions were accurate. A comparison of predicted results and experimental results is presented in Table 4.1. However the problem is prediction of ultimate capacity with lesser amount of end anchorage so that it cannot fully prevent premature failure.

Table 4.1: Comparison of ACI-440-2R predictions and experimental results

Description of the specimen	ACI-440-2R predictions	Experimental results	Percentage deviation from experimental results
Beam strengthened with FRP external reinforcement			
Moment capacity	5.32 kNm	5.61 kNm	-5.17 %
Ultimate load	35.53 kN	39.73 kN	-10.57 %
Failure mode	Premature failure including end debonding and cover separation	Concrete cover separation	-
Beam strengthened with FRP external reinforcement and end anchored with 60 mm wide CFRP inclined wraps			
Moment capacity	7.44 kNm	7 kNm	+6.28 %
Ultimate load	49.69 kN	49.05 kN	+1.3%
Failure mode	FRP rupture	FRP rupture	-

The predictions show very good agreement with experimental results, with a deviation less than 10% of the experimental results. When premature failure is concerned, the predictions are at the safe side and predictions for classical failure are in unsafe side.

4.2.2 FIB-bulletin-14 design guide

The International Federation for Structural Concrete (FIB - Fédération internationale du béton) has established in 1998, for the purpose of developing an international

level of study on performance of concrete construction. They make a special concern on scientific and practical methods which can improve technical, economic, aesthetic and environmental aspects of construction concrete. In order to achieve their objectives, they take measures to stimulation of research, synthesis of findings from research and practice, produce publications and guidance documents and organize international congresses and symposia. More than 1000 members representing 43 national member groups are actively corporate with the association.

As a result of their attempt, FIB has published a technical report on externally bonded FRP reinforcement for reinforced concrete structures in 2001. It is known as FIB-bulletin-14 and it includes the design and construction guidelines that should be adopted in FRP/concrete composites. The guideline is in accordance with the format of the CEB (Comité euro-international du béton)-FIP (Fédération internationale de la précontrainte) Model Code and Eurocode2. The report is a combined effort of 60 professionals, from most European universities, research institutes and industrial companies working in the field of advanced composite reinforcement for concrete structures, as well as corresponding members from Canada, Japan and USA.

4.2.2.1 Stress distribution profile adopted in the design
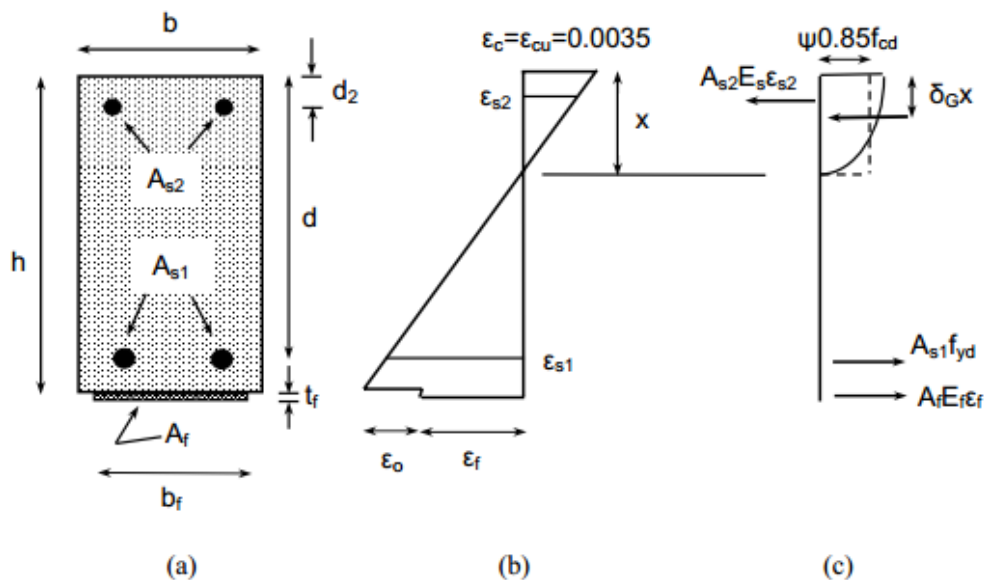
Figure 4.3: Analysis of cross section for the ultimate limit state in bending: (a) geometry, (b) strain distribution and (c) stress distribution (FIB Bulletin 14).

Similar to ACI-440-2R method, FIB-bulletin-14 also idealize the concrete compressive stress distribution in to a rectangular distribution. It neglects tension stresses in concrete and represent stresses in tension reinforcement by point loads as same as ACI. However, FIB-bulletin-14 takes the compressive stresses in steel reinforcement in to consideration in the calculations.

4.2.2.2 Prediction of load carrying capacity and failure mode

FIB- bulletin-14 has proposed separate design equations to predict failure load of the system due to steel yielding followed by concrete crushing and steel yielding followed by FRP rupture. They have specified a minimum anchorage length required for flexural reinforcement in order to prevent debonding failure. They have predicted end shear failure including concrete rip off failure with different set of equations.

The minimum anchorage length requirement for the test specimens according to FIB-bulletin-14 is 118.7 mm. The actual anchorage in the test specimens is 300 mm. Therefore, it can be predicted that debonding does not take place in the system. However provision of adequate anchorage length does not grantee the prevention of cover separation failure.

According to the predictions conducted in Appendix C.2.2. and Appendix C.2.3., classical failure will occur due to steel yielding followed by FRP rupture. The ultimate capacity is 54.87 kN. As predicted in Appendix C.2.4. end shear failure or cover separation failure will take place at a load of 31.5 kN. In conclusion, it can be predicted that the test specimens without end anchorage will fail due to concrete cover separation. Experimental results validate these predictions by resulting the same mode of failure and ultimate load carrying capacity of 39.73 kN.

The enhanced shear capacity of the end anchored specimen is 107.89 kN. Therefore the beam will fail in a flexural failure mode which has lesser ultimate capacity compared to shear capacity.

4.2.2.3. Comparison with experimental results

The end anchored beams failed due to FRP rupture and their ultimate capacity was 49.05 kN. The predicted capacity for this failure mode is 54.87 kN. The deviation is only 10.76 %. The percentage difference of the non anchored beam capacity is 20.7 % and the failure mode is accurate including the sub failure type. Therefore, design equations provided in the FIB- bulletin-14 are capable of accurately predicting the behavior of beams with no additional end anchorage as well as beams with full end anchorages.

The comparison given in Table 4.2 proves this fact. However when it comes to specimens with U-wrap end anchorage, which does not adequate enough to prevent premature failure, the guidelines fail to predict the capacity.

Table 4.2: Comparison of FIB-bulletin-14 predictions and experimental results

Description of the specimen	FIB- bulletin-14 predictions	Experimental results	Percentage deviation from experimental results
Beam strengthened with FRP external reinforcement			
Moment capacity	4.37 kNm	5.61 kNm	-22.1 %
Ultimate load	31.5 kN	39.73 *kN*	-20.7 %
Failure mode	End shear failure or concrete cover separation	Concrete cover separation	-
Beam strengthened with FRP external reinforcement and end anchored with 60 mm wide CFRP inclined wraps			
Moment capacity	7.88 kNm	7 kNm	+12.57 %
Ultimate load	54.35 kN	49.05 *kN*	+10.76 %

Failure mode	FRP rupture	FRP rupture	-

4.2.3 Method proposed by Li et al. (2013)

This method has proposed based on experimental results and results of parametric study using a finite element model. The design method is focused on low strength concrete where concrete grade is less than 15 MPa. Li et al.(2013) study have investigated the effect of concrete grade, on effectiveness of the composite system. According to their findings, the bond strength between concrete substrate and FRP sheet reduces with the reduction of concrete strength.

4.2.3.1 Stress distribution profile adopted in the design

Li. et. al. (2013) has idealized the behaviour of CFRP flexural strengthened concrete member in to a Brace Arch model. When the failure process of a strengthened low-strength RC beam is considered, large number of cracks occurs due to bending moment and shear force within the span. Secondary cracks also arise in the bottom of the beam as a result of high interfacial stresses. When the distance between two cracks becomes less than effective length L_e, the concrete tooth debonds from the beam. Therefore, under the ultimate load, the strengthened beam could be regarded as a brace arch. The top concrete acts as a compressive cord, and the bottom longitudinal steel bars and CFRP sheets functions as tensile chords. Illustration of Brace Arch model is shown in Figure 4.4.
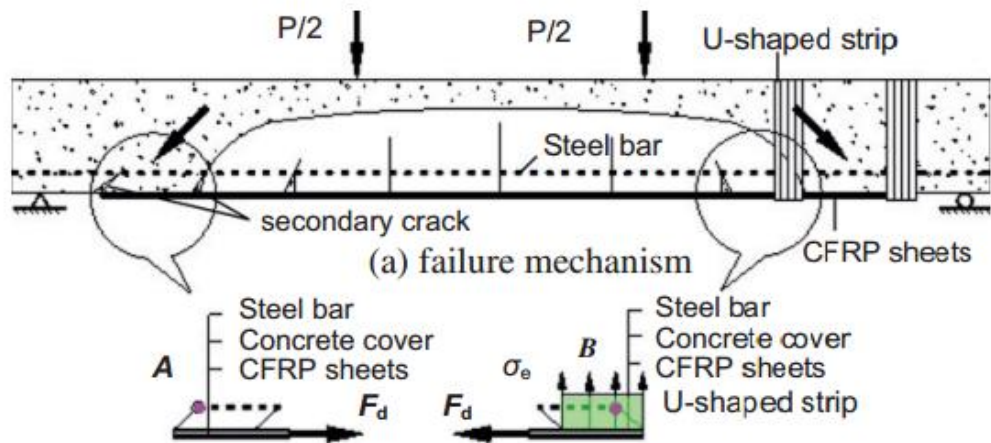
Figure 4.4: Brace arch model applied for low strength concrete beams strengthened with CFRP sheets for flexure and end anchored with U-wraps (Li et al. 2013)

According to Li. et.al. (2013), when the stresses at the root of the tooth exceeded the tensile strength of the concrete, the concrete cover between two adjacent cracks broke. When the CFRP sheet edges are confined with U-wraps, the stresses of concrete tooth reduces. Therefore, the load bearing capacity enhances.

Li. et.al. (2013) have added this stress increment to tensile strength of concrete, in order to define the enhanced stress level which cause concrete cover separation or tooth breakage at the edge of CFRP flexural reinforcement.

$$\sigma_A - \sigma_e \leq f_t$$

$$\sigma_A \leq f_t + \sigma_e \ \ldots\ldots\ldots\ldots..\ldots\ldots\ldots\ldots..\text{ Equation 4.1}$$

Where, σ_A is the stress at the concrete teeth edge, f_t tensile strength of concrete and σ_e confinement stress.

The reduction of vertical stress of concrete tooth, due to the confinement provided by U-wraps is calculated as in Equation 4.2.

$$\sigma_e = \frac{2\tau_u W_u L_{ue}}{bW_u} \ \ldots\ldots\ldots\ldots\ldots\ldots\ldots\ldots..\text{ Equation 4.2}$$

Where, W_u is the width of the U-shaped strips and L_{ue} is the effective bond length of the U-shaped strips.

103

Since the single-shear bond test specimens failed in concrete, the ultimate bond strength between the CFRP sheets and the low-strength concrete is suggested to be equated to the tensile strength of concrete, f_t.

$$\tau_u = f_t \quad \text{.. Equation 4.3}$$

When it comes to normal strength concrete beams, strengthened with CFRP and end anchored with U-wraps, the failure mode does not limit to concrete cover separation as in low strength concrete beams. Failure of end wrap may be due to CFRP rupture of the end wrap, CFRP debonding form the interface or delemination of end wrap from concrete substrate. Therefore, applicability of the model proposed by Li et al.(2013), on normal strength concrete beams cannot be guaranteed without further studies.

Calculations conducted in this section are done according to Li et al.(2013) method, in order to investigate the compatibility of this method for normal use concrete. As shown in Figure 4.5, end anchorage is provided with vertical wraps in this study. Similar to FIB method, in this method also, the compression of contribution of top reinforcement has considered. The terms and abbreviations used in the calculations are clearly described in Figure 4.5.
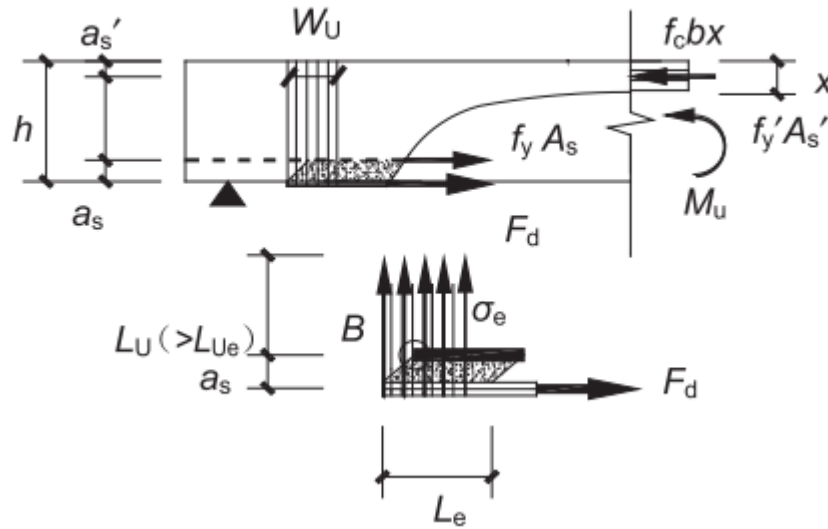
Figure 4.5: Illustration of dimensional variables used in the calculations (Li et al.2013)

4.2.3.2 Prediction of load carrying capacity and failure mode

In this design method the authors have assumed that yielding stress of steel and concrete crushing stress have achieved by the time of FRP debonding. Based on this assumption, a simplified equation has proposed to calculate the depth to the neutral axis. The same set of equations can be utilized to predict the behaviour of beams with different anchorage conditions by replacing the tensile force of CFRP (F_d), according to the analysis. Li et al.(2013) method has provide design equations to predict the strength increment with increasing amount of end anchorage. The other important fact is that the guidelines are developed for vertical U-wraps.

As far as the suitability of this method for normal strength concrete is concerned, the predictions are not accurate in case of premature failure. The theoretical load carrying capacity of the system under premature failure is 11.7 kN which is much lower than results obtained in experimental investigations (39.73 kN). This may because of the aforementioned assumption regarding sequence of occurrence of failure. When normal strength concrete is concerned, crushing of concrete may not begin at the moment of debonding.

When it comes to classical failure, the predictions are close enough to the experimented results (Appendix C.3.1.). This may because the assumed condition is similar to the conditions of current study. However the applicability is highly depending on the concrete grade. If the depth to neutral axis is calculated in a more accurate method instead of the straightforward method given in the theory, the rest of the equations may become valid for specimens casted with normal weight concrete.

Table 4.3: Comparison of predictions using Li et al.(2013) and experimental results in current study

Description of the specimen	Li et al.(2013) model predictions (Current study)	Experimental results (Current study)	Percentage deviation from experimental results
Beam strengthened with FRP external reinforcement			
Moment capacity	1.74 kNm	5.61 kNm	-68.98 %
Ultimate load	11.7 kN	39.73 kN	-70.55 %
Failure mode	FRP debonding	Concrete cover separation	-
Beam strengthened with FRP external reinforcement and end anchored with 60 mm wide CFRP inclined wraps			
Moment capacity	7.76 kNm	7 kNm	+10.85 %
Ultimate load	51.83 kN	49.05 kN	+5.67%
Failure mode	FRP rupture	FRP rupture	-
Capacity of end anchored beams			
Moment capacity	11.8 kNm	7 kNm	+68.57 %

Ultimate load	78.77 kN	49.05 kN	+60.59 %
Failure mode	Debonding of end wrap	FRP rupture	

Li et al.(2013) method have proposed a set of equations to predict the behaviour of end anchored beams. However this prediction yields much higher ultimate capacity for the specimens than experimented. The percentage difference is 60.59%. Therefore this method is not applicable for normal strength concrete. The modifications proposed to address this issue are presented in Chapter 5.

4.3 Conclusions

In order to initiate proposing of new theoretical model, the compatibility of existing models were assessed for different failure modes experimented in the study. Capacity of the test specimens were predicted using three selected design methods namely, ACI-440-2R, FIB-bulletin-14 and method proposed by Li et al.(2013). ACI-440-2R and FIB-bulletin-14 are well known design guidelines published by recognized research organizations. However these two design guides do not include methods to compute the capacity of beams where FRP flexural reinforcement is anchored with end wraps. Li et al.(2013) method proposed a design method to predict the combined behaviour. Since it method proposed for low strength concrete, it's applicability for moderate strength concrete should be assessed.

Table 4.4: Comparison of predictions according to different theoretical models

Design method	Capacity under premature failure	Ultimate capacity if classical failure is assumed	Capacity with end U-wrap anchorage
Experimental results	39.73 kN (F1 & F2)	49.05 kN (FA1 & FA2)	49.05 kN (FA1 & FA2)
ACI-440-2R	35.53 kN	49.69 kN	-
% difference from	-10.57 %	+1.3%	-

experimental results			
FIB-bulletin-14	31.5 kN	54.35kN	-
% difference from experimental results	-20.7 %	+10.76%	-
Li. et al 2013	11.7 kN	51.83kN	78.77 kN
% difference from experimental results	-70.55 %	+5.67 %	-60.59 %

Results of the theoretical study are summarized in Table 4.4. Accordingly, ACI-440-2R guide is capable of predicting the failure mode and failure load more accurately compared to FIB-bulletin-14 design guide, for flexural strengthened members without additional end anchorage. The maximum deviation of the predicted results using ACI-440-2R is about 10% and that for FIB-bulletin-14 is around 20%. Most of the times the predictions of these two design guides are less than the actual value and therefore they can be recommended as safe design methods to predict the behaviour of CFRP strengthened non anchored beams.

Predictions in Li et al.(2013) method were deviated more than 70% of the actual capacity. Therefore Li et al (2013) method is not suitable to predict the capacity of specimens cast out of moderate strength or high strength concrete.

CHAPTER 5

5 Proposed theoretical model

5.1 Introduction

Application of external reinforcement is a very popular option to increase the flexural capacity of reinforced concrete beams. Generally, when a reinforced concrete beams subjected to bending, larger strains occur at the middle of the element. Ultimately failure occurs due to mid span flexural cracks. In contrast, mid span strain of flexural strengthened members is very small and large strains are present at the reinforcement edges. Large strain is an indication of high stress concentrations at the edges. Transferring of these stresses to concrete element happens in the termination region of external reinforcement. As a consequence the beams are highly vulnerable to debonding failure. Provision of end wraps is a very good technique to prevent the aforementioned premature failure by the means of providing additional anchorage at the edges of external reinforcement.

Beyond the boundary of research, when practical application of this technique is concerned, a proper design methodology becomes essential. This chapter presents a theoretical model which is capable of predicting the capacity of flexural strengthened and end anchored beams. It includes the development of theory, proposed theoretical model, calculation procedure and validation of the model.

5.2 Theory

Failure of a flexural strengthened beam is mainly classified in to two categories; premature failure and classical failure. When the anchorage length L, is greater than effective bond length L_e debonding failure which is a sub-mode of premature failure is prevented. As a result of high stress concentrations, the beam is liable to end shear failure including cover separation failure. However this cannot be prevented by increasing anchorage length. Because, the shear stresses are limited to the region marked by the bond development length and the excessive bonded length is ineffective in terms of anchorage.

The mechanism of increasing the flexural capacity by end anchorage is that they provide a confinement effect to flexural reinforcement. It helps to reduce the vertical

stresses which are caused due to transfer of stresses in CFRP flexural reinforcement to concrete substrate. Thus, the overall moment capacity of the member increases.

When a flexural strengthened beam is subjected to bending, the tension capacity of concrete below the neutral axis can be neglected. However, the concrete zone above the neutral axis takes the compression force of the momentum. Closer to the support where shear effects are high, presence of concrete cannot be neglected. The bond stresses are also inactive beyond the effective bond length from the strip edge. This behaviour can be simulated by a Brace Arch model. Li et. al. (2013), in their prediction of load carrying capacity of flexural strengthened end anchored beams built up of low strength beams, have use Brace Arch model. The Brace arch model matched for the beam's behaviour is shown in Figure 5.1.
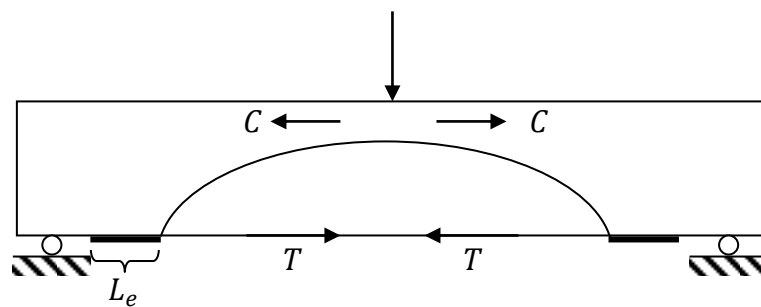
Figure 5.1 : Illustration of Brace Arch Model

The compressive force C, is the compression capacity of concrete before crushing. Tension T, is generated by externally applied FRP reinforcement and steel tension reinforcement. L_e is the effective bond length of flexural reinforcement.

5.3   Proposed model

The design procedure proposed here is a strength based model. The strength enhancement due to the confinement provided to the flexural reinforcement by end wraps can be computed with this model. The strength gain due to the effects of end wrap is then added to the resistance of end shear failure. This yields the total load carrying capacity under cover separation failure of flexural strengthened and end anchored beams. The new end shear capacity can then be compared with the flexural

capacity predicted using the available models and finally the failure load and failure mode can be determined.

5.3.1 Prediction of flexural capacity gain due to end wraps

When an end wrap is applied at the plate end, it provides a confinement effect to the CFRP flexural reinforcement. The distribution of forces in different components of the beam after applying the end wrap is shown in Figure 5.2.
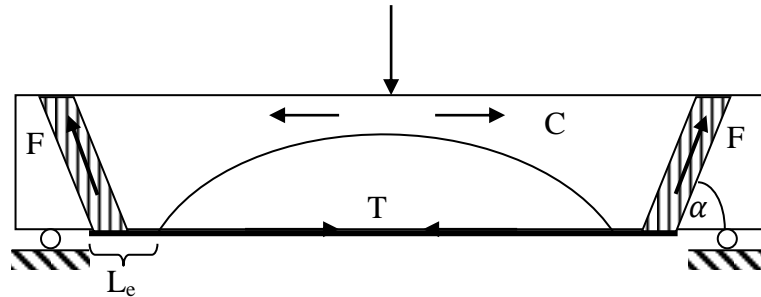
Figure 5.2: Brace Arch model for end anchored beams with inclined end-wraps

As a result of force in side straps, a vertical stress is generated on the flexural FRP, by the end wraps. This effect is descriptively presented in Figure 5.3.
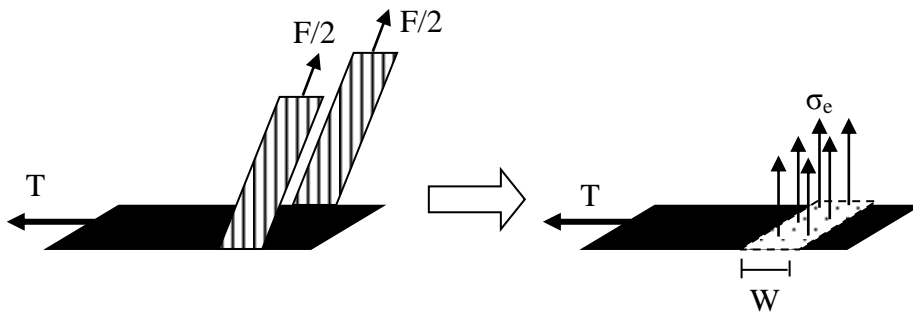
Figure 5.3: Confinement effect induced by end-wraps

The ultimate vertical stress that the wrap can provide depends on the failure mode of the wrap. As far as failure modes are concerned, the end wrap may fail due to one of three main reasons. They are;

      (a). Debonding from concrete substrate with a thin layer of concrete attached to the end wrap

      (b). Rupture of the two side straps of the FRP end wrap

(c) . Debonding of the end wrap from FRP/concrete interface

However, in Li et. al. (2013) model, the bond strength of the end wrap (τ_u) has assumed to be equal to the tensile strength of concrete (f_t).

$$\tau_u = f_t \text{ .... Equation 5.1}$$

Accordingly, the confinement stress enhancement due to end wrap (σ_e), is calculated as the stress developed over the area of effective bond length.

$$\sigma_e = \frac{2\tau_u W_u L_{ue}}{b W_u} = \frac{2 f_t L_{ue}}{b} \text{ .... Equation 5.2}$$

When it comes to normal strength concrete, failure is not the due to only one failure criteria. In order to verify the exact failure criteria of the end wrap, maximum bearable force under each criterion is computed. The minimum of the three values is taken as ultimate force which creates a vertical stress on longitudinal CFRP. The ultimate force carried by the end wrap is computed as in Equation 5.3.

Ultimate tensile force = min(Debonding from concrete substrate. Rupture of the FRP end wrap, Debonding of the end wrap from FRP/concrete interface)

$$F_u = \min(F_1, F_2, F_3) \text{ ……………………. Equation 5.3}$$

In order to debond the wrap from concrete substrate, the force should be large enough to overcome tensile strength of concrete across the bonded area of the wrap. Therefore failure criterion of the wrap is calculated by multiplying the concrete strength by area of side straps of the end wrap (Equation 5.4).

Failure load due to concrete debonding = 2×Tensile strength of concrete× Area of the end wrap

$$F_1 = 2 f_c' W d \sin \alpha \text{ ………………………….. Equation 5.4}$$

When CFRP rupture is concerned, the ultimate force resisted by two side straps of the end wrap is equal to tensile strength of CFRP multiplied by the cross sectional area of the wrap (Equation 5.5). The factor "2" stands for two straps of the wrap.

Failure load under CFRP rupture = 2 × Rupture strain of CFRP × Cross sectional area of CFRP end wrap

$$F_2 = 2f_f W t_f \text{ .... Equation 5.5}$$

Debonding of end wrap occurs if the applied force exceeds total interfacial shear strength. Therefore, the force F_3 is calculated as the multiplication of bond stress by effective bond area. Effective bond area is obtained by multiplying wrap width and effective bond length. The effective bond length for end wraps is assumed to be same as effective bond length of shear reinforcement. Equation 5.6 shows the expression for F_3.

Failure load under debonding of end wrap = 2 × Bond stress of epoxy adhesive × Area over effective bond length.

$$F_3 = 2f_b W L_{ue} \text{ .... Equation 5.6}$$

Once F_u is determined, the confinement stress induced by end wrap σ_e, can be derived using Equation 5.7. The ultimate force F_u is excreted over the area covered by the end wrap in the beam soffit. Therefore the force is divided by the area in order to obtain the stress. Since the force is inclined to the longitudinal axis of the beam, the expression should also be multiplied by $\sin \alpha$ to get the vertical stress.

$$\sigma_e = \frac{F_u \sin \alpha}{bW} \text{ .... Equation 5.7}$$

In the next step, moment capacity enhanced due to confinement of end wraps M_e, can be calculated using first principals as in Equation 5.8.

$$M_e = \frac{I\sigma_e}{y} \text{ .... Equation 5.8}$$

Where,

$I = \frac{bd^3}{12} = \frac{b_f W^3}{12}$ for beams with rectangular cross sections where, b_f is the width of CFRP flexural reinforcement

y in Equation 5.8 is the distance to the centre of end wrap from point A of the Brace Arch Model (Figure 5.4 (a)). If wrap width W is less than effective bond length L_e, point A locates at L_e distance towards the mid span from the edge of the flexural CFRP reinforcement.

In case of $L_e < W$, position of point A is assumed to be located at a distance of W, from the edge of the CFRP sheet(Figure 5.4 (b)). The reason is that, when the confinement effect of end wrap is present, the concrete volume covered by the end wrap becomes effective in compression. Therefore, the arch of the Brace Arch model will begin from the place where the wrap terminates. Even though, the effective bond length does remain the same. The confinement effect is active beyond the length L_e, in this scenario.

When the value of M_e, is known the increment of load carrying capacity can be calculated. It is added to the load carrying capacity under end shear failure. The resulting value is the load carrying capacity of end anchored beams under end shear failure.
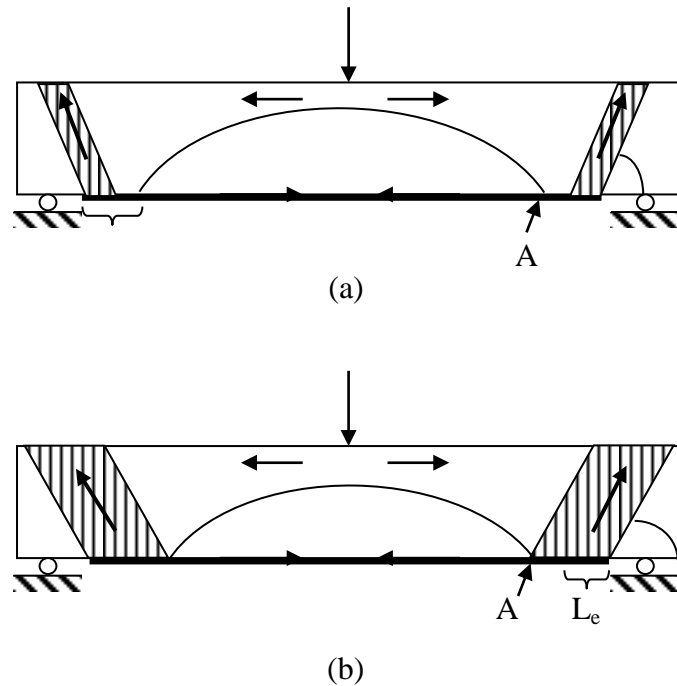
Figure 5.4: Location of point A (a) When $L_e > W$, (b) when $L_e < W$

5.3.2 Comparison of predictions with experimental results

The failure criterion of CFRP strengthened and end anchored beams were predicted using the new proposed model. The results are summarized in Table 5.1.

Table 5.1 : Theoretical predictions and experimental results

Parameter	Li.et.al. (2013) predictions for current study	Predictions of the proposed model	Experimental results
Moment capacity under flexural failure M_u	7.76 kNm	6.85 kNm	7.00 kNm
Ultimate load corresponding to flexural failure W_m	51.73 kN	48.02 kN	49.05 kN
End shear capacity of non anchored beam V_{Rd}	76.61 kN	15.62 kN	-
Ultimate load corresponding to end shear failure V_f	78.66 kN	39.68 kN	-
Moment capacity enhancement due to confinement induced by end anchors M_e	0.592 kNm	1.33 kNm	-
Corresponding load carrying capacity W_e	6.3 kN	8.87 kN	-
Load carrying capacity under end shear failure	84.96 kN	48.55 kN	-
Failure load	51.73 kN	48.02 kN	49.05 kN FA1(1) and FA1(2)
% difference of failure load compared to experimental results	+5.46%	-2.09%	-
Failure mode	Flexural	Flexural	Flexural

	failure	failure due to FRP rupture	failure due to FRP rupture

5.4 Validation of the model

A total of thirteen test beams included in seven papers published, were selected for the validation. All the selected specimens are flexural strengthened with single layer of CFRP and end anchored with CFRP or GFRP end wraps. A plot of predicted capacity vs. experimented load is shown in Figure 5.5.

As far as the available experimental results are concerned, very few number specimens have failed in end shear in presence of end wraps. Therefore the specimens referred for the validation of the model were selected without limiting the failure mode. Load carrying capacities under different failure criteria including end shear failure were predicted and the minimum capacities were taken as failure load. The corresponding failure criterion was named as the failure mode. Although accuracy levels cannot be determined with this procedure, validity of the model can be clearly presented.

As shown in Figure 5.5, the predicted loads are lower than experimental loads. However the values lie within the range defined by + or − 15% deviations. It indicates the condition of predicted load being equal to experimented load.
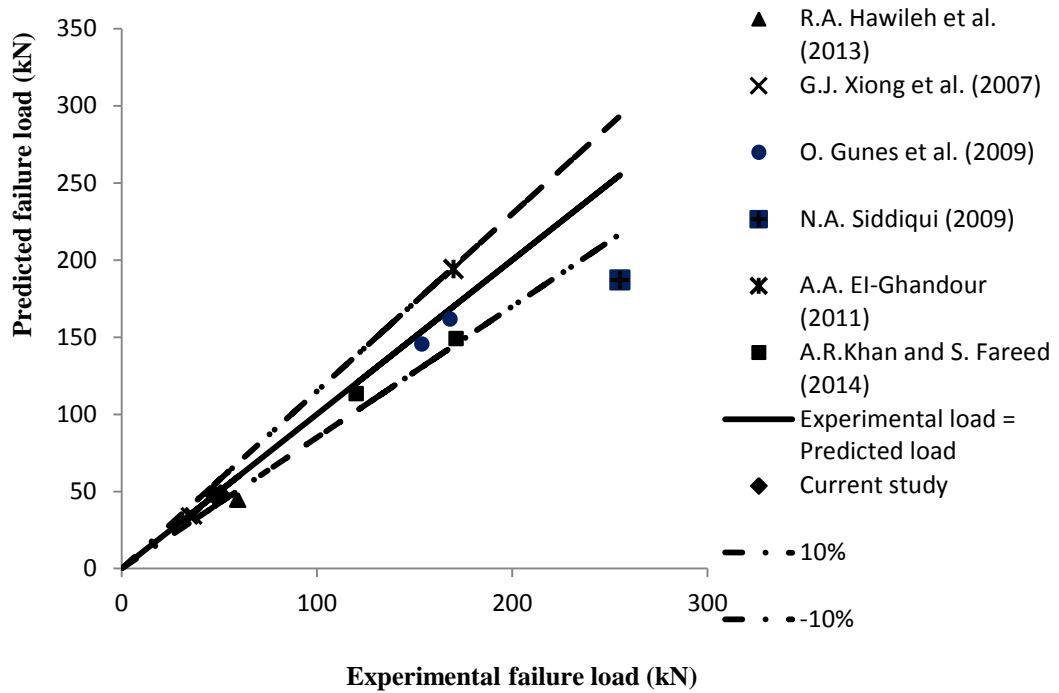
Figure 5.5:Predicted failure load vs. Experimental failure load

The failure modes are compared in Table 5.2. The predicted failure modes are accurate for all the test specimens. When end debonding is liable the failure can further be characterized in to sub failure modes such as debonding of the wrap, rupture of the end wrap or debonding of concrete etc, with the proposed model. The details of these studies are listed in Appendix D.

Table 5.2: Comparison of predicted results and actual results

Reference	Beam designation	Experimental failure load (kN)	Experimented failure mode	Predicted failure load (kN)	Predicted failure mode	% difference
Current study	FA1 (1)	50.81	FRP rupture at mid span	48.02	FRP rupture at mid span	-5.49 %
	FA1 (2)	47.28	FRP rupture at mid span	48.02	FRP rupture at mid span	+1.56 %

R.A. Hawileh et al. (2013)	B50PW	59.56	Concrete cover delamination	44.15	Cover separation failure	25.87 %
	FE-B50PW	60.1	Concrete cover delamination	44.15	Cover separation failure	-26.54 %
	FE-B50PW1	58.88	FRP rupture at mid span	44.3	FRP rupture at mid span	-24.76 %
G.J. Xiong et al. (2007)	F1C/2G(1)	34.8	Steel yielding	34	Flexural failure	-2.29 %
	F1C/2G(2)	37	Steel yielding	34	Flexural failure	-8.10 %
O. Gunes et al. (2009)	S4PS1M	153.8	FRP debonding	145.4	FRP cover debonding	-5.45 %
	S4PS2M	168.2	FRP debonding	161.6	FRP cover debonding	3.92 %
N.A. Siddiqui (2009)	BFS2	255.2	concrete crushing	187	Flexural failure	-26.72 %
A.A. EI-Ghandour (2011)	B1F	170	Flexural CFRP rupture	194	FRP rupture at mid span	+14.12 %
A.R.Khan and S. Fareed (2014)	WSAB1	120.3	Flexural failure due to steel yielding	113.37	Flexural failure	-5.76 %
	WSAB2	171.3	Shear	149	Flexural	13.02

			compression failure		failure	%

5.5 Conclusions

A new theoretical model was proposed to predict the load carrying capacity and failure mode of externally strengthened and end anchored beams with FRP materials. The model was developed based on Brace Arch model and Li et. al.(2013).

The proposed model can accurately predict the behaviour of flexural strengthened and end anchored beams. According to the model, end shear failure capacity increases with increasing end wrap width. However the variation is not linear. The failure mode of end wrap depends on tensile properties of concrete, adhesive properties and FRP material properties.

The model shows -5.49% maximum deviation from experimental results of current study. The difference can be due to the effect of parameters such as bond strength, concrete grade, loading pattern, steel reinforcement ratio etc., which were not studied in the current program.

CHAPTER 6

6 Conclusions and recommendations

6.1 Conclusions

This dissertation presents a study conducted to investigate the effect of provision of end anchorage on flexural performance of reinforced concrete beams strengthened with CFRP external reinforcement. The available methods to predict the behaviour of beams externally strengthened and end anchored with FRP wraps were evaluated. Little research has conducted on predicting the aforementioned behaviour of flexural members. ACI-440-2R guide and FIB-bulletin-14 guide does not contain a method predict the combined effect of flexural reinforcement and end anchorage. X. Li et al. (2013) have proposed a method to evaluate the behaviour of reinforced concrete members made with low strength concrete and externally strengthened with CFRP in a similar way. However this method is not applicable for moderate strength concrete. Therefore an experimental program was conducted to study the behaviour moderate strength reinforced concrete beams external strengthened with CFRP for flexure and end anchored with CFRP end wraps. The wrap configuration selected for this study was inclined wraps due to their high performance over other end wrap configurations.

The experimental program was consisting of eight medium scale beams. Their behaviour was observed by the means of deflection, strain of bottom fibres, applied load, ductility and failure criteria. The results were analyzed and discussed in order to identify mechanism that the end anchors affect on flexural strength gain. Once the mechanism is identified, a theoretical model was proposed to predict the behaviour of flexural strengthened and end anchored reinforced concrete beams.

Remarkable strength increments can be achieved with external strengthening of concrete beams with CFRP. In current study, 99.53% gain of ultimate strength was achieved by the strengthened beams over un-strengthened beams. As far as serviceability conditions are concerned, the strength gain was 99.97%. Interface debonding failure of these beams was prevented by allowing adequate anchorage

length as given in design guides. As a result, FRP debnding was not observed in the experiments. However, concrete cover separation failure was still observed.

When a 60 mm wide inclined end wrap is applied to the flexural CFRP, 23.45% strength gain over non anchored beams was achieved. It is 145% strength increment over control beams. In the context of serviceability, the strength increments are 18% and 153% over non anchored beam and non strengthened beam respectively.

As far as failure modes of end anchored beams are concerned, the end wraps could totally prevent debonding failure. Consequently, the beams failed due to flexural CFRP rupture at the mid span. Therefore it can be concluded that, failure modes have changed due to provision of end anchorage from cover separation failure which is a premature failure mode to CFRP rupture which is a classical failure mode.

With the introduction of mid span U-wrap, ultimate load carrying capacity of end anchored beams increased by 4.15% over a similar beam, but without U-wrap at the middle. Although the ultimate failure loads are large in mid span anchored beams, they failed in serviceability prior to the beams with only end anchorage. The failure mode did not change from the beam without middle wrap and the CFRP rupture occurs at an edge of the mid span wrap.

The control beams failed due to propagation of flexural crack occurred at the mid span. Accordingly, mid span strains of control beams were larger than end strains. In contrast, flexural strengthened members indicated large strain values at the ends of CFRP flexural reinforcement. The mid span strains were almost zero throughout the test. When the beams anchored at ends, the strain profile altered so that end strains are less than mid span strains. However in this case, large strains were observed at both mid span and ends.

The maximum strain observed in CFRP flexural reinforcement of end anchored beams was 9.3 times higher than that of beams without anchorage. It indicates a better utilization of CFRP's tensile strength for the improvement of performance of beams with end anchorage. Accordingly, CFRP is more effectively contributed to strength gain in the presence of end anchorage.

Although the actual bond length is greater than effective bond length calculated according to ACI-440-2R, the total bond strength does developed within the bond length of test specimens. The reason is very high bond strength of epoxy adhesive, which makes the ultimate bond strength is not achieved, by the time of CFRP rupture. However, the development of bond strength increases with increasing end anchorage.

It was found that fracture energy, which is the amount of energy required for the failure of the beam, is increasing with provision of end anchorage. The mode of fracture is also changing from Mode I fracture to Mode II fracture with the introduction of end wrap anchors.

Shear capacity of reinforced concrete beams reduced with application of external CFRP flexural reinforcement. The reason is large stress concentrations occurred at the edges of the CFRP reinforcement. As a result, cover separation failure, which is a consequence of end shear failure, occurred. Even though provision of adequate anchorage length could successfully prevent debonding, it was not contributing to avoid cover separation failure.

When the predictions of different design guidelines are concerned, both ACI-440-2R and FIB-bulletin-14 showed a good compatibility with experimental results for non anchored beams. The predicted loads had a maximum deviation of -10% in ACI method and -20% in FIB method. Therefore both ACI guide and FIB guide can be named as better methods of predicting results with considerable safety factors of 1.1 and 1.25 respectively. As far as compatibility of Li. Et. al.(2013) method is concerned, it can predict concrete cover separation up to 5.67% accuracy, in normal strength concrete beams. Predictions of all the other failure modes are much deviated from experimental results. Accordingly, Li. Et. al. (2013) method cannot be used to predict the behaviour of normal strength reinforced concrete beams.

It was observed that end wraps enhance the flexural capacity of beams by means of resisting concrete cover separation at beam edges. End wraps also contribute to anchor the externally applied flexural reinforcement by reducing the anchorage length requirement (FIB-bulletin-14). If the anchorage length requirement is satisfied

by the length of flexural CFRP itself, end wrap is important only for prevention of end shear failure.

The confinement force exerted by the end wraps on flexural FRP is the key to increase end shear capacity in end anchored beams. The moment capacity enhancement can be evaluated by using Equations 5.3 to 5.8.

The enhanced shear capacity (V_{es}) of the system due to introduction of end wrap anchorage can be determined by adding the capacity enhancement due to end anchors (V_e) to existing end shear capacity of the beam (V_{Rd}). This relationship is mathematically expressed in Equation 6.1.

$$\boldsymbol{V_{es} = V_a + V_{Rd}} \cdots\cdots\cdots\cdots\cdots\cdots\cdots\cdots\cdots\cdots \text{Equation 6.1}$$

The model proposed in Chapter 6 is valid for experimental results of current study as well as experimental results obtained by seven other authors. Details of the test specimens are included in Appendix D.

6.2 Proposed guidelines

In the proposed design method, the failure criteria of end anchorage wrap is evaluated first. The failure criteria are; failure from concrete substrate, rupture of the FRP wrap and debonding of the wrap from epoxy adhesive. The critical failure mode is determined by comparing the failure load under each criterion. The effective vertical confinement stress provided by the end wrap to the edge of the edge of the longitudinal CFRP is evaluated in the next step. When effective stress (σ_e) is known, the enhanced moment capacity can be calculated straightforward. There are two criteria to evaluate the section modulus of affected area by the end wrap. The criteria depend on the comparative dimensions of effective bond length and width of the FRP wrap. The enhancement in force is then evaluated using first principals. The load enhancement depends on the loading pattern and the geometry of the beam.

Once the capacity enhancement is calculated in terms of an external load, it can be directly summed to the capacity of a beam under concrete cover separation failure; which can be calculated using available design guidelines. The resulting value is the load carrying capacity of CFRP strengthened beam and anchored with end wraps

under end debinding failure. The whole design procedure is summarised in Figure 6.1.

$$F_{d=} \min(F_1, F_2, F_3)$$

$$F_1 = 2f_c' W d \sin \alpha$$

$$F_2 = 2f_f W t_f$$

$$F_3 = 2f_b W L_{ue}$$

$$\sigma_e = \frac{F_u \sin \alpha}{bW}$$

$$M_e = \frac{I\sigma_e}{y}$$

$$L_e < W$$

$$\frac{I}{Y} = \frac{b_f W^3 \times 2}{12 \times W}$$

Yes

$$\frac{I}{Y} = \frac{b_f W^3}{12 \times (L_e - W/2)}$$

No

Increase in load carrying capacity due to M_e

(Calculated according to the loading pattern and beam geometry)

$$V_{es} = V_a + V_{Rd}$$
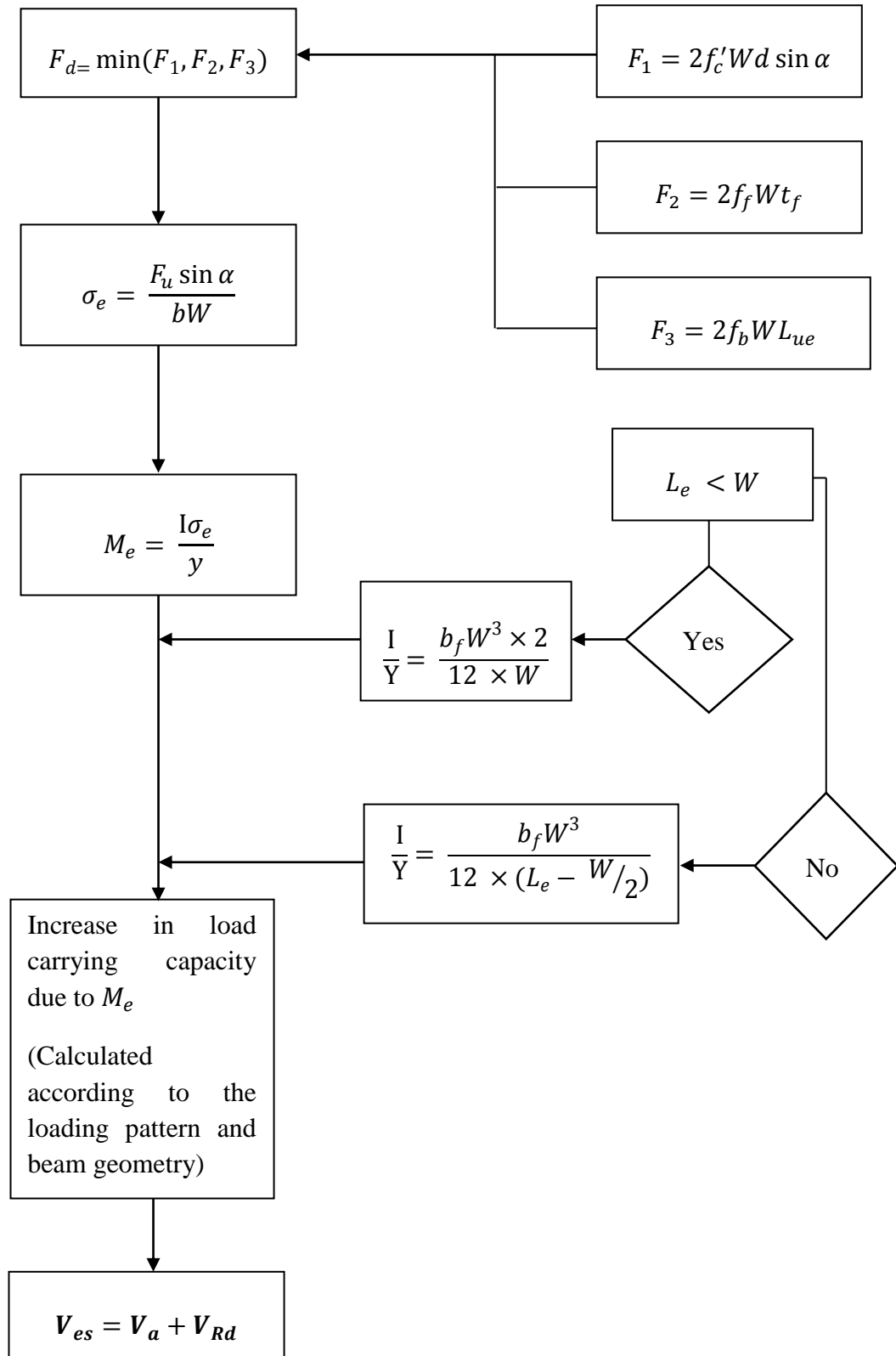
Figure 6.1: Summary of proposed design method

6.3 Limitations

The model proposed in current study is suggested for the specimens that fulfil anchorage length requirement. Applicability of this model for the beams where anchored length is less than specified length should be further studied.

The proposed model is applicable only for beams with rectangular cross section. Validity of this model for beams with different cross section should be evaluated and modification should be proposed if required.

In this study, it is assumed that the effective bond length of end anchoring wraps is same as the effective bond length of shear straps. Studies should be conducted to verify the applicability of this assumption.

Validity of the model has checked for the concrete strength values range from 25 N/mm^2 to 55 N/mm^2. It is stated that Li et.al. (2013) method is applicable only for concrete strengths from 10 N/mm^2 to 15 N/mm^2. The rage in between 15 – 25 N/mm^2 and above 55 N/mm^2 are still uncovered.

6.4 Recommendations

The design can be optimized with this model by controlling the width of end wrap. The effective depth of the end anchor may also be able to optimize. Studies on this aspect are also recommended.

The validity of the model should be further verified with the results of parametric studies which cover different aspects engaged with the design such as bond strength, concrete grade, loading pattern, internal reinforcement configuration etc.

Safety factors required in order to use the proposed model for practical applications are not included in this study. It is very important to introduce safety factors and material strength reduction factor for the design.

The current proposal is the only one theoretical model to predict the behaviour of flexural strengthened and end anchored beams. Just one study is not adequate to generate a proper design guideline. Therefore more investigations on the same topic

are encouraged in order to make a contribution for the preparation of design guideline on this regard.

REFERENCES

Achintha, P.M.M. & Burgoyne, C.J., (2008), "Fracture mechanics of plate end debonding". *ASCE Journal of Composites for Construction,* vol. 12, no. 04, pp. 396-404.

ACI Committee 440 and American Concrete Institute, *Guide for the design and construction of externally bonded FRP systems for strengthening concrete structures.* Farmington Hills, Mich.: American Concrete Institute, 2008.

Ahmed, O., Gemert, D. V. & Vandewalle, L., (2001), "Improved model for plare end shear of CFRP strengthened RC beams". *Cement & Concrete Composites*, vol. 23, pp. 3-19,.

Al-Amery, R. & Al-Mahaidi, R., (2006), "Coupled flexural shear retrofitting of RC beams using CFRP straps". *Composite Structures*, vol.75, no. (1-4), pp. 457-464.

American concrete institute, http://www.concrete.org/aboutaci.aspx, viewed 5th Feb. 2015

Anania, L., Badal, A. & Failla, G., (2005), "Increasing the flexural performance of RC beams strengthened withCFRP materials". *Construction and Building Materials*. Vol. 19, pp. 55–61.

Antonoiades, K.K., Salonikios, T.N. and Kappos, A.J., (2003), Cyclic tests on seismically damaged reinforced concrete walls strengthened using fibre-reinforced polymer reinforcement. ACI Structural Journal, vol 100, no 4, 510-518.

Antonopoulos, C.P. & Triantafillou, T.C., (2003), "Experimental investigation of FRP strengthened RC beam-column joints". *Journal of Composites for Construction*, vol. 7, no. 1, pp. 39-49.

Aram, R.M., Czaderski, C. & Motavalli, M., (2008), "Debonding failure modes of flexural FRP-strengthened RC beams". *Composites: Part B*, vol. 39, pp. 826–841.

Attari, N., Amziane, S. & Chemrouk, M., (2012), "Flexural strengthening of concrete beams using CFRP, GFRP and hybrid FRP sheets". *Construction and Building Materials,* vol. 37, pp. 746–757.

Borosnyi, A., (2002), *Servicability of CFRP prestressed concrete beams,* Budapest: Budapest Universiy of technology and Economics Faculty of Civil Engineering.

Bukhari, I.A., Vollumt, R.L., Ahmad, S. & Sagaseta, J., (2010), "Shear strengthening of reinforced concrete beams with CFRP". *Magazine of Concrete Research,* 62(No.1), pp. 65-77.

Buyukozturk. O., Gunes. O. & Karaca. E., (2004), "Progress review on understanding debonding problems in reinforced concrete and steel members strengthened using FRP composites". *Cunstruction and Building Materials*, vol. 18., pp. 9-19.

Carbon Fiber Strengthening, Viewed October 21 2014, http://www.bristolroofcompany.co.uk/structural-repairs/carbon-fiber-strengthening.html

Carlton, A. & Taljsten, B., (2005), "Experimental study on strengthening for increased shear bearing capacity". *Journal of composite for constructution,* vol. 9. pp. 488-496.

Carolin, A., (2003), *Carbon fiber reinforced polymers for strengthening of structural elements.* Lulea: Lulea Univercity of Technology.

Ceroni, F., Pecce, M., Matthys, S. & Taerwe, L., (2008), "Debonding strength and anchorage devices for reinforced concrete elements strengthened with FRP sheets". *Composites: Part B*, vol. 39, pp. 429–441.

Chaallal, O., Nollet, M.J. & Perraton, D., (1998), *Strengthening og reinforced concrete beams with externelly bonded fiber reinforced plastic plates: design guidelines for shear and flexure.* Montreal, Canada: Universilt du Quebec.

Chen, G.M., Teng J.G. & Chen, J.F., (2012), "Precess of debonding in RC beams shear strengthened with FRP U-strips or side strips". *International Journal of Solids and Structures*, vol. 49, pp. 1266-1282.

Civil construction retrofitting, Viewed October 21 2014, http://dir.indiamart.com/mumbai/civil-construction-contractors.html

Dash, N., (2009), *Strenghtening of reonforced concrete beams using glass fiber reinforced polymer composites,* Rourkela: National Institute of Technology.

Direct industry, The online industrial exhibition n.d., Viewed January 3 2015, http://www.directindustry.com/prod/von-roll/grp-panels-composite-12485-145701.html

El-Ghandour, A.A., (2011), "Experimental and analytical investigation of CFRP flexural and shear strengthening efficiencies of RC beams", *Construction and Building Materials,* vol 25, pp.1419–1429.

El-Sayed, A.K., (2014), "Effect of longitudinal CFRP strengthening on the shear resistance of reinforced concrete beams", *Composites: Part B, Elsevier Ltd,* Vol. 58, pp. 422–429.

Faella, C., Martinelli, E. & Nigro, E., (2008), " Formulation and validation of a theoretical model for intermediate debonding in FRP strengthened RC beams". *Composites: Part B*, vol. 39, pp. 645-655.

FIB Bulletin 14. Externally bonded FRP reinforcement for RC structures. *Design and use of externally bonded fibre reinforced polymer reinforcement (FRP EBR) for reinforced concrete structures*. Task Group 9.3, July 2001.

FIB official website, http://www.fib-international.org/about

Gite,B.E., Suvidha & Margaj, R., (2011), *Carbon fiber as a recent material use in consruction,* Sangamner: Amrutvahini College of Engineering.

Godati, A., Qu, Z., Lu, X.Z., Labossiere, P., Ye, L.P. & Neale, K.W., (2010), Size effects for reinforced concrete beams strengthened in shear with CFRP strips. *Journal of Composite for Construction,* vol. 14, No.3(June 1,), pp. 60-71.

Grelle, S.V. & Sneed, L.H., (2013), "Review of anchorage systems for externally bonded FRP laminaates". *International Journal of Concrete Strucutres and Materials*.vol. 7, no.1, pp. 17-33.

Gunes, O., Buyukozturk, O. & Karaca, E., (2009), "A fracture-based model for FRP debonding in strengthened beams", *Engineering Fracture Mechanics,* vol. 76, pp.1897–1909.

Hamara Kuwait co. w.l.l., (n.d), Commercial division, Viewed December 21 2014, http://www.hamrakt.com/Pages/CommercialServices.aspx

Hawileh, R.A., Naser, M.Z. & Abdalla, J.A., (2013), "Finite element simulation of reinforced concrete beams externally strengthened with short-length CFRP plates". *Composites: Part B,* vol. 45. pp. 1722–1730.

Hawileh,R. A., Rasheed,H.A., Abdalla,J. A. & Al-Tamimi, A. K., (2014), "Behavior of reinforced concrete beams strengthened with externally bonded hybrid fiber reinforced polymer systems", *Materials and Design,* vol. 53, pp.972–982.

Hosny,A., Shaheen, H., Abdelrahman, A., & Elafandy, T., (2006), "Performance of reinforced concrete beams strengthened by hybrid FRP laminates", *Cement & Concrete Composites.*, vol. 28, pp. 906-913.

Isaac, P.M., (2009), *Effect of Adhesive Stiffness on FRP Anchorage Strengthening of Steel.*, Department of Architecture and Civil Engineering, University of Bath.

Jankowiak, I., (2012), "Analysis of RC beams strengthened by CFRP strips—Experimental and FEA study", *Archives of civil and mechanical engineering.,* Elsevier Urban & Partner, Poznan,vol. 12, pp. 376–388.

Jayanath, B.C.R., (2013), Behaviour of reinforced concrete flexural members strengthened with externally bonded carbon fibre reinforced polymers, University of Moratuwa, Sri Lanka.

Kachlakev, D. & McCurry, D.D., (2000), "Behavior of full-scale reinforced concrete beams retrofitted for shear and flexural with FRP laminates", *Composites: Part B., Elsevier Science Ltd.,* vol. 31, pp. 445-452, 2000.

Kalfat, R., Al-Mahaidi, R. & Smith,S., " Anchorage devices used to improve the performance of reinforced concrete beams retrofitted with FRP composites: A-state-of-the-art-review". *Journal of composites for construction*, ASCE. Doi:10.1061/(ASCE)CC.1943-5614.0000276

Khalifa,E.S., & Al-tersawy, S.H., (2013), "Experimental and analytical investigation for enhancement of flexural beams using multilayer wraps", *Composites: Part B, Elsevier Ltd,* vol. 45, pp.1432–1440.

Khan, A.R. & Fareed, S., (2013), "Behaviour of Reinforced Concrete Beams Strengthened by CFRP Wraps with and without End Anchorages", *Fourth International Symposium on Infrastructure Engineering in Developing Countries*. IEDC, Karachi., vol. 77, pp. 123–130.

Kopeliovich, D., (n.d.), Carbon Fiber Reinforced Polymer Composites, http://www.substech.com/dokuwiki/doku.php?id=carbon_fiber_reinforced_pol ymer_composites

Kotynia, R., (2005), Debonding failures of RC beams strengthened with externally bonded strips. *In Proceedings of the International Symposium on Bond Behaviour of FRP in Structures* (BBFS 2005), Hong Kong: International Institute for FRP in construction, pp. 7-9, December 2005.

Li, X., Gu, X.L., Song, X.B., Ouyang, Y. & Feng, Z.L., (2013), "Contribution of U-shaped strips to the flexural capacity of low-strength reinforced concrete beams strengthened with carbon fibre composite sheets*", Composites: Part B, vol. 45*,pp. 117–126.

Lijuan Li, Guo,Y.,and Liu,F., "Test analysis for FRC beams strengthened with externally bonded FRP sheets", *Construction and Building Materials., Elsevier Ltd.,* vol. 22, pp. 315-323, 2008.

Lorenzis, L. D., Nanni, A. & Tegola, A. L., (2000), "Strengthening of Reinforced Concrete Structures with Near Surface Mounted FRP Rods" , bibl. International Meeting on Composite Materials, PLAST 2000, Milan, Italy, May 9-11, 2000, http://transportation.mst.edu/media/research/transportation/documents/strngth_rods.pdf

Madureira, E. L. & Ávila, J.I.S.L., (2012), Numerical simulation of the mechanical performance of deep beam, http://dx.doi.org/10.1590/S1983-41952012000600002 , Viewed 4 Feb 2015, IBRACON Estrut. Mater. vol.5 no.6 São Paulo Dec. 2012

Masuelli, & Alberto, M., (2013), *Introduction of fibre-reinforced polymers − polymers and composites: concepts, properties and processes.* [Online]Available at: http://dx.doi.org/10.5772/54629, [Accessed June 2013].

Meier, U. & Rostasy, (1995), Strengthening of structures using carbon fibre/ epoxy composites, *Constrction and Building Materials Journal,* vol. 9, No. 6, pp. 341-351.

Michels, J., Martinelli, E., Czaderski, C. & Motavalli, M., (6 January 2014), Prestressed CFRP Strips with Gradient Anchorage for Structural Concrete Retrofitting: Experiments and Numerical Modeling , http://www.mdpi.com/2073-4360/6/1/114/htm

Mohamed, T. K. H., (2002), *Flexural performance and bond characteristics of FRP strengthening techniques for concrete structures.* Manitoba, Canada: The University of Manitoba.

Morsy, A. & Mahmoud, E.T., (2012), "Bonding techniques for flexural strengthening of R.C. beams using CFRP laminates", *Ain Shams Eng J.*, http://dx.doi.org/10.1016/j.asej.2012.11.004.

Mostofinejad, D. & Moghaddas, A., (2014), "Bond efficiency of EBR and EBROG methods in different flexural failure mechanisms of FRP strengthened RC beams", *Construction and Building Materials, Elsevier Ltd*, Vol. 54, pp.605–614.

Obaidat,Y.T., Heyden,S., Dahlblom,O., Abu-Farsakh,G. & Abdel-Jawad, Y., (2011), "Retrofitting of reinforced concrete beams using composite laminates", *Construction and Building Materials., Elsevier Ltd.,* Vol. 25, pp. 591–597.

Qeshta, I.M.I., Shafigh, P., Jumaat, M.Z., Abdulla, A.I. & Ibrahim, Z., (2014), "Alengaram, U.J., The use of wire mesh–epoxy composite for enhancing the flexural performance of concrete beams". *Materials and Design*, vol. 60, pp. 250–259.

Ramanathan K.N., (2006), *Influence of frp width-to-spacing ratio on bond performance of externally bonded frp systems on one way concrete slabs* Graduate Faculty of Swanson School of Engineering, Osmania University.

Reinforced concrete buildings n.d., Viewed December 28 2014, http://www.iitk.ac.in

Sagawa, Y., Matsushita, H. & Tsuruta, H., (2001), "Anchoring method for carbon fibre sheet for strengthening of reinforced concrete beams". ". In *Proceedings of 5th International Conference on Fiber Reinforced Plastics for Reinforced Concrete Structures.* Landon: FRPRCS-5, pp. 16-18., July 2001.

Sawada, S., Kishi, N., Mikami, H. & Kurihashi, Y., (2003), "An experimental study on debond control of AFRP's for flexurally strengthened RC beams". In *Proceedings of 6th International Conference on Fiber Reinforced Polymer (FRP) Reinforcement for Concrete Structures.* Singapore: FRPRCS-6, 8-10 July 2003.

Sethunge, S., (2002), Review of strengthening techniques using externally bonded fibre reinforced polymer composites, CRC Construction Innovation.

Shahawy, M. A., Arockiasamy, M., Beitelmant, T. & Sowrirajan, R., (1996), "Reinforced concrete rectangular beams strengthened with CFRP laminates", *Composites: Part B, Elsevier Science Limited*, Vol. 27B, pp. 225-233.

Shahawy, M.A., Arockiasamy, M., Beitelman, T. & R. Sowrirajan, (1995), *Reinforced concrete rectangular beams strengthened with CFRP laminates,* Florida: Elsevier Science Limited.

Siddiqui, N. A., (2009), "Experimental investigation of RC beams strengthened with externally bonded FRP composites", *Latin American Journal of Solids and Structures,* Vol.6, pp.343 – 362.

Siddiqui, N. A., (2009). Experimental investigation of RC beams strengthened with externally bonded FRP composites. *Latin American Journal of solids and structures,* Vol 6, pp. 343-362.

Smith, S.T. & Teng, J.G., (2002), "FRP strengthened rc beams. I: Review of debonding strength models". *Engineering Structures*, vol. 24, pp. 385-395.

Spadea, G., Swamy R.N. & Bencardino, F., (2001), Strength and ductility of RC beams repaired with bonded CFRP laminates. *Journal of Bridge Engineering*, ASCE, Vol 6, no 5, pp. 349-355.

Srisangeerthanan, S., (2013), "*Investigation on alternatives to prevent debonding of reinforced concrete members*" Department of Civil Engineering, University of Moratuwa, Sri Lanka.

Structural Retrofit, (n.d.), http://civil-engg world.blogspot.com/2011/06/structural-retrofit.html, Viewed July 26 2014.

Structural Retrofit, (n.d.), http://civil-engg-world.blogspot.com/2011/06/structural-retrofit.html, Viewed December 11 2014.

Sveinsdottir, S. L., (2012), *Experimental research on strengthening of concrete beams by the use of epoxy adhesive and cement based bonding material,* Haskolinn: Reykjavik Univercity.

The mechanical properties of steel, (n.d.), http://www.tatasteelconstruction.com/en/reference/teaching-resources/architectural-teaching-resource/technology/the-nature-of-steel/the-mechanical-properties-of-steel, Viewed 10 January 2015.

Wu, Z. M., Hu, C. H., Wu,Y. F. & Zheng, J. J., (2011), "Application of improved hybrid bonded FRP technique to FRP debonding prevention", *Construction and Building Materials, Elsevier Ltd*, Vol. 25, pp. 2898–2905.

Xiong , G.J., Jiang, X., Liu, J.W. & Chen. L., (2007), "A way for preventing tension delamination of concrete coverin midspan of FRP strengthened beams", *Construction and Building Materials, Elsevier Ltd*, Vol. 21 pp.402–408.

Zhou, Y., Gou,M., Zhang,F., Zhang,S. & Wang,D., (2013), "Reinforced concrete beams strengthened with carbon fiber reinforced polymer by friction hybrid bond technique: Experimental investigation", *Materials and Design, Elsevier Ltd,* Vol.50, pp.130–139, 2013.

APPENDIX A
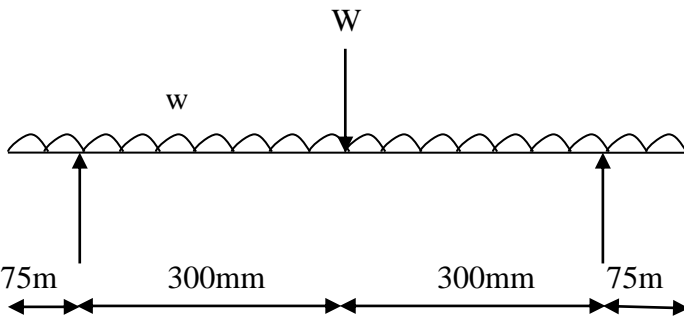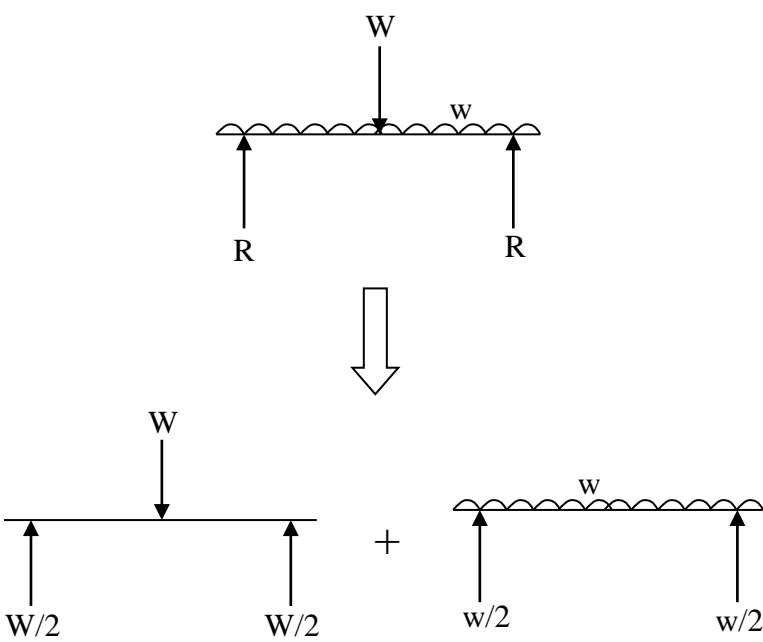
A.1. Preliminary design calculations
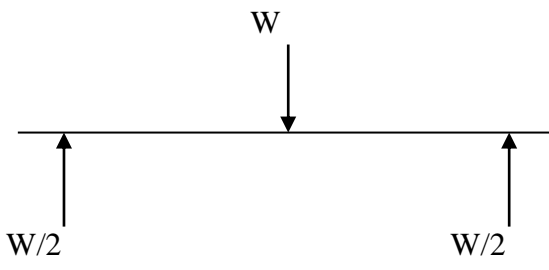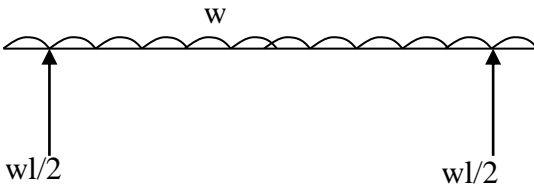
Table A.1.: Design data

Symbol	Value
Overall thickness of the member d	150 mm
Width of the beam b	100 mm
Considered cover for reinforcement	25 mm
Depth to tensile steel reinforcement from the extream compression fiber d'	150-25-6/2-4 118 mm
Span of the beam	600 mm
Concrete ultimate strain ε_{cu}	0.0035
Elastic modulus of steel E_s	200 GPa (Assumed)
Yield stress of steel f_y	230 MPa (Measured)
Concrete cube strength f_{cu}	30 MPa (Assumed)

A.1.1. Expected failure load in flexure (BS 8110: 1985 part 11)

Reference	Calculations	Out put
BS8110: part 1 – Clause 3.4.4	Depth to neutral axis, Compressive force in concrete (f_c) $= $ Tensile force in steel (f_t) $0.9X \times b \times 0.67 f_{cu} = f_y A_s$ $0.9X \times 100\ mm \times 0.67 \times 30\ \dfrac{N}{mm^2} = 250\ \dfrac{N}{mm^2} \times \pi$ $X = 7.8\ mm$	$X = 7.8\ mm$
BS8110: part 1 – Clause 3.4.4.4	Lever arm Z, $Z = d - \dfrac{0.9X}{2}$ $= 118 - \dfrac{0.9 \times 7.8}{2}$	Z $= 114.5\ mm$

	$= 114.5 \; mm$	
	Flexural capacity, M, $$M = F_t Z$$ $$= f_y A_s Z$$ $$= 250 \frac{N}{mm^2} \times \pi \times 3^2 mm^2 \times 2 \times 114.5 \; mm$$ $$= 1.62 \times 10^6 \; Nmm$$ $$= 1.62 \; kNm$$	M $= 1.62 \; kNm$
	Evaluation of failure load Loads applied on the beam 	
	Using principle of superposition 	

	a) Point load Maximum moment will occur between two point loads Therefore, for 0.075m < X <0.375m; Moment, $M_1 = \frac{W}{2}(X - 0.075)$	
	b) Self weight Moment $M_2 = \frac{wl}{2}(X - 0.075) - w\frac{X^2}{2}$	
	Total moment By adding (a) and (b); Total moment $M = \frac{W}{2}(X - 0.075) + \frac{wl}{2}(X - 0.075) - w\frac{X^2}{2}$ For maximum moment, $\frac{d(m)}{dX} = 0$ $\qquad X = 0.375m$ Therefore maximum moment, $\qquad M_{max} = 0.15W - 0.04219w$ $\qquad M_{max} = 1.62\ kNm$ $\quad w = 0.15 \times 0.1 \times 2.4 \times 9.81 Nm^{-1}$ $\qquad = 0.3532\ \text{Nm}^{-1}$ $\quad 1.62 = 0.15W - 0.04219 \times 0.3532$ $\qquad W = 10.9\ kN$	W $= 10.9\ kN$

	Expected failure load in flexure $\quad= \mathbf{10.9\ kN}$ $\qquad$ **Fail due to steel yielding**	

A.1.2. Expected shear capacity (According to BS 8110: Part1 1: 1985)

Reference	Calculations	Out put
	Expected shear capacity = shear capacity of concrete + shear capacity of steel	
BS8110: part 1 - table 3.8	Shear capacity of concrete $$= 0.79 \left(\frac{100 A_s}{b_v d}\right)^{\frac{1}{3}} \left(\frac{400}{d}\right)^{\frac{1}{4}} \left(\frac{f_{cu}}{25}\right)^{\frac{1}{3}}$$ $$= 0.79 \left(\frac{100 \times 56.55}{100 \times 150}\right)^{\frac{1}{3}} \times \left(\frac{400}{150}\right)^{\frac{1}{4}} \times \left(\frac{30}{25}\right)^{\frac{1}{3}}$$ $$= 0.775$$ Where, $\frac{100 A_s}{b_v d} \leq 3; \frac{400}{d} \geq 1$	
BS8110: part 1 – Clause 3.4.5.3	Shear capacity of stirrups $= \frac{A_{sy} f_y}{s b_v}$ $$\text{(S= 50mm)}$$ $$= \frac{2\pi \times 2^2 \times 363.01}{50 \times 100}$$ $$= 1.825$$	
	Expected shear capacity $= 0.775 + 1.825$ $$= 2.6 \ N/mm^2$$	$V = 2.6 \ N/mm^2$
	Shear force due to applied load $$0.075 < X \ < 0.6m$$ Shear force, S $= \frac{W}{2}$	
	Shear force due to self weight $$\text{Shear force, S} = \frac{wl}{2} - \ wX$$	
	Total shear force, $$S = \frac{W}{2} + \frac{wl}{2} - \ wX$$	

	Maximum shear occurs at the support. i.e. X = 0.075m $$S_{max} = \frac{W}{2} + \frac{wl}{2} - 0.075w$$	
	Allowable shear force, $$S = 2.72 \times 150 \times 100 \times 10^{-3} \ kN$$ $$= 40.8 \text{ kN}$$	
	Failure load under shear $$\frac{W}{2} + \frac{wl}{2} - 0.075w = 40.8$$ $$\frac{W}{2} + \frac{0.3532 \times 0.75}{2} - 0.075 \times 0.3532 = 40.8$$ $$W = 81.39 \text{ kN}$$	W = 81.39 kN

Expected failure load in shear = 81.39 kN

Expected failure load in shear >> Expected failure load in flexure

Therefore the beam will fail in flexure and thus the selected specimen details are suitable for the study.

A.2. Mix design data

Table A.2: Summary of mix design

Stage	Item		Reference or calculation	Values
1	1.1	Characteristic strength	Specified	30 N/mm^2 at 28 days Proportion defective 5%
	1.2	Standard deviation	Fig 3	8 N/mm^2
	1.3	Margin	Specified	1.64×8 = 13.12
	1.4	Target mean strength		30+13.12 = 43.12
	1.5	Cement strength class	Specified	42.5

	1.6	Aggregate type Coarse Fine		Crushed Uncrushed
	1.7	Free water/ Cement ratio	Fig 2	0.55
	1.8	Maximum free water/cement ratio	Specified	0.65
				Use 0.55
2	2.1	Slump	Specified	75mm
	2.2	Maximum aggregate size	Specified	20mm
	2.3	Free – Water content	Table 3	**205 kg/m^3**
3	3.1	Cement content		205/0.55 = 372.73 kg/m^3
	3.2	Maximum cement content	Specified	550 kg/m^3
	3.3	Minimum cement content	Specified	290 kg/m^3
	3.4	Modified free water/cement ratio		0.55
				Use cement content **373.73 kg/m^3**
4	4.1	Relative density of aggregate	Assumed	2.65
	4.2	Concrete density	Fig 5	2370 kg/m^3
	4.3	Total aggregate content		2370-373-205 = 1792 kg/m^3
5	5.1	Grading of fine aggregate		% passing 60μm sieve = 60%
	5.2	Proportion of fine aggregate	Fig 6	38%
	5.3	Fine aggregate content		1792 × 0.38 = **681 kg/m^3**
	5.4	Coarse aggregate content		1792 – 681 = **1111 kg/m^3**

APPENDIX B

B.1. Material test data

B.1.1. Concrete cube strength

Cube number	Cross section area (mm^2)	Height (mm)	Weight (kg)	Compressive strength (N/mm^2)	Density
C - C1	153×150	150	8.25	47.3	
C – C2	153×150	151	8.25	45.2	
F – C1	153×152	151	8.35	50.5	
F – C2	152×150	151	8.35	46.3	
FA1 – C1	150×151	151	8.3	46.6	
FA1 – C2	151×150	149	8.3	53.9	
FA2 – C1	151×150	152	8.3	44.5	
FA2 – C2	152×151	150	8.3	45.9	

Therefore average compressive strength f_{cu};

$$f_{cu} = \frac{47.3 + 45.2 + 50.5 + 46.3 + 46.6 + 53.9 + 44.5 + 45.9}{2}$$

$$= 47.46 \, Nmm^{-2}$$

B.1.2. Tensile strength of 6mm diameter mild steel

Applied load (in MT)	Applied load (in kN)	Number of revelutions	
		Specimen 1 (R1)	Specimen 2 (R2)
0.00	0.00	0	0
0.05	0.49	52	131
0.10	0.98	66	140
0.15	1.47	81	154
0.20	1.96	93	165

0.25	2.45	111	176
0.30	2.94	190	200
0.30	2.94	-	385
0.32	3.14	190	-
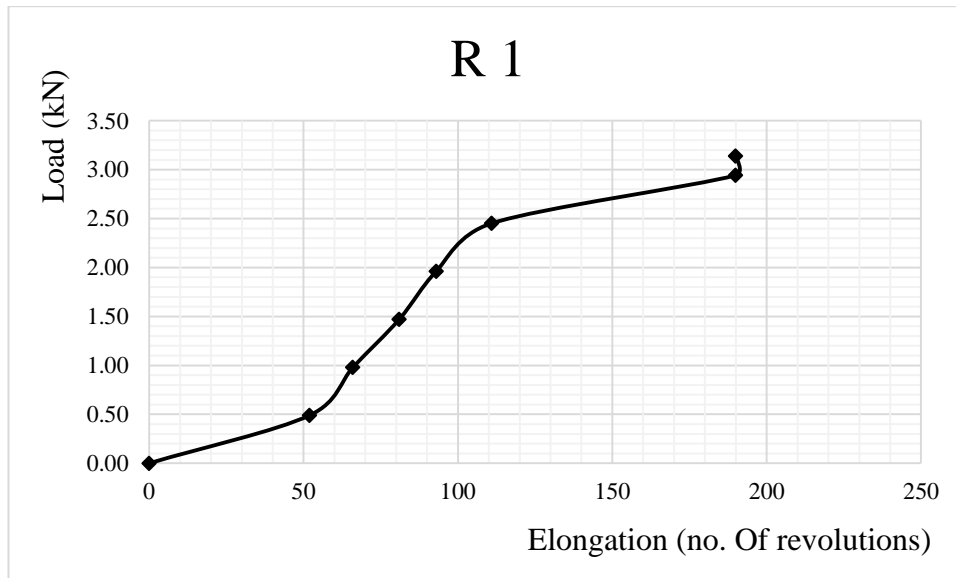
Figure 1: Load Vs elongation for R1
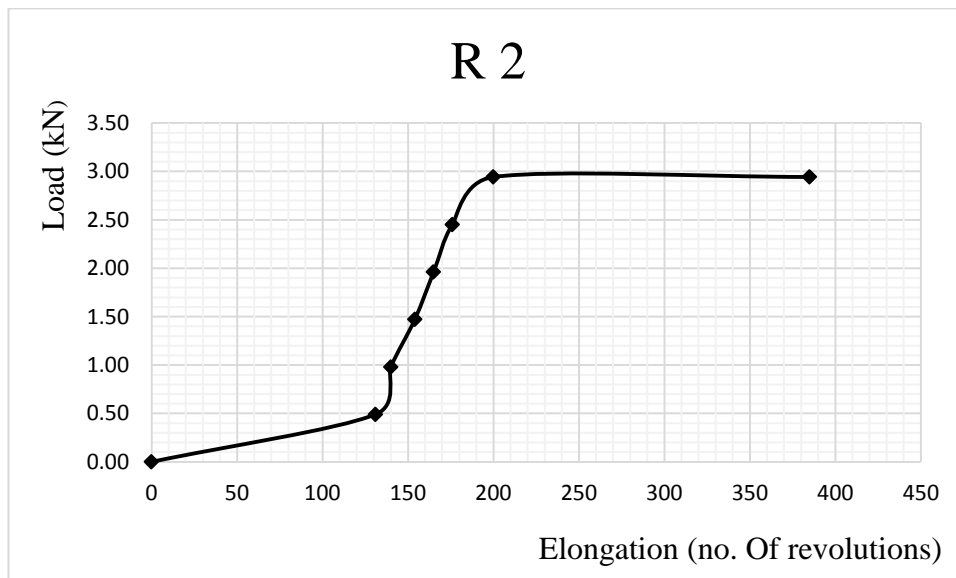
Figure 2: Load Vs elongation for R2

For specimen 1 (R1)

Yield stress $= \dfrac{Yield\ load\ (N)}{Average\ Area\ (mm^2)}$

$$f_{y1} = \frac{2.94 \times 1000\ N}{\pi r^2 mm^2}$$

$$= \frac{2940}{\pi \times 2^2}$$

$$= 233.96\ Nmm^{-2}$$

For specimen 2 (R2)

Yield stress $= \dfrac{Yield\ load\ (N)}{Average\ Area\ (mm^2)}$

$$f_{y2} = \frac{2.54 \times 1000\ N}{\pi r^2 mm^2}$$

$$= \frac{2940}{\pi \times 2^2}$$

$$= 202.126\ Nmm^{-2}$$

Hence design f_y;

$$= \frac{233.96 + 202.126}{2}\ Nmm^{-2}$$

$$= 218.043\ Nmm^{-2}$$

B.1.3. Galvanized steel tensile strength

Applied load (MT)	Applied load (kN)	Number of revolutions	
		Specimen 1 (GS1)	Specimen 2 (GS2)
0.00	0.00	0	0
0.05	0.49	106	40
0.10	0.98	122	59
0.15	1.47	132	70

0.20	1.96	140	79
0.25	2.45	146	87
0.30	2.94	151	94
0.35	3.43	156	100
0.40	3.92	162	106
0.45	4.41	168	117
0.50	4.91	173	123
0.55	5.40	180	129
0.60	5.89	186	139
0.65	6.38	193	143
0.70	6.87	210	168
0.75	7.36	235	187
0.80	7.85	260	211
0.85	8.34	286	250
0.90	8.83	336	358
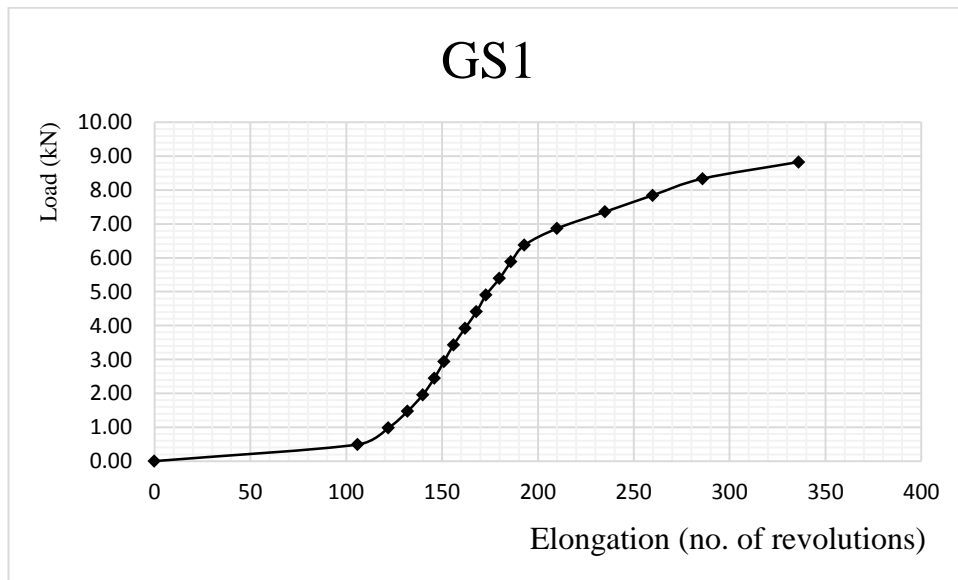
Figure 3: Load Vs elongation for GS1

GS 2
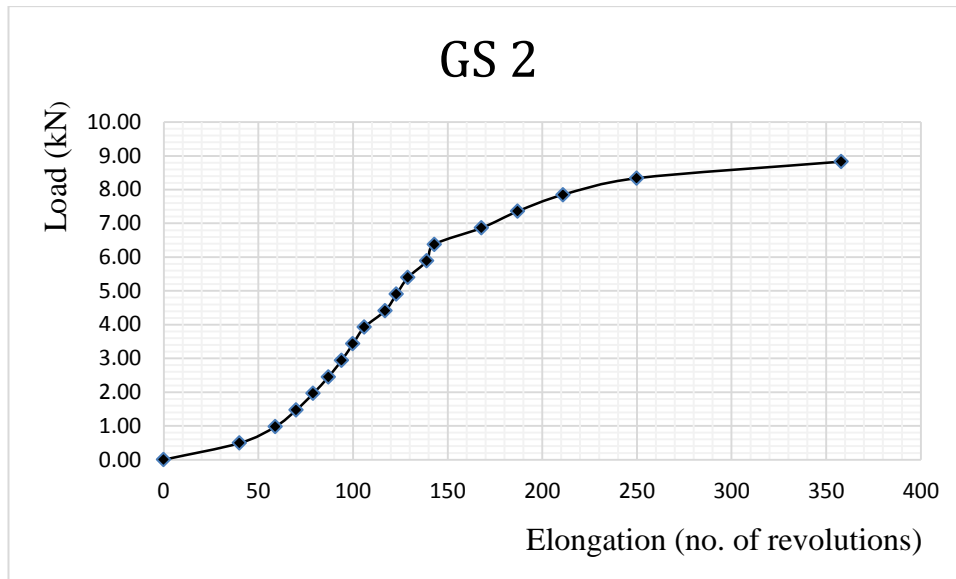
Figure 4: Load Vs elongation for GS2

For specimen 1 (GS1)

$$\text{Yield stress} = \frac{Yield\ load\ (N)}{Average\ Area\ (mm^2)}$$

$$f_{y1} = \frac{7.85 \times 1000\ N}{\pi r^2 mm^2}$$

$$= \frac{7850}{\pi \times 3^2}\ Nmm^2$$

$$= 277.66\ Nmm^{-2}$$

For specimen 2 (GS2)

$$\text{Yield stress} = \frac{Yield\ load\ (N)}{Average\ Area\ (mm^2)}$$

$$f_{y2} = \frac{7.85 \times 1000\ N}{\pi r^2\ mm^2}$$

$$= \frac{7850}{\pi \times 3^2}\ Nmm^2$$

$$= 277.66\ Nmm^{-2}$$

Hence Average yield stress $(f_y) = 277.66 \ Nmm^{-2}$

B.2. Failure modes of specimens
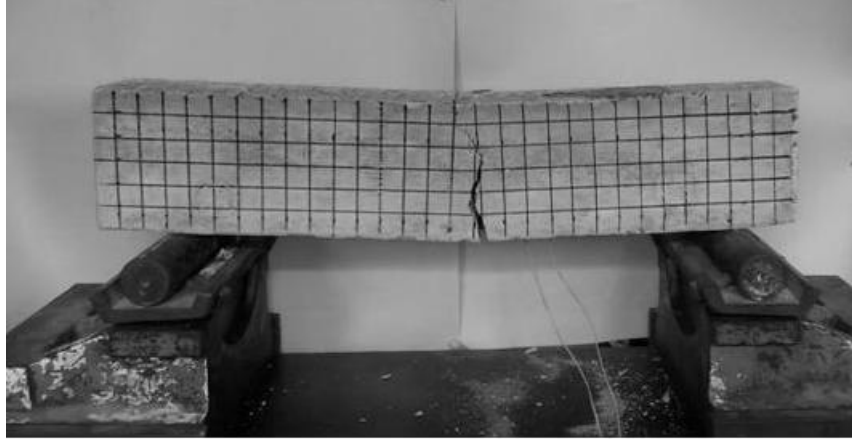
Figure B.1: Failure of specimen C(1)

Figure B.2: Failure of specimen C(2)
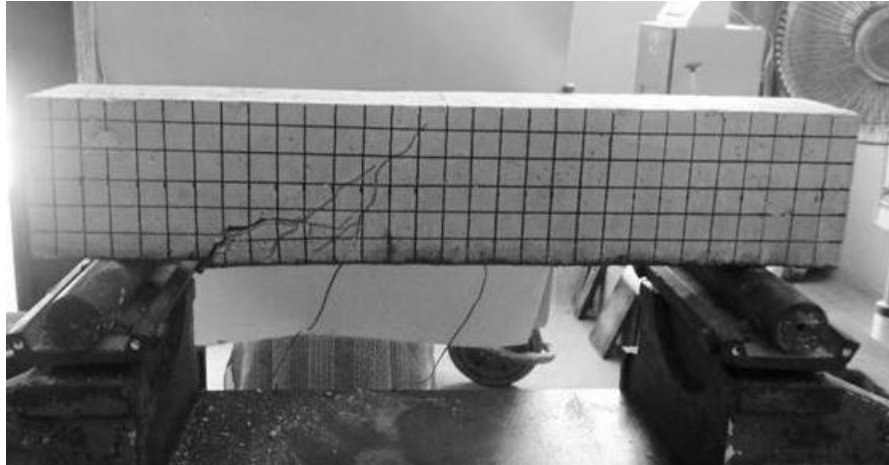
Figure B.3: Failure of specimen F(1)

Figure B.4: Failure of specimen F(2)
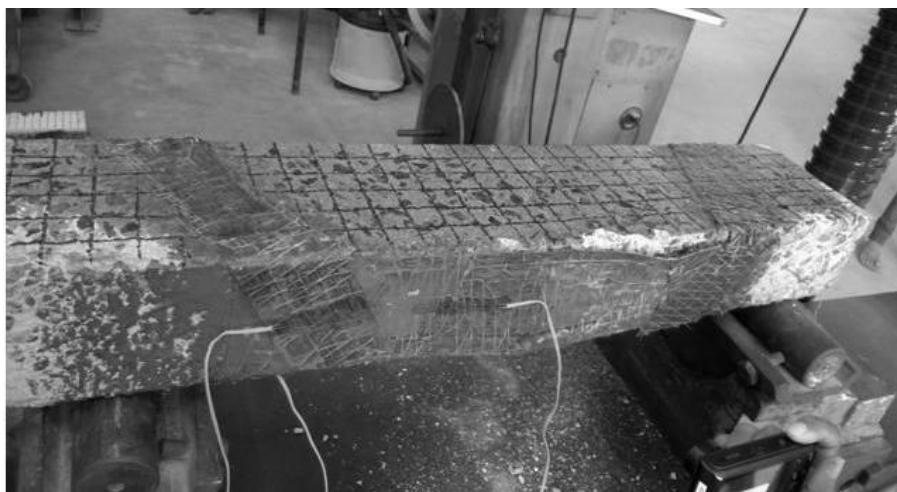
Figure B.5: Failure of specimen FA1(1)

148
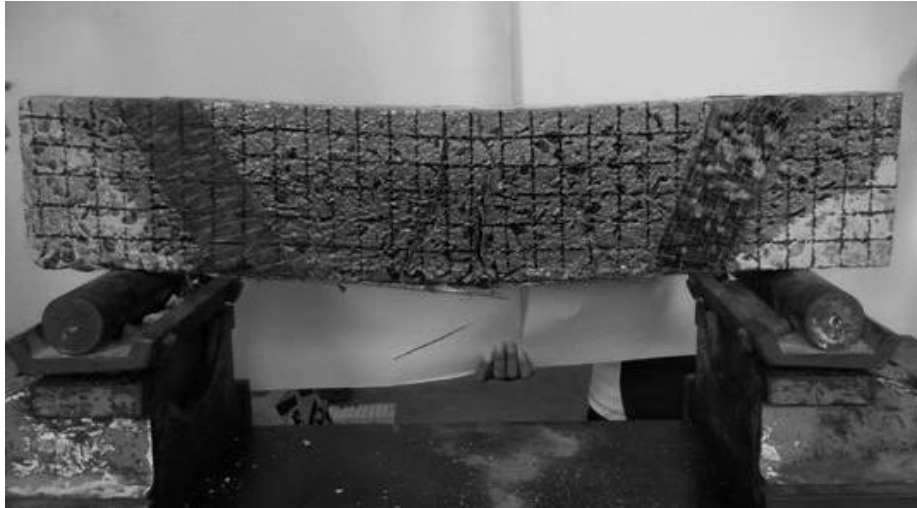
Figure B.6: Failure of specimen FA1(2)

Figure B.7: Failure of specimen FA2(1)

Figure B. 8: Failure of specimen FA2(2)

APPENDIX C

C.1   Prediction of flexural capacity according to ACI-440-R design guide

The beam geometry required for calculations is shown in Figure 4.1.

Table 1: Design data

Symbol	Value
Overall thickness of the member h	150 mm
Width of the beam b	100 mm
Width of the FRP plate w_f	90 mm
Depth to tensile steel reinforcement from the extream compression fiber d	150-25-6/2-4 118 mm
Depth to FRP reinforcement from the extream compression fiber h′	150+0.1+0.19 mm 150.29 mm
Thickness ofthe FRP plate t_f	0.19 mm
Concrete ultimate strain ε_{cu}	0.003
f'_c	47.46 MPa
E_s	195 GPa
f_y	230 MPa
f_{frp}	2600 MPa
E_{frp}	640 GPa

C.1.1. Flexural capacity under premature failure

Reference	Calculations	Out put
ACI 440.2R-02 Table 8.1	FRP System design material properties Assume the beam is located in an interior space and a CFRP material is be used. However the environmental reduction factor was equate to 1 for a proper comparison	$C_E = 1$

Reference	Calculations	Out put
ACI 440.2R-02 Section 8.4	Design tensile strength of FRP $f_{fu} = C_E \times f_{frp}$ $\quad = 1 \times 2600\ N/mm^2$ $\quad = 2600\ N/mm^2$ Design tensile strain in FRP $\varepsilon_{fu} = f_{fu}/E_{frp}$ $\quad = 2600\ Nmm^{-2}/640000Nmm^{-2}$ $\quad = 0.00406$	f_{fu} $= 2600\ N$ $/mm^2$ $\varepsilon_{fu} = 0.00406$
ACI 318-99 Section 10.2.7.3	Calculation of β_1 $\beta_1 = 0.85 - 0.05\frac{f'_c - 4000}{1000}$, $0.65 \leq \beta_1 \leq 0.85$(f'$_c$ in ksi) $\quad = 1.05 - 0.05\frac{f'_c}{1000}$ $\quad = 1.05 - 0.05 \times \frac{47460/6.894757}{1000}$ $\quad = 0.705$	$\beta_1 = 0.705$
	Existing strain on the soffit ε_{bi} Assume no initial strain when bonding FRP $\varepsilon_{bi} = 0$	$\varepsilon_{bi} = 0$
ACI 440.2R-02 Section 9.2.1	Bond depended coefficient of the FRP system K_m $nE_f t_f = 1 \times 640000\ Nmm^{-2} \times 0.19\ mm$ $\quad = 121600 > 180000$ Therefore; $K_m = \frac{1}{60\varepsilon_{fu}} \times \frac{90000}{nE_f t_f} \leq 0.9$ $\quad = \frac{1}{60 \times 0.00406} \times \frac{90000}{180000}$ $\quad = 2.05 \leq 0.9$	$K_m = 0.9$

Reference	Calculations	Out put
	Assumed depth to the neutral axis c $$c = 70 \; mm$$	
ACI 440.2R-02 Section 9.2.2	Effective level of strain in FRP ε_{fe} $$\varepsilon_{fe} = 0.003 \times \frac{h' - c}{c} - \varepsilon_{bi} \leq K_m \varepsilon_{fu}$$ $$= 0.003 \times \frac{150.29mm - 70mm}{70mm} - 0$$ $$\leq 0.9 \times 0.00406$$ $$= 0.003441 \; \leq 0.00365$$ Strain in the existing reinforcing steel ε_s $$\varepsilon_s = \left(\varepsilon_{fe} + \; \varepsilon_{bi} \right) \times \frac{d - c}{h' - c}$$ $$= \; 0.003441 \times \frac{118mm - 70mm}{150.29mm - 70mm}$$ $$= 0.00204$$	ε_{fe} $= 0.003441$ System will fail due to concrete crushing $\varepsilon_s = 0.00204$

Reference	Calculations	Out put
ACI 440.2R-02	**Stress levels in FRP and steel**	
Section 9.2.3 ACI 440.2R-02 Section 9.6	Depth to neutral axis by checking force equilibrium $$f_s = \frac{\varepsilon_s E_s}{\gamma_m} \leq \frac{f_y}{\gamma_m}$$ $$c = \frac{A_f f_{fe} + A_s f_s}{\gamma \frac{f'_c}{\gamma_m} \beta_1}$$ $$= \frac{0.00204 \times 195000 Nmm^{-2}}{1.15} = \frac{230 Nmm^{-2}}{1.15}$$ $$= \frac{0.19mm \times 90mm \times 2182.4 \ Nmm^{-2} + 345.91 \ mm^2 \times \frac{230N}{1.15} \times 200 N/mm^2}{0.85 \times \frac{47.46 \ Nmm^{-2}}{1.5} \times 0.705 \times 100mm}$$ $$= 645.91 \ mm^2 \times \frac{\pi}{4} \times 230 N/mm^2$$ $$= 21.04 \ mm \qquad f_{fe} = \frac{\varepsilon_{fe} E_f}{\gamma_m}$$ $$= \frac{0.003441 \times 640000 Nmm^{-2}}{1.4}$$	$f_s = 200 \ Nmm^{-2}$ The assumed c $f_{fe} = 1573.03$ value is not Nmm^{-2} correct
	$$= 1573.028 \ N/mm^2$$	

	By iteration $c = 21.9\ mm$	$c = 21.9\ mm$
	Strain level in FRP $\varepsilon_{fe} = 0.00365$	$\varepsilon_{fe} = 0.00365$
	Strain in steel reinforcement $\varepsilon_s = 0.00273$	System will fail due to de bonding
ACI 440.2R-02 Section 9.2.3	Stresses in FRP f_{fe} $$f_{fe} = \frac{\varepsilon_{fe}E_f}{\gamma_m}$$ $$= \frac{0.00365 \times 640000 Nmm^{-2}}{1.4}$$ $$= 1668.57\ N/mm^2$$ Stress in steel f_s $$f_s = \frac{\varepsilon_s E_s}{\gamma_m} \leq \frac{f_y}{\gamma_m}$$ $$= \frac{0.00273 \times 195000 Nmm^{-2}}{1.15}$$ $$\leq \frac{230 Nmm^{-2}}{1.15}$$ $$= 462.91 \frac{N}{mm^2} \leq 200\ N/mm^2$$	Steel yielding also occurs
ACI 440.2R-02 Section 9.6	Moment carrying capacity M_n $$M_n = A_s f_s \left(d - \frac{\beta_1 c}{2}\right) + \varphi A_f f_{fe} \left(h' - \frac{\beta_1 c}{2}\right)$$ $$= 56.55 mm^2 \times 200 Nmm^{-2} \left(118mm - \frac{0.705 \times 21.9\ mm}{2}\right)$$ $$+ 1 \times 17.1 mm^2$$ $$\times 1668.57\ Nmm^{-2} \left(150.29mm\right.$$ $$\left. - \frac{0.705 \times 21.9\ mm}{2}\right)$$	

	$= 5\ 315.16\ kNmm$	
	$= 5.315\ kNm$	$\boldsymbol{M_n}$ $= \boldsymbol{5.32\ kNm}$
From chapter 3	Maximum moment $M_{max} = 0.15W - 0.04219w$ $M_{max} = 5.315\ kNm$ $w = 0.15\ \times 0.1 \times 2.4 \times 9.81 Nm^{-1}$ $= 0.3532\ \text{Nm}^{-1}$ Ultimate load $0.15W = M_{max} + 0.04219 \times 0.3532$ $W = 35\ 532.67\ N = 35.53\ kN$	$\boldsymbol{W =}$ $\boldsymbol{35.53}\ \text{kN}$

C.1.2. Flexural capacity under classical failure

Reference	Calculations	Out put
ACI 440.2R-02	FRP System design material properties	

Table 8.1	Assume the beam is located in an interior space and a CFRP material is be used. However; environmental-reduction factor $C_E = 1$	$C_E = 1$
ACI 440.2R-02 Section 8.4	Design tensile strength of FRP $f_{fu} = C_E \times f_{frp}$ $= 1 \times 2600 \ N/mm^2$ $= 2600 \ N/mm^2$ Design tensile strain in FRP $\varepsilon_{fu} = f_{fu}/E_{frp}$ $= 2600 \ Nmm^{-2}/640000 Nmm^{-2}$ $= 0.00406$	f_{fu} $= 2600 \ N/mm^2$ $\varepsilon_{fu} = 0.00406$
ACI 318-99 Section 10.2.7.3	Calculation of β_1 $\beta_1 = 0.85 - 0.05\frac{f'_c - 4000}{1000}$, $0.65 \leq \beta_1 \leq 0.85$(f'$_c$ in ksi) $= 1.05 - 0.05\frac{f'_c}{1000}$ $= 1.05 - 0.05 \times \frac{47460/6.894757}{1000}$ $= 0.705$	$\beta_1 = 0.705$
	Existing strain on the soffit ε_{bi} Assume no initial strain when bonding FRP $\varepsilon_{bi} = 0$	$\varepsilon_{bi} = 0$
ACI 440.2R-02 Section 9.2.1	No Bond depended coefficient is introduced	

	Assumed depth to the neutral axis c $$c = 70 \ mm$$	
ACI 440.2R-02 Section 9.2.2	Effective level of strain in FRP ε_{fe} $$\varepsilon_{fe} = 0.003 \times \frac{h' - c}{c} - \varepsilon_{bi} \leq \varepsilon_{fu}$$ $$= 0.003 \times \frac{150.29mm - 70mm}{70mm} - 0$$ $$= 0.00344$$	$\varepsilon_{fe} = 0.00344$ System will fail due to concrete crushing
	Strain in the existing reinforcing steel $$\varepsilon_s = (\varepsilon_{fe} + \varepsilon_{bi}) \times \frac{d - c}{h' - c}$$ $$= 0.00344 \times \frac{118mm - 70mm}{150.29mm - 70mm}$$ $$= 0.00206$$	$\varepsilon_s = 0.00206$
ACI 440.2R-02 Section 9.2.3	<u>Stress levels in FRP and steel</u> $$f_s = \frac{\varepsilon_s E_s}{\gamma_m} \leq \frac{f_y}{\gamma_m}$$ $$= \frac{0.00206 \times 195000 Nmm^{-2}}{1.15}$$ $$\leq \frac{230 Nmm^{-2}}{1.15}$$ $$= 311.53 \frac{N}{mm^2} \leq 200 \ N/mm^2$$ $$f_{fe} = \frac{\varepsilon_{fe} E_f}{\gamma_m}$$ $$= \frac{0.00344 \times 640000 Nmm^{-2}}{1.4}$$ $$= 1572.57 \ N/mm^2$$	$f_s = 200 \ Nmm^{-2}$ $f_{fe} = 1572.57 \ Nmm^-$

ACI 440.2R-02 Section 9.6	Depth to neutral axis by checking force equilibrium $$c = \frac{A_f f_{fe} + A_s f_s}{\gamma \dfrac{f'_c}{\gamma_m} \beta_1 b}$$ $$= \frac{\begin{aligned}&0.19mm \times 90mm \times 2202 \ Nmm^{-2} + \\ &6^2 mm^2 \times \frac{\pi}{4} 230 N mm^{-2} \times 2\end{aligned}}{0.85 \times \dfrac{47.46 N mm^{-2}}{1.5} 0.705 \times 100mm}$$	
	$$= 21.05 \ mm$$	The assumed c value is not correct
	By iteration $c = 29.41 \ mm$	$c = 29.41 \ mm$
	Strain level in FRP $\varepsilon_{fe} = 0.008443$ Strain in steel reinforcement $\varepsilon_s = 0.002757$	
ACI 440.2R-02 Section 9.2.3	Stresses in FRP f_{fe} $$f_{fe} = \frac{\varepsilon_{fe} E_f}{\gamma_m} < f_{yfe}$$ $$= \frac{0.01236 \times 640000 N mm^{-2}}{1.4}$$ $$= 5639.18 \frac{N}{mm^2} < 2600 \ N mm^2$$ Stress in steel f_s $$f_s = \frac{\varepsilon_s E_s}{\gamma_m} \le \frac{f_y}{\gamma_m}$$ $$= \frac{0.00297 \times 195000 N mm^{-2}}{1.15}$$ $$\le \frac{230 N mm^{-2}}{1.15}$$	FRP ruptures Steel yielding also occurs

	$= 504.55 \dfrac{N}{mm^2} \leq 200 \; N/mm^2$	
ACI 440.2R-02 Section 9.6	Moment carrying capacity M_n $$M_n = A_s f_s \left(d - \dfrac{\beta_1 c}{2} \right) + \varphi A_f f_{fe} \left(h' - \dfrac{\beta_1 c}{2} \right)$$ $$= 56.55 mm^2 \times 200 mm^{-2} \left(118mm - \dfrac{0.705 \times 29.41mm}{2} \right)$$ $$+ 17.1 mm^2$$ $$\times 2600 \; Nmm^{-2} \left(150.29mm \right.$$ $$\left. - \dfrac{0.705 \times 29.41mm}{2} \right)$$ $= 7\,438.304 \; kNmm$ $= 7.438 \; kNm$	$\boldsymbol{M_n}$ $\boldsymbol{= 7.438 kNm}$
From chapter 3	Maximum moment $$M_{max} = 0.15W - 0.04219w$$ $$M_{max} = 7.438 \; kNm$$ $$w = 0.15 \; \times 0.1 \times 2.4 \times 9.81 Nm^{-1}$$ $$= 0.3532 \; Nm^{-1}$$ Ultimate load $$0.15W = M_{max} + 0.04219 \times$$ 0.3532 $$W = 49\,686 \; N = 49.69 \; kN$$	$\boldsymbol{W = 49.69}$ kN

C.1.3. Shear capacity of end anchored beams

Reference	Calculations	Out put
ACI 440 2R section 10.4	Shear contribution of FRP system	

	$$V_f = \dfrac{A_{fv}f_{fe}(\sin\alpha + \cos\alpha)d_f}{s_f}$$	
ACI 440 2R Equation 10.4	Area of fiber reinforcement $$A_{fv} = 2nt_fw_f$$ $$= 2 \times 1 \times 0.19 \times 60$$ $$= 22.8\ mm^2$$	$A_{fv} = 22.8\ mm^2$
ACI 440 2R Equation 10.6. (b)	$$\varepsilon_{fe} = \varepsilon_{fu} \le 0.004$$ $$= \dfrac{2600}{640000} = 0.00406 \le 0.004$$ $$= 0.004$$	$\varepsilon_{fe} = 0.004$
ACI 440 2R Equation 10.5	$$f_{fe} = \varepsilon_{fe}E_f$$ $$= 0.004 \times 640000$$ $$= 2560\ Nmm^{-2}$$	f_{fe} $= 2560\ Nmm^{-2}$
ACI 440 2R Equation 10.3	$$V_f = \dfrac{A_{fv}f_{fe}(\sin\alpha + \cos\alpha)d_f}{s_f}$$ $$= \dfrac{22.8 \times 2600\ (0.446 + 0.8928) \times 150}{300}$$ $$= 39\ 682\ N$$	$V_f = 39.68\ kN$
ACI 440 2R Equation 10.2	Total shear capacity $$\boldsymbol{V_n = (V_c + V_s + V_f)}$$ $$= 40\ 800 + 39\ 682$$ $$= 80\ 482\ N$$	$\boldsymbol{V_n = 80.48\ kN}$
	Therefore, ultimate load, $$\dfrac{W}{2} + \dfrac{wl}{2} - 0.075w = 80.48$$ $$\dfrac{W}{2} + \dfrac{0.3532 \times 0.75}{2} - 0.075 \times 0.3532$$ $$= 80.48$$ $$W = 160.96\ kN$$	$\boldsymbol{W = 160.96\ kN}$

C.2. Prediction of flexural capacity according to FIB bulletin-14 design guide

Symbol	Value

Overall thickness of the member h	150 mm
Width of the beam b	100 mm
Width of the FRP plate w_f	90 mm
Depth to tensile steel reinforcement from the extream compression fiber d	150-25-6/2-4 118 mm
Depth to compression steel reinforcement from the extream compression fiber d_2	25+4+3 32 mm
Depth to FRP reinforcement from the extream compression fiber h′	150+0.1+0.19 mm 150.29 mm
Thickness ofthe FRP plate t_f	0.19 mm
Concrete ultimate strain ε_{cu}	0.0035
f'_c	47.46 MPa
E_s	200 GPa
f_{yd}	230 MPa
f_{fud}	2600 MPa
E_f	640 GPa

C.2.1. Anchorage length

Reference	Calculations	Out put
FIB bulletin 14 Equation A1-2	$$l_{b,max} = \sqrt{\frac{E_f t_f}{c_2 f_{ctm}}}$$ $$= \sqrt{\frac{640000 \times 0.19}{2 \times 3.5}}$$ $$= 118.7 \, mm$$	$l_{b,max}$ $= \mathbf{118.7 \, mm}$

C.2.2. Flexural capacity under failure due to steel yielding followed by concrete crushing

Reference	Calculations	Out put
FIB bulletin	Full composite action in the system is assumed.	

14 Section 4.4.1.1	Depth to neutral axis; X is calculated considering strain compatibility and internal force equilibrium. Assume $x = 50mm$	
	Ultimate strain in FRP ε_{fud} $$\varepsilon_{fud} = f_{fud}/E_f$$ $$= 2600/640000$$ $$= 0.00406$$	
FIB bulletin 14 Equation 4-6	Strain in compression steel ε_{s2} $$\varepsilon_{s2} = \varepsilon_{cu}\frac{x - d_2}{x}$$ $$= 0.0035\frac{50 - 32}{50}$$ $$= 1.26 \times 10^{-3}$$ $E_{s2}\varepsilon_{s2} \leq f_{yd}$ $\quad 195000\ Nmm^2 \times 0.00126 \leq 230\ Nmm^2$ $\quad\quad 245.7\ Nmm^2 > 230Nmm^2$ Therefore, $$\varepsilon_{s2} = f_{yd}/E_s$$ $$= 0.00118$$	ε_{s2} $= 1.18 \times 10^{-3}$
FIB bulletin 14 Equation 4-7	Strain in FRP ε_f $$\varepsilon_f = \varepsilon_{cu}\frac{h - x}{x} \leq \varepsilon_{fud}$$ $$= 0.0035\frac{150 - 50}{50}$$ $$= 7 \times 10^{-3} \leq 4.06 \times 10^{-3}$$	ε_f $= 4.06 \times 10^{-3}$
	Strain in tension steel ε_{s1} $$\varepsilon_{s1} = \varepsilon_{cu}\frac{d - x}{x} \geq \frac{f_{yd}}{E_s}$$ $$= 0.0035\frac{118 - 50}{50} \geq 0.00118$$ $$= 4.76 \times 10^{-3}$$	ε_{s1} $= 4.76 \times 10^{-3}$

FIB bulletin 14 Equation 4-5	$0.85 \times \varphi \times f_{cd}bx + A_{s2}E_s\varepsilon_{s2}$ $= A_{s1}f_{yd} + A_f E_{fu}\varepsilon_f$ $0.85 \times 0.8 \times 47.46 \times 100 \times x +$ $56.55 \times 195000 \times 0.00118 = 56.55 \times 230 +$ $0.19 \times 90 \times 640000 \times 4.062 \times 10^{-3}$ $x = 14.19$ mm	The assumed c value is not correct
	By iteration ; Depth to neutral axis $x = 22.63\ mm$	$x = 22.63\ mm$
FIB bulletin 14 Equation 4-8	Moment capacity $M_{Rd} = A_{s1}f_{yd}(d - \delta_G x) + A_f E_f \varepsilon_f (h - \delta_G x)$ $+ A_{s2}E_{s2}\varepsilon_{s2}(\delta_G x - d_2)$ $= 56.55 \times 230 \times (118 - 0.4 \times 22.63)$ $+ 17.1 \times 640000 \times 4.06 \times 10^{-3}(150 - 0.4 \times 22.63)$ $+ 56.55 \times 195000 \times (-0.00117) \times (0.4 \times 22.63 - 32)$ $= 7\ 967\ 207.547\ Nmm$	
	$M_{Rd} = 7.97\ kNm$	$M_{Rd} = 7.97\ kNm$
From chapter 3	Maximum moment $M_{max} = 0.15W - 0.04219w$ $M_{max} = 7.97\ kNm$ $w = 0.15 \times 0.1 \times 2.4 \times 9.81 Nm^{-1}$ $= 0.3532\ Nm^{-1}$ Ultimate load $0.15W = M_{max} + 0.04219 \times 0.3532$ $W = 55\ 535\ N = 55.53\ kN$	$W = 55.53$ kN
	If additional reduction factor of 0.85 is considered for FRP, (in order to address the damage to FRP while installing)	$W = 49.22\ kN$

$M_n = 7.03\ kNm$	
$W = 49.22\ kN$	

C.2.3. Flexural capacity under failure due to steel yielding followed by FRP rupture

Reference	Calculations	Output
FIB bulletin 14 Section 4.4.1.1	Full composite action until failure is assumed	
	$\varepsilon_f = \varepsilon_{fud} = 0.00406$	
	Assume depth to neutral axis; $x = 60\ mm$	
	Maximum strain in concrete compression fibers ε_c $$\varepsilon_c = \varepsilon_{fud}\frac{x}{h-x}$$ $$= 0.00406\frac{60}{150-60}$$ $$= 0.0027$$	
FIB bulletin 14 Equation 4-11	$0.002 \leq \varepsilon_c \leq 0.0035$ $$\varphi = 1 - \frac{2}{3000\varepsilon_c}$$ $$= 1 - \frac{2}{3000 \times 0.0027}$$ $$= 0.75$$	
FIB bulletin 14 Equation 4-12	$$\delta_G = \frac{1000\varepsilon_c(3000\varepsilon_c - 4) + 2}{2000\varepsilon_c(3000\varepsilon_c - 2)}$$ $$= 0.396$$	
FIB bulletin 14 Equation 4-6	Strain in compression steel ε_{s2} $$\varepsilon_{s2} = \varepsilon_{cu}\frac{x - d_2}{x}$$	$\varepsilon_{s2} = 0.00117$

	$$= 0.0027 \frac{60 - 32}{60}$$ $$= 1.26 \times 10^{-3} \ < \ \frac{f_{yd}}{E_s} =$$ 0.00117	
	Strain in tension steel ε_{s1} $$\varepsilon_{s1} = \ \varepsilon_{cu} \frac{d - x}{x}$$ $$= 0.0027 \frac{118 - 60}{60}$$ $$= 2.61 \ \times 10^{-3}$$	$\varepsilon_{s1} = 0.00117$
FIB bulletin 14 Equation 4-5	$$0.85 \times \varphi \times f_c bx + \ A_{s2}E_s\varepsilon_{s2}$$ $$= \ A_{s1}f_{yd} + \ A_f E_{fu}\varepsilon_{fud}$$ $$0.85 \times 0.75 \times 47.46 \times 100 \times x +$$ $$56.55 \times 195000 \times 0.00117 = 56.55 \times 230 +$$ $$0.19 \times 90 \times 640000 \times 4.06 \times 10^{-3}$$ $$x = 15.48 \text{ mm}$$	The assumed c value is not correct
	By iteration ; Depth to neutral axis $x = 21.32 mm$	$x = 21.32\, mm$
FIB bulletin 14 Equation 4-8	Moment capacity $$M_{Rd} = \ A_{s1}f_{yd}(d - \delta_G x) + \ A_f E_f \varepsilon_f (h - \delta_G x)$$ $$+ \ A_{s2}E_{s2}\varepsilon_{s2}(\delta_G x - d_2)$$ $$= 56.55 \times 230 \times (118 - 0.34 \times 21.32)$$ $$+ 17.1 \times 640000 \times 4.06 \times 10^{-3}(150 - 0.34 \times 21.32)$$ $$+ 56.55 \times 195000 \times (-0.00037)(0.34 \times 21.32 - 32)$$ $$= 7\,877 \ Nm$$	
	$M_{Rd} = 7.877 \ kNm$	M_{Rd} $= 7.877 \ kNm$
From chapter 3	Maximum moment $$M_{max} = 0.15W - 0.04219w$$ $$M_{max} = 7.877 \ kNm$$	$W = 54.87 \text{ kN}$

	$w = 0.15 \times 0.1 \times 2.4 \times 9.81 Nm^{-1}$ $= 0.3532 \text{ Nm}^{-1}$ Ultimate load $\quad 0.15W = M_{max} + 0.04219 \times 0.3532$ $\quad W = 54\,868 \ N = 54.87 \ kN$	
	If additional reduction factor of 0.85 is considered for FRP, (in order to address the damage to FRP while installing) $\quad M_n = 6.932 \ kNm$ $\quad W = 48.57 \ kN$	**W** **$= 48.57 \ kN$**

Failure load under yielding of steel reinforcement followed by concrete crushing (55.53 kN) > Failure load under yielding of steel reinforcement followed by FRP rupture (54.87 kN)

Therefore failure will occur due to steel yielding followed by FRP rupture.

C.2.4. Flexural capacity under end shear failure

Reference	Calculations	Output
FIB-bulletin-14 section 4.4.2.3.	$$\rho_s = \frac{A_{s1}}{bd}$$ $$= \frac{56.55}{100 \times 150}$$ $$= 0.0037$$	$\rho_s = 0.0037$
FIB bulletin 14 Equation 4.17	$$a_L = \sqrt[4]{\frac{(1 - \sqrt{\rho_s})^2}{\rho_s} dL^3}$$ $$= \sqrt[4]{\frac{(1 - \sqrt{0.0037})^2}{0.0037} 118 \times 75^3}$$ $$= 330 \ mm \ < 300 \ mm$$	$a_L = 330 \ mm$

Reference	Calculations	Output
FIB bulletin 14 Equation 4.15	$V_{sd} < V_{Rd} = \tau_{Rd}bd$ $$\tau_{Rd} = 0.15 \sqrt[3]{3\frac{d}{a_L}} \left(1 + \sqrt{\frac{200}{d}}\right) \sqrt[3]{100\rho_s f_{ck}}$$ $$= 0.15$$ $$\times \sqrt[3]{3\frac{150}{300}} \left(1\right.$$ $$\left. + \sqrt{\frac{200}{150}}\right) \sqrt[3]{100 \times 0.0037 \times 47.46}$$ $$= 1.041 \, N/mm^2$$ $$V_{Rd} = 1.041 \times 100 \times 150$$ $$= 15620.97 \, N$$ $$= 15.62 \, kN$$	
	Therefore, applicable load before end shear failure $$\frac{W}{2} + \frac{wl}{2} - 0.075w = S$$ $$\frac{W}{2} + \frac{0.3532 \times 0.75}{2} - 0.075 \times 0.3532$$ $$= 15.62$$ $$W = 31.5 \, kN$$	$W = 31.5 \, kN$

C.2.5. Shear capacity of end anchored beams

Reference	Calculations	Output
FIB bulletin 14 Equation 5.2	FRP contribution to shear capacity $$V_{fd} = 0.9\varepsilon_{fd,e}E_{fu}\rho_f b_w d(\cos\theta + \cot\alpha)\sin\alpha$$	
	Design value of FRP strain, Minimum of (peeling stress, fracture stress)	

FIB bulletin 14 Clause 5.1.2.1	$$\rho_f = \frac{2t_f}{b_w} \times \frac{b_f}{s_f}$$ $$= \frac{2 \times 0.19 \times 60}{100 \times 300}$$ $$= 0.00076$$	
FIB bulletin 14 Equation 5.4 a	Strain at peeling off $$\varepsilon_{fe} = 0.65 \left(\frac{f_{cm}^{\frac{2}{3}}}{E_{fu}\rho_f} \right)^{0.56} \times 10^{-3}$$ $$= 0.65 \left(\frac{47.46^{\frac{2}{3}}}{640 \times 0.00076} \right)^{0.56} \times 10^{-3}$$ $$= 0.085$$	
FIB bulletin 14 Equation 5.4 b	Strain at FRP fracture $$\varepsilon_{fe} = 0.17 \left(\frac{f_{cm}^{\frac{2}{3}}}{E_{fu}\rho_f} \right)^{0.3} \times \varepsilon_{fu}$$ $$= 0.17 \left(\frac{47.46^{\frac{2}{3}}}{640 \times 0.00076} \right)^{0.3} \times 0.00406$$ $$= 0.00185$$ FRP fracture will occur first.	
	$$V_{fd} = 0.9\varepsilon_{fd,e}E_{fu}\rho_f b_w d(\cos\theta + \cot\alpha)\sin\alpha$$ $$= 0.9 \times 0.00185 \times 640 \times 0.00076 \times 100$$ $$\times 125 \times \left(\frac{2}{2.24} + \frac{2}{1} \right) \times \frac{1}{2.24}$$ $$= 13.073 \ kN$$	
	$$V_{rd} = V_{cd} + V_{wd} + V_{fd}$$ $$v_{cd} = 0.79 \left(\frac{100A_s}{b_v d} \right)^{\frac{1}{3}} \left(\frac{400}{d} \right)^{\frac{1}{4}} \left(\frac{f_{cu}}{25} \right)^{\frac{1}{3}}$$	**V_{rd}** **$= 24.758 \ kN$**

<table>
<tr><td></td><td>

$$= 0.79 \left(\frac{100 \times 56.55}{100 \times 150}\right)^{\frac{1}{3}} \times \left(\frac{400}{150}\right)^{\frac{1}{4}}$$

$$\times \left(\frac{47.46}{25}\right)^{\frac{1}{3}}$$

$$= 0.90 \ N/mm^2$$

$$v_{wd} = \frac{2\pi \times 2^2 \times 363.01}{50 \times 100}$$

$$= 1.825 \ N/mm^2$$

$$V_{rd} = V_{cd} + V_{wd} + V_{fd}$$

$$= 0.9 \times 150 \times 100 \times 10^{-3} + 1.825 \times 150$$

$$\times 100 \times 10^{-3} + 13.073$$

$$= 53.948 \ kN$$

</td><td></td></tr>
<tr><td></td><td>

Therefore, ultimate load,
$$\frac{W}{2} + \frac{wl}{2} - 0.075w = S$$
$$\frac{W}{2} + \frac{0.3532 \times 0.75}{2} - 0.075 \times 0.3532$$
$$= 53.948$$
$$W = 107.896 \ kN$$

</td><td>

W

$= 107.896 \ kN$

</td></tr>
</table>

C.3. Prediction of flexural capacity according to method proposed by Li et al. (2013)

Table 2: Design data for Li et al method

Symbol	Value
Overall thickness of the member h	150 mm
Width of the beam b	100 mm
Width of the FRP plate w_f	90 mm
Depth to tensile steel reinforcement from the extream compression fiber d	150-25-6/2-4 118 mm
Depth to compression steel reinforcement from the extream compression fiber d_2	25+4+3 32 mm

Depth to FRP reinforcement from the extream compression fiber h′	150+0.1+0.19 mm 150.29 mm
Thickness ofthe FRP plate t_f	0.19 mm
Concrete ultimate strain ε_{cu}	0.0035
f'_c	47.46 MPa
E_s	195 GPa
f_{yd}	230 MPa
f_{fud}	2600 MPa
E_f	640 GPa

C.3.1. Capacity of beams flexural strengthened with CFRP under classical failure

Reference	Calculations	Output
Equation 9	$$x = \frac{f_y A_s + F_d}{f_c b}$$ $$= \frac{230 \times 56.55 + 2600 \times 0.91 \times 90}{30 \times 100}$$ $$= 19.16 \, mm$$	x $= 19.16 \, mm$
Equation 8	$$M_u = f_y A_s \left(h - a_s - \frac{x}{2} \right) + F_d \left(h - \frac{x}{2} \right)$$ $$= 230 \times 56.55 \left(150.29 - 25 - \frac{19.16}{2} \right) + 2600$$ $$\times 0.19 \times 90 \left(150.29 - \frac{19.16}{2} \right)$$ $$= 7760 \, 948 \, Nmm$$ $$= 7.76 \, kNm$$	M_u $= 7.76 \, kNm$
From chapter 3	Maximum moment $$M_{max} = 0.15W - 0.04219w$$ $$M_{max} = 7.76 \, kNm$$ $$w = 0.15 \times 0.1 \times 2.4 \times 9.81 Nm^{-1}$$ $$= 0.3532 \, Nm^{-1}$$	$W = 51.83$ kN

	Ultimate load	
	$$0.15W = M_{max} + 0.04219 \times 0.3532$$ $$W = 51\,832\,N = 51.83\,kN$$	

C.3.2. Capacity of beams when debonding occurs

Reference	Calculations	Output
Equation 9	$$x = \frac{f_y A_s + F_d}{f_c b}$$ $$= \frac{230 \times 56.55 + 54 \times 0.91 \times 90}{30 \times 100}$$ $$= 4.64\,mm$$	$x = 4.64\,mm$
Equation 8	When debonding occurs, interfacial shear stress is equal to bond strength. Therefore stress in FRP sheet is assumed to be equal to bond stress at failure. $$M_u = f_y A_s \left(h - a_s - \frac{x}{2} \right) + F_d \left(h - \frac{x}{2} \right)$$ $$= 230 \times 56.55 \left(150.29 - 25 - \frac{4.64}{2} \right) + 54$$ $$\times 0.19 \times 90 \left(150.29 - \frac{4.64}{2} \right)$$ $$= 1\,736\,044\,Nmm$$ $$= 1.74\,kNm$$	M_u $= 1.74\,kNm$
From chapter 3	Maximum moment $$M_{max} = 0.15W - 0.04219w$$ $$M_{max} = 1.74\,kNm$$ $$w = 0.15 \times 0.1 \times 2.4 \times 9.81 Nm^{-1}$$ $$= 0.3532\,Nm^{-1}$$ Ultimate load $$0.15W = M_{max} + 0.04219 \times 0.3532$$ $$W = 11\,699\,N = 11.7\,kN$$	$\boldsymbol{W = 11.7\,kN}$

C.3.4 Capacity of end anchored beams

Reference	Calculations	Output
Equation 4	Assume failure due to FRP rupture $$F_u = b_f t_f \sigma_{t,max}$$ $$= 90 \times 0.19 \times 2600$$ $$= 44460 \ N$$	$F_u = 44460 \ N$
	Ultimate bond strength τ_u; In the experiments, the beam was failed at FRP / concrete interface. Therefore τ_u can be taken as ultimate strength of the adhesive layer. $$\tau_u = 54 \ Nmm^{-2}$$	$\tau_u = 54 \ Nmm^{-2}$
Equation 6	Effective bond length L_e; $$L_e = \frac{F_u}{b_f \tau_u}$$ $$= \frac{44460}{90 \times 54}$$ $$= 9.148 \ mm$$	$L_e = 9.148 \ mm$
Equation 16	Tensile force, when concrete cover separation occurs in presence of end U wraps F_{e2}; $$F_{e2} = f_t \left(1 + \frac{2L_{ue}}{b}\right)\frac{b_f L_e^2}{6a_s}$$ $$= 2600 \left(1 + \frac{2 \times 9.148}{100}\right)\frac{90 \times 9.148^2}{6 \times 25}$$ $$= 154\,435 \ N$$	$F_{e2} = 154\,435 \ N$

Equation 17	Tensile force before sheets debonding F_{e1}; $$F_{e1} = b_f\sqrt{0.4E_f t_f f_t} + \tau_f b_f w \leq \varepsilon_{fu}E_f A_f$$ $$= 90\sqrt{0.4 \times 640000 \times 0.19 \times 2600} + 54$$ $$\times 90 \times 60$$ $$\leq 0.007 \times 640000 \times 90 \times 0.19$$ $$= 1\,303\,705\,N \leq 76\,608\,N$$	F_{e1} $= 76\,608\,N$
Equation 10	$$F_d = \min(F_{e1}, F_{e2})$$ $$F_d = 76\,608\,N$$ Beam fails due to FRP rupture	$\boldsymbol{F_d}$ $= \boldsymbol{76\,608\,N}$
Equation 9	$$x = \frac{f_y A_s + F_d}{f_c b}$$ $$= \frac{230 \times 56.55 + 76\,608}{30 \times 100}$$ $$= 29.87\,mm$$	$x = 3.095\,mm$
Equation 8	$$M_u = f_y A_s\left(h - a_s - \frac{x}{2}\right) + F_d\left(h - \frac{x}{2}\right)$$ $$= 230 \times 56.55\left(150.29 - 25 - \frac{29.87}{2}\right)$$ $$+ 76\,608\left(150.29 - \frac{29.87}{2}\right)$$ $$= 11\,804\,160\,Nmm$$ $$= 11.80\,kNm$$	$\boldsymbol{M_u}$ $= \boldsymbol{11.8\,kNm}$

APPENDIX D

Table 1: Geometric details of database beams

Reference	Beam designation	Beam height h (mm)	Beam width b (mm)	Clear Span (mm)	Shear span L_s (mm)	Width of U wrap L_a (mm)	Loading type	Percentage strength gain % over non anchored beam
R.A. Hawileh et al. (2013)	B50PW1	180	110	1690	561.5	139	Two point loading	23.43
R.A. Hawileh et al. (2013)	FE - B50PW1	180	110	1690	561.5	139	Two point loading	23.75
E.S. Khalifa and S.H. Al-tersawy (2013)	B2 - 1W2U	200	100	1700	650	100	Two point loading	35.36
O. Gunes et al. (2009)	S4PS1M	180	150	1350	450	80	Two point loading	31
O. Gunes et al. (2009)	S4PS2M	180	150	1350	450	160	Two point loading	43.27
N.A. Siddiqui	BFS2	300	200	2000	750	100	Two point	29.41

							loading	
A.A. EI-Ghandour	B1F	300	120	1800	900	50	One point loading	9.7
A.A. EI-Ghandour	B3FS	300	120	1800	900	205	One point loading	24
A.R.Khan and S. Fareed	WSAB1	232	152.4	1728	518.16	216	Two point loading	16.68
A.R.Khan and S. Fareed	WSAB2	232	152.4	1728	381	216	Two point loading	20.8

Table 2: Material properties of database beams

Reference	Beam designation	Compressive strength of concrete f_{cu} (N/mm^2)	Elastic modulus of CFRP E_f (kN/mm^2)	Thickness of CFRP sheet t_f (mm)	Tensile strength of CFRP f_f (N/mm^2)	Modulus of elasticity of steel E_s (kN/mm^2)	Yield stress of steel reinforcement f_{ys} (N/mm^2)	Tensile steel reinforcement
R.A. Hawileh et	B50PW1	54	160	1.4	2800	202	611	2T10

al. (2013)								
R.A. Hawileh et al. (2013)	FE - B50PW1	54	160	1.4	2800	202	611	2T10
E.S. Khalifa and S.H. Al-tersawy (2013)	B2 - 1W2U	25	230	0.13	3600	200	230	2T12
O. Gunes et al. (2009)	S4PS1M	41.4	165	1.2	2800	200	440	2T#5
O. Gunes et al. (2009)	S4PS2M	41.4	165	1.2	2800	200	440	2T#5
N.A. Siddiqui (2009)	BFS2	35	77.28	1	846	200	420	3T14

A.A. EI-Ghandour	B1F	48.1	240	0.176	3800	200	400	3T16
A.A. EI-Ghandour	B3FS	48.1	240	0.176	3800	200	400	3T16
A.R.Khan and S. Fareed	WSAB1	40	270	1.2	4100	200	418	3T12
A.R.Khan and S. Fareed	WSAB2	40	270	1.2	4100	200	418	3T12

APPENDIX E - List of publications

Wijerathna D.M.N., Gamage J.C.P.H., Fawzia S.**"Effects of end anchorage on flexural performance of CFRP strengthened concrete beam"** Materials and structures. Manuscript Submitted

Wijerathna D.M.N., Gamage J.C.P.H., **"A Review on Alternative Bonding Techniques to Delay End Debonding of CFRP/Concrete Composites"** *Proceedings of the 5thInternational Conference on Sustainable Built Environment (ICSBE 2014).* Kandy, Sri Lanka, 12-15 Dec 2014

E.1. Effects of end anchorages on flexural performance of CFRP strengthened Concrete beams

D.M.N. Wijerathne[1], J. C. P. H. Gamage[2*], S. Fawzia[2]

[1]*Post Graduate student,, Department of Civil Engineering, University of Moratuwa, Sri Lanka*

[2]*Senior Lecturer, Department of Civil Engineering, University of Moratuwa, Sri Lanka*

[3]*School of Civil Engineering and built Environment, Queensland University of Technology, Brisbane, Australia*

*Corresponding Author Email: kgamage@uom.lk

Abstract

Purpose

Strengthening of structures with Carbon Fiber Reinforced Polymer (CFRP) can be identified as an efficient technique for upgrading reinforced concrete structures. Although the strengthening system is capable of providing high load carrying capacity increments, research studies have shown that debonding failure limits the ultimate capacity in concrete members, flexural strengthened using CFRP. There are various alternatives proposed to overcome debonding failure, among which CFRP end wraps are more beneficial and convenient. Proper understanding on the extended benefits of CFRP end anchors is a necessity to optimize the system performance and allocated resources. Purpose of this study is to investigate the mechanical response of CFRP flexural strengthened reinforced concrete beams and propose a constitutive model to predict the flexural behavior.

Method

Experimental program was conducted on CFRP strengthened reinforced concrete beam specimens. Data available on similar research was also collected. Based on the results and collected data from literature, a theoretical model was proposed to predict the behavior of CFRP strengthened beams with end wrap anchorages.

Results

This paper presents the outline of test programme, results, bond characteristics such bond stress vs. slip, fracture energy in relation with failure mode etc and modified braced arch model for CFRP strengthened normal strength concrete beams.

Conclusions

Remarkable strength increments can be achieved with inclined CFRP end anchorage. CFRP end wraps prevent debonding failure and shift the failure mode from premature failure to classical failure. The developed theoretical model can predict the flexural capacity of CFRP flexural strengthened and end anchored beams with CFRP end wraps with a reasonable accuracy.

E.2. A Review on Alternative Bonding Techniques to Delay End Debonding of CFRP/Concrete Composites

D.M.N. Wijerathne[1*], J. C. P. H. Gamage[2]

[1]University of Moratuwa, Moratuwa, Sri Lanka

[2]University of Moratuwa, Moratuwa, Sri Lanka

*E-Mail: dmanasiwijerathna@gmail.com, TP: +94711687502

Abstract: Externally bonded Fiber Reinforced Polymers (FRP) has been widely used for flexural strengthening of reinforced concrete structures. End debonding is a critical issue which causes a significant reduction of ultimate capacity of the strengthening system. End debonding occurs due to cracks induced by high interfacial shear and normal stresses caused by the abrupt termination of the plate. The failure can be in two modes; plate end shear failure and anchorage failure at last crack. The common attribute of both these failure modes is that delamination occurs along the track with minimum fracture energy. By introducing a proper anchorage, stresses can be effectively transferred to the concrete element and energy required to the failure can be increased. There are many research works that have been carried out to investigate possible techniques to delay end debonding failure. However there is no any record of effort taken to scale those techniques in to a single study. This research paper presents a review on usage of FRP wraps to delay end debonding. It summarizes different wrapping methods used to delay end debonding which have proposed by different authors and compares them in terms of efficiency.

Keywords: CFRP/Concrete, Debonding, Flexure.